

Aus dem Department für Diagnostische Labormedizin der  
Universität Tübingen

Institut für Medizinische Mikrobiologie und Hygiene

**The impact of antibiotic pressure on the phenotypic  
evolution of clinical antibiotic resistant  
*Pseudomonas aeruginosa* in a Morbidostat device**

Inaugural-Dissertation  
zur Erlangung des Doktorgrades  
der Medizin

der Medizinischen Fakultät  
der Eberhard Karls Universität  
zu Tübingen

vorgelegt von

Jentzsch, Benedikt Alexander

2022

Dekan: Professor Dr. B. Pichler

1. Berichterstatter: Professor Dr. M. Willmann  
2. Berichterstatter: Professorin Dr. C. Wolz

Tag der Disputation: 20.12.2021

# I. Table of Content

I.	Table of Content.....	I
II.	List of Figures .....	IV
III.	List of Tables .....	IV
IV.	List of Abbreviations .....	V
<b>1</b>	<b>Introduction .....</b>	<b>1</b>
1.1	<i>Pseudomonas</i> .....	1
1.2	<i>Pseudomonas aeruginosa</i> .....	1
1.3	<i>Biofilm formation</i> .....	2
1.4	<i>Virulence</i> .....	5
1.5	<i>Antimicrobial resistance</i> .....	6
1.6	<i>Colistin as last-resort antibiotic</i> .....	7
1.6.1	Colistin-resistance .....	8
1.7	<i>Combination with metronidazole</i> .....	10
1.8	<i>Morbidostat</i> .....	12
1.9	<i>Objective of this study</i> .....	14
<b>2</b>	<b>Material &amp; Methods.....</b>	<b>15</b>
2.1	<i>Material</i> .....	15
2.1.1	Laboratory equipment .....	15
2.1.2	Plastic devices .....	16
2.1.3	Bacterial strains .....	16
2.1.4	Antibiotics .....	17
2.1.5	Chemicals .....	17
2.1.6	Growth media for bacterial cultivation.....	18
2.1.7	Animals .....	18
2.1.8	Others .....	19
2.2	<i>Bacterial strains</i> .....	19
2.3	<i>Morbidostat</i> .....	19
2.3.1	General principal.....	19

2.3.2	Control run using LB medium .....	20
2.3.3	Sample collection .....	21
2.3.4	Cleaning .....	21
2.4	<i>Cultivation of bacteria</i> .....	21
2.5	<i>Susceptibility tests</i> .....	22
2.6	<i>Biofilm formation</i> .....	23
2.6.1	Principle of assay .....	23
2.6.2	Crystal violet staining method .....	23
2.6.3	Peg-lid method biofilm assay .....	24
2.7	<i>Virulence</i> .....	26
2.7.1	The <i>Galleria mellonella</i> infection model .....	26
2.7.2	Preparation .....	26
2.7.3	Injection .....	26
2.7.4	Survival control .....	27
2.7.5	Growth curve .....	28
2.8	<i>Correlation analysis</i> .....	28
2.9	<i>Statistical analysis</i> .....	29
2.10	<i>Ethics</i> .....	29
<b>3</b>	<b>Results</b> .....	<b>30</b>
3.1	<i>Sample collection from the morbidostat and growth failure</i> .....	30
3.2	<i>Colistin resistance development under antibiotic exposure</i> .....	30
3.3	<i>Alterations in biofilm formation ability after antibiotic exposure</i> .....	33
3.3.1	Irregular production of biofilm biomass under antibiotic influence .....	33
3.3.2	Increased quantity of viable cells in biofilm under colistin exposure .....	38
3.4	<i>Exposure to colistin leads to loss of virulence</i> .....	45
3.4.1	Partly clear connection between loss of virulence and increasing MIC.....	49
3.4.2	No growth restriction due to antibiotic exposure .....	51
<b>4</b>	<b>Discussion</b> .....	<b>54</b>
<b>5</b>	<b>Summary</b> .....	<b>66</b>
<b>6</b>	<b>Zusammenfassung auf Deutsch</b> .....	<b>68</b>

<b>7</b>	<b>Supplementary.....</b>	<b>70</b>
7.1	<i>Crystal violet staining method - OD<sub>600nm</sub> values.....</i>	70
7.2	<i>Peg-lid method – CFU count .....</i>	74
7.3	<i>Galleria mellonella infection model – Kaplan Meier curves.....</i>	78
7.4	<i>Galleria mellonella infection model – Hazard ratios.....</i>	83
<b>8</b>	<b>References .....</b>	<b>85</b>
<b>9</b>	<b>Erklärung zum Eigenanteil der Dissertationsschrift .....</b>	<b>93</b>
<b>10</b>	<b>Publications .....</b>	<b>94</b>
<b>11</b>	<b>Acknowledgements.....</b>	<b>95</b>

## II. List of Figures

Figure 1: Schematically illustrated mechanism of biofilm development.....	4
Figure 2: Chemical structure of colistin.....	7
Figure 3: Chemical structure of metronidazole.....	10
Figure 4: Comparison of conventional culture devices to morbidostat culture. ....	12
Figure 5: Results for crystal violet staining biofilm assay.....	36
Figure 6: Spearman correlation between ratios and MIC (violet staining biofilm assay).. ....	38
Figure 7: Results for peg-lid method biofilm assay.....	42
Figure 8: Spearman correlation between ratios and MIC (peg-lid method biofilm assay).. ....	44
Figure 9: Kaplan Meier curves monitoring the survival of <i>G. mellonella</i> larvae after infection with ID21.. ....	46
Figure 10: Results for <i>Galleria mellonella</i> infection model.. ....	49
Figure 11: Spearman correlation between ratios and MIC ( <i>G. mellonella</i> infection model).....	50
Figure 13: Growth curves and corresponding linear regression.. ....	53
Figure 14: Results for crystal violet staining biofilm assay.....	73
Figure 15: Results for peg-lid method biofilm assay.. ....	77
Figure 16: Kaplan Meier curves monitoring the survival of <i>G. mellonella</i> larvae after infection.. ....	82
Figure 17: Hazard ratios for <i>Galleria mellonella</i> infection model.. ....	84

## III. List of Tables

Table 1: MICs for baseline isolates and morbidostat-derived strains.....	32
--	----

#### IV. List of Abbreviations

<i>A. baumannii</i>	<i>Acinetobacter baumannii</i>
bp	Base pairs
BMD	Broth microdilution
CF	Cystic Fibrosis
CFU	Colony forming units
CHAPS	3-[(3-Cholamidopropyl)dimethylammonio]-1-propanesulfonate
DNA	Desoxyribonucleic acid
dH <sub>2</sub> O	Deionized water
ddH <sub>2</sub> O	Double distilled water
ECDC	European Centre for Disease Prevention and Control
EDTA	Ethylenediaminetetraacetic acid
e.g.	Exempli gratia
EPS	Extracellular polymeric substance
FACS	Fluorescence-activated Cell Sorting
<i>G. mellonella</i>	<i>Galleria mellonella</i>
h	Hour
ICU	Intensive care unit
LB	Lysogeny broth
LPS	Lipopolysaccharide
M	Molar
MDR	Multi-drug-resistant
MIC	Minimal inhibitory concentration
min	Minute
NGS	Next Generation Sequencing
OD <sub>x</sub>	Optical density at x nm
PBS	Phosphate buffered saline

PDR	Pan-drug-resistant
<i>P. aeruginosa</i>	<i>Pseudomonas aeruginosa</i>
TSA	Tryptic Soy Agar
TSB	Tryptic Soy Broth
TSP	transferable 96-peg solid phase plate
WHO	World Health Organization
XDR	Extensively-drug-resistant



# 1 Introduction

## 1.1 Pseudomonas

*Pseudomonas* species are Gram-negative rod-shaped bacteria, which belong to the family of *Pseudomonadaceae*. Their name derives from the Greek ψευδής (“false”) and μονάς (“unit”) - as a term that was used to describe a motile unicellular organism - and was first described by Walter Migula in 1894 (Etymologia *Pseudomonas* 2012). There are more than 140 species, of which 25 are associated with humans. The bacteria measuring 1.5 to 3 µm are motile due to a single polar flagellum. *Pseudomonas* are aerobic, catalase- and oxidase-positive and not able to form spores. They inhabit soil and water and are found on the skin, throat and stool of a healthy human person. *Pseudomonas* species usually cause opportunistic infections including endocarditis, pneumonia and infections of the urinary tract, wounds, skin and the musculoskeletal system (Iglewski 1996).

## 1.2 *Pseudomonas aeruginosa*

*Pseudomonas aeruginosa* is an ubiquitous environmental organism that requires minimal survival resources and has a remarkable adaptability to a wide range of environmental challenges (Hardalo *et al.* 1997). It produces a green-blue color when grown in nutrient medium due to its production of pyocyanin and pyoverdine giving it the Latin name aerugo for verdigris. Furthermore, it is known for its grapelike odor (Sykes 2014). With an average size of 6.3 Mbp - and a G+C content of around 66.6% - its genome is remarkably larger than most bacterial genomes which allows the adaptation into different ecological niches (Stover *et al.* 2000, Lee *et al.* 2006).

According to the European Centre for Disease Prevention and Control (ECDC), *Pseudomonas aeruginosa* causes 8.9% of nosocomial infections in European hospitals and even up to 33.3% of pneumoniae acquired in intensive care units (ICUs) (ECDC-Surveillance-Report 2012, ECDC-Annual-Epidemiological-Report 2017). Although only 4-12% of the population are fecal carriers it is a real danger

for hospital-acquired infections because of its ability to survive even in adverse circumstances (Bodey *et al.* 1983). Being found in moist environments like faucets, sink drains, water jugs and respiratory equipment in hospitals *P. aeruginosa* poses a particular threat for patients suffering from burn wounds, cystic fibrosis (CF), acute leukemia or neutropenia, organ transplants, mechanical ventilation and vascular as well as urinary catheterization (Bodey *et al.* 1983). Depending on the underlying disease, most commonly the opportunistic bacteria cause pneumonia (CF patients and patients requiring ventilation), wound infections (burn patients), urinary infections (patients with urinary catheters) and blood stream infections (neutropenic patients and patients with long-term vascular catheters) (Gould *et al.* 1985). Prognosis for *P. aeruginosa* infections in immunocompromised patients are poor, especially for patients with bacteremia with a 30-day mortality of 39% (Kang *et al.* 2003). Risk factors increasing the mortality are pneumonia, a severe underlying disease and a delayed start of adequate antibiotic therapy (Kang *et al.* 2003).

### **1.3 Biofilm formation**

A major cause of chronic *P. aeruginosa* infections is the formation of bacterial biofilm on medical devices, wounds, the middle ear or the lung of CF patients. The mechanism of biofilm development includes the attachment to a solid surface, followed by the creation of microcolonies, and the production of extracellular polymeric substance (EPS) matrix resulting in a matured biofilm (Costerton *et al.* 1999).

The attachment of *P. aeruginosa* to the surface initiated by flagella-mediated motility, whereas the formation of a stable, dense monolayer requires the presence of type IV pili (O'Toole *et al.* 1998). These type IV pili are also involved in the twitching motility of adherent bacteria necessary for the expansion of microcolonies into mushroom-shaped complexes (Klausen *et al.* 2003). Furthermore, the ability of *P. aeruginosa* to attach and detach to a surface depends on the expression of *sadB*. After the stimulation of outer membrane signal transduction proteins like *GacS* and *AdrA* through contact to the surface the intracellular concentration of the second messenger cyclic-diguanosin-5-

monophosphate (c-di-GMP) increases. *SadB* among other regulatory proteins is activated by the binding of c-di-GMP regulating flagellum motility and the production of exopolysaccharides which are key aspects of the initial formation of biofilms (Caiazza *et al.* 2004, Merritt *et al.* 2007, Muriel *et al.* 2019) (Figure 1 A).

In addition, initial microcolony formation and the biofilm dispersion in the mushroom-shaped structure is mediated by the biosurfactant rhamnolipid produced by *P. aeruginosa* (Pamp *et al.* 2008). Rhamnolipid increases the hydrophobicity of the bacterial cell surface due to a release of lipopolysaccharides (LPS) from the outer membrane enhancing the bacteria's solubility in the EPS and their ability to deplete organic compounds (Al-Tahhan *et al.* 2000).

To form a mature biofilm, the bacteria have to produce an EPS matrix consisting of polysaccharides, proteins and nucleic acids that provide a safe and stable environment. The exopolysaccharides synthesized by *P. aeruginosa* are *Pel*, *Psl*, and alginate of which the latter in particular can protect the bacteria from antibiotics and therefore increase their resistance against many drugs (Harmsen *et al.* 2010). Similar to the attachment and microcolony formation, the expression of genes encoding for the production of the EPS matrix is correlated to the intracellular concentration of c-di-GMP (Lee *et al.* 2007, Lory *et al.* 2009).

In order to execute the individual steps of biofilm formation, *P. aeruginosa* utilizes quorum sensing. Quorum sensing is a form of cell-to-cell communication leading to induced or repressed gene expression depending on the bacteria's environment and cell density. The three systems known in *P. aeruginosa* are the *Las*, the *Rhl*, and the *Pqs* system. Only the interplay of these systems leads to the production of the right quantity of proteins at the right time and the consequent development of the biofilm (Fuqua *et al.* 1994, Juhas *et al.* 2005) (Figure 1 A).

Bacterial cells in a matured biofilm matrix can detach and may colonize a surface in another location. This can either occur when part of the biofilm has broken off in a flow (e.g. in vascular catheters) or when planktonic bacteria are released deliberately from the biofilm (Kim *et al.* 2016) (Figure 1 B). This is one of the major problems with *P. aeruginosa* infections that include the formation of biofilms. The constant detachment and dispersal of planktonic bacteria can lead to severe

bloodstream infections and the expansion of the infection to various parts of the body.

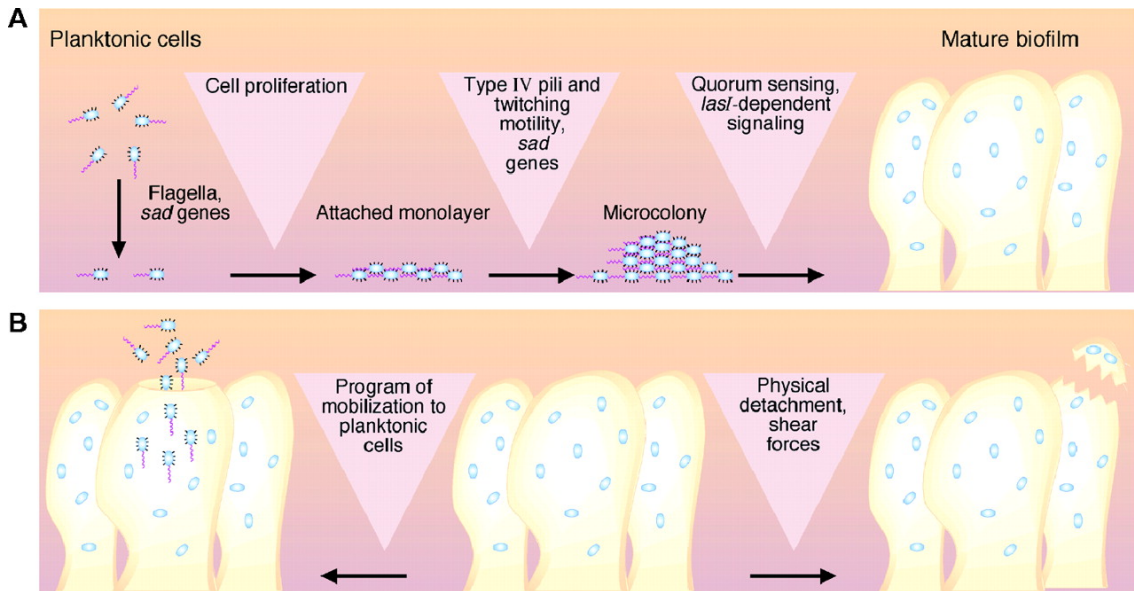


**Figure 1: Schematically illustrated mechanism of biofilm development.** (Costerton *et al.* 1999)

One of the most important reasons why the formation of biofilms leads to persistent infections is that bacteria in a biofilm have the ability to withstand antimicrobial treatment and to evade the host's immune system (Rybtke *et al.* 2015). Regulated by quorum sensing, *P. aeruginosa* release an abundance of proteins and nucleic acids in a biofilm to protect them against specific antibiotics and lead to necrosis of polymorphonuclear neutrophils (Jensen *et al.* 2007, Rybtke *et al.* 2015). Furthermore, distinct subpopulations in the cluster of bacteria can persist as dormant cells. This is a reaction of the bacteria to difficult environmental conditions resulting in growth arrest and adapted gene expression, therefore making the bacteria less vulnerable to oxidant stress induced by either antibiotic drugs or the immune system (Pamp *et al.* 2008, Nguyen *et al.* 2011). Hence, *P. aeruginosa* infections with biofilm formation are a concern in hospitals and difficult to treat. Further investigations into whether some strains are particularly prone to biofilm formation could contribute to a better understanding of the underlying mechanisms and could help in the clinical management of these persistent *P. aeruginosa* infections.

## 1.4 Virulence

Virulence is the ability of a pathogen to infect an organism and to cause a certain degree of disease. In contrast to the expression “pathogenicity” (which is the absolute ability to produce a disease), “virulence” is a quantitative term describing the severity of an infection (Steinhaus *et al.* 1970, Shapiro-Ilan *et al.* 2005). The production of virulence factors is a survival strategy for bacteria to obtain nutritional resources from the host and to escape the host’s immune system. These factors can be secreted proteins, including toxins and proteases or cell-associated structures like LPS.

*P. aeruginosa* produces a variety of virulence factors. The most important ones being the effector proteins of the type III secretion system (*ExoS*, *ExoT*, *ExoU*, *ExoY*), which are exotoxins that are transported directly into the host cells via a needle-like apparatus (Hauser 2009). Furthermore, it produces cytotoxic exotoxins pyocyanin and exotoxin A, the siderophore pyoverdine, the cytotoxic phospholipase C *PlcB*, and a vast amount of proteases (Moradali *et al.* 2017). Moreover, a polysaccharide region integrated into the lipid A moiety of the LPS known as the O antigen is highly associated with virulence of the bacteria (Cryz *et al.* 1984, Tang *et al.* 1996). These antigens are recognized by macrophages, leading to excessive secretion of interleukins and cytokines. As a result, *P. aeruginosa* overstimulate the host’s immune system, which can cause a septic shock and even lead to death (Rocchetta *et al.* 1999).

Similar to biofilm formation, the production of most of these factors depend on quorum sensing systems (see 1.3) and stress responses (Passador *et al.* 1993, Jimenez *et al.* 2012, Francis *et al.* 2017).

Apart from these proteins and polysaccharides having a direct impact on the severity of the disease, there are also other characteristics in *P. aeruginosa* that can increase the level of virulence. These involve the ability to persist in the host, what is achieved e.g. by the formation of biofilms, to spread in the host and the environment, and to evade the immune system (Francis *et al.* 2017, Moradali *et al.* 2017).

The extent of production of all these factors and the associated degree of virulence is multifactorial and may vary from one strain to the other (Lee *et al.*

2006). Thus, it is still difficult to estimate the outcome of an infection with *P. aeruginosa*. Elucidating connections in the evolution of virulence during an infection and finding biomarkers that are associated with the level of virulence could be key to better predict the severity of the disease and could therefore optimize the treatment of the infection.

### **1.5 Antimicrobial resistance**

Finding the optimal antimicrobial therapy against *P. aeruginosa* in particular represents a substantial challenge in modern health care. This is primarily due to the increasing number of multi-drug-resistant (MDR) strains (Lister *et al.* 2009). According to the ECDC and the Centers for Disease Control and Prevention (CDC), MDR is defined as non-susceptible to one or more antibiotics in at least three antimicrobial categories usually effective against the bacterium. Extensively-drug-resistant (XDR) is defined as non-susceptible to at least one agent in all but two antimicrobial categories, and pan-drug-resistant (PDR) as non-susceptible to all antibiotic drugs (Magiorakos *et al.* 2012).

One reason for multi-drug resistance in *P. aeruginosa* is its high intrinsic resistance against a wide range of  $\beta$ -lactam antibiotics including cephalosporins, glycopeptides and macrolides due to its low permeability of the cell wall, efflux pumps and chromosomally encoded  $\beta$ -lactamases like *ampC* (Lambert 2002, Santajit *et al.* 2016). Moreover, multi-drug resistance in *P. aeruginosa* can arise because of its genetic capacity to express multiple resistance mechanisms, to import resistance genes from other organisms like carbapenemases or the predisposition for chromosomal mutations (Lambert 2002, Santajit *et al.* 2016). Furthermore, a major problem with *P. aeruginosa* is that this acquired resistance to multiple classes of antibiotic drugs can even occur within the treatment of the infection (Noteboom *et al.* 2015). In addition, mortality for patients suffering from bloodstream infections (especially nosocomial infections acquired in intensive care units (ICU)) with MDR strains is up to 2 times higher than for patients with non-MDR strains (Tumbarello *et al.* 2011).

This is why *P. aeruginosa* was listed as one of the pathogens with critical priority for further research and development of novel antibiotics by the WHO (World Health Organization) (Tacconelli *et al.* 2018).

### 1.6 Colistin as last-resort antibiotic

As a result of the rise in MDR- and XDR-*P. aeruginosa* related infections (Buhl *et al.* 2015) and the lack of novel antimicrobial agents (Livermore 2004), antibiotics that had previously almost disappeared from the market had to be used more frequently in recent years. One of them is colistin (Levin *et al.* 1999, Falagas *et al.* 2005).

Colistin belongs to the group of polymyxins which are branched, cationic, cyclic decapeptides linked to a fatty acid residue, in the case of colistin via an  $\alpha$ -amide linkage, originally produced by *Bacillus polymyxa* (Katz *et al.* 1977) (Figure 2).

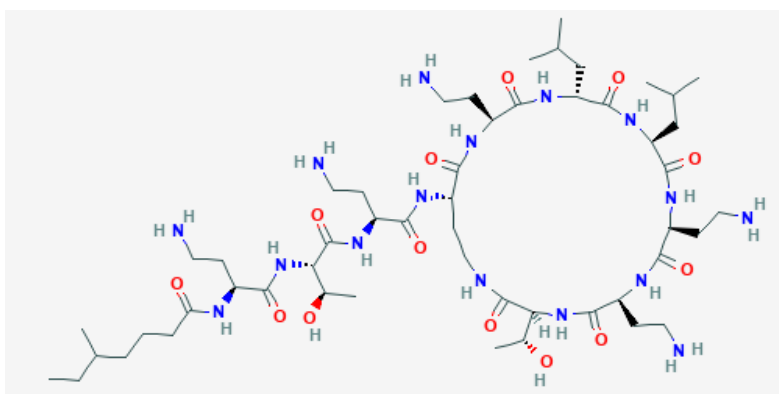


**Figure 2: Chemical structure of colistin.** National Center for Biotechnology Information. PubChem Database. Colistin, CID=5311054, <https://pubchem.ncbi.nlm.nih.gov/compound/Colistin> (accessed on Aug. 26, 2019)

Out of that antibiotic family, polymyxin B and polymyxin E (colistin) are currently the only agents used in clinical settings because of their lower toxicity to eukaryotic cells. They have broad bactericidal activity against Gram-negative pathogens but much less against Gram-positive bacteria. Colistin binds to the outer membrane by electrostatic interactions between the cationic peptide and the anionic LPS membrane of Gram-negative bacteria and hydrophobic interactions between the peptide fatty acid and the membrane. Colistin is able to displace magnesium- and calcium ions from the membrane lipids which leads to

a disturbed LPS envelope and an increased permeability of the outer and cytoplasmic membrane. These interactions cause a leakage of cytoplasmic material of the bacteria which in the end results in cell death (Storm *et al.* 1977). The use of colistin was abandoned mainly because of dose-dependent adverse reactions like nephrotoxicity and neurotoxicity (Falagas *et al.* 2005). However, recent studies show that especially nephrotoxicity might be a less frequent effect than expected (Katz *et al.* 2016). Despite the poor knowledge on its pharmacokinetics, pharmacodynamics and toxicodynamics, colistin still displays an important alternative or even last effective antimicrobial agent against MDR or XDR *P. aeruginosa* (Li *et al.* 2006).

### **1.6.1 Colistin-resistance**

Unfortunately, the inadequate use of colistin as antimicrobial drug may have led to the current situation of emerging colistin-resistant Gram-negative pathogens that leave clinicians with limited or even no treatment options (Antoniadou *et al.* 2007). Resistance against colistin in *P. aeruginosa* can occur through chromosomal alterations of the outer LPS membrane. By addition of 4-amino-4-deoxy-L-arabinose (L-Ara4N) to the lipid A moiety, the hydrophobic anchor of the LPS, the net negative charge of the outer membrane is reduced thereby limiting the interaction of colistin as a cationic antimicrobial peptide (Raetz *et al.* 2007, Fernández *et al.* 2010, Lee *et al.* 2016). This action is induced by several two-component regulators that can directly promote the transcription of the *arnBCADTEF*, a LPS modification operon (McPhee *et al.* 2003). There are currently five of these two-component regulators being involved in colistin-resistance in *P. aeruginosa*: *pmrA/pmrB*, *phoP/phoQ*, *parR/parS*, *colR/colS* and *cprR/cprS* (Olaitan *et al.* 2014). *PmrB/pmrA* and *phoP/phoQ* usually respond to limited magnesium concentrations but are also likely to mutate especially under exposure to low colistin concentrations resulting in overexpression of genes on the *arnBCADTEF* operon and thus colistin-resistance (Macfarlane *et al.* 2000, MCPhee *et al.* 2003, Moskowitz *et al.* 2012, Lee *et al.* 2014). Moreover, mutations in *parR/parS*, *colR/colS* and *cprR/cprS* also occur particularly under subinhibitory concentrations of colistin and lead to extended resistance against polymyxins.



These mutations are considered to have direct impact on the modification of lipid A by L-Ara4N through upregulation of the *arnBCADTEF* operon as well as an enhanced activation of the *pmrB/pmrA* and *phoP/phoQ* regulators (Fernández *et al.* 2010, Muller *et al.* 2011, Fernández *et al.* 2012, Gutu *et al.* 2013).

Apart from chromosomal mutations, plasmid-mediated colistin-resistance has been described first in *Escherichia coli* isolated from farm animals: The acquisition of the *mcr-1* plasmid through bacterial conjugation was the first mechanism of transmitted resistance against polymyxins (Liu *et al.* 2016). Nevertheless, the emergence *mcr-1* in other Gram-negative bacteria including *P. aeruginosa* suggest the problem of spreading colistin-resistance to a clinical setting (Liu *et al.* 2016, Caselli *et al.* 2018). Furthermore, this enhances the risk of transferring colistin-resistance from one patient to another in the hospital (Liu *et al.* 2016, Caselli *et al.* 2018). Similar to most chromosomal mutations, activation of the plasmid leads to modifications of lipid A as a binding site for colistin. In this case, *mcr-1* causes the addition of phosphoethanolamine (PEtN) to the lipid A moiety (Liu *et al.* 2017).

Thus, correlations between specific mutations in the regulator systems or plasmids and resistance to colistin have been found. In addition, these mutations lead to alterations in the structure of the LPS in the membrane of *P. aeruginosa*. Those modifications might have a significant impact on phenotypic qualities of the bacteria such as biofilm formation or virulence. These bacterial characteristics in particular are highly dependent on the composition of the LPS in the outer membrane and can influence the dynamics and the outcome of an infection with the pathogen (see 1.3 and 1.4). However, the mutations resulting in colistin resistance did not seem to be consistent or similar in different *P. aeruginosa* strains and the exact processes are still not fully understood (Lee *et al.* 2014). Particularly, the evolutionary dynamics of acquired resistance and the presumably associated phenotypical evolution under antibiotic stress, which may have an effect on a different approach to clinical treatment, is yet to be investigated.

## 1.7 Combination with metronidazole

Metronidazole is the most commonly used antimicrobial drug from the group of nitroimidazoles (Figure 3). It was initially discovered in the 1950s as a product of *Streptomyces spp.* (Maeda *et al.* 1953, Dingsdag *et al.* 2017). After its original purpose as a treatment against *Trichomonas vaginalis* metronidazole is still used effectively against anaerobes, microaerophiles, and protozoa but not against aerobic bacteria (Shinn 1962, Tally *et al.* 1972, Dingsdag *et al.* 2017).

Metronidazole acts as a prodrug, which means the molecule has to be activated at its target site in order to exert an effect against the bacteria. The activation is carried out by reduction of the nitro group through cleavage of the imidazole ring. This process on the one hand results in the formation of cytotoxic derivatives. On the other hand, the reaction produces nitro-radicals which themselves react with oxygen. The oxygen radicals that emerge from that reaction as well as cytotoxic derivatives cause DNA strand breaks and DNA destabilization (Müller 1986). However, the reductive activation of metronidazole usually only happens through the enzyme pyruvate ferredoxin oxidoreductase which is expressed obligately in anaerobes explaining the lower effect on aerobic bacteria (Edwards 1986, Tocher *et al.* 1988, Tocher *et al.* 1992).

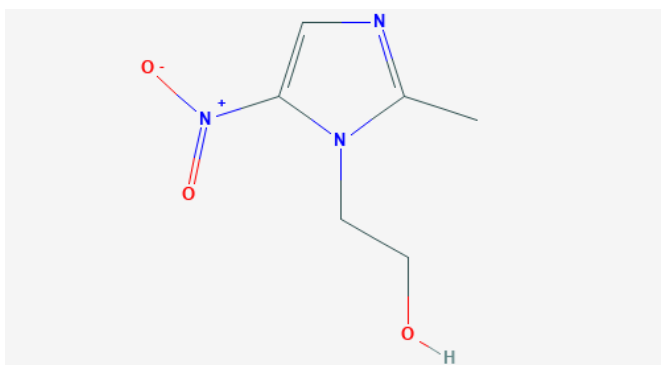


**Figure 3: Chemical structure of metronidazole.** National Center for Biotechnology Information. PubChem Database. Metronidazole, CID=4173, <https://pubchem.ncbi.nlm.nih.gov/compound/Metronidazole> (accessed on Aug. 29, 2019)

Anaerobic bacteria can cause a variety of infections including central nervous system-, skin-, upper respiratory tract-, genital- and intraabdominal-infections. Metronidazole is the first-choice therapy for intracranial and intraabdominal infections (especially *Clostridium difficile* infections) and can also be applied for most other infections caused by anaerobes (Miller 2007, Brook 2016). It is also part of the triple or quadruple therapy against *Helicobacter pylori* next to a proton-pump inhibitor, clarithromycin and/or amoxicillin (Löfmark *et al.* 2010). Moreover, metronidazole is commonly used as a prophylaxis prior to gastrointestinal or head and neck surgeries mostly in combination with a cephalosporin or an aminoglycoside (Freeman *et al.* 1997, Giske *et al.* 2017).

Thus, due to colistin`s wide range of applications, patients having a *P. aeruginosa* infection treated with colistin may also need metronidazole because of a second infection with anaerobic bacteria or for prophylaxis.

In previous studies it has been shown that a combination therapy of ciprofloxacin or amikacin with metronidazole contributes to the emergence of resistance to ciprofloxacin or amikacin in *P. aeruginosa*. This phenomenon can be attributed to the induction of the SOS response in the bacteria by metronidazole (Hocquet *et al.* 2013). The SOS response is a coordinated, induced, cellular response to DNA damage leading to DNA repair, inhibition of cell division and prophage induction, regulated by *recA* and *lexA* gene products (Radman 1975). *LexA* is a repressor of the genes responsible for the SOS response. This transcription repressor is cleaved and inactivated by the *recA* protein, which is induced by single strand DNA segments or inhibition of replication in general (Little *et al.* 1982). After activation, polymerases and repair proteins, that are encoded on the SOS response genes, start the DNA repair. In addition, the SOS response reduces the cell metabolism of the bacteria making them less vulnerable to antibiotics. However, the repair mechanisms are highly error-prone leading to mutations, which enable the bacteria to persist and develop resistance in a short period of time (Cirz *et al.* 2006). Despite the lack of antimicrobial effects of metronidazole against *P. aeruginosa* the DNA strand breakage triggered by the antibiotic drug can cause an activation of the SOS response (Hocquet *et al.* 2013).

However, it is not known whether the induction of the SOS response by metronidazole could also accelerate the development of resistance against other antimicrobial drugs like colistin in *P. aeruginosa*.

### 1.8 Morbidostat

The morbidostat is a culture device that continuously pressures the bacteria with constantly increasing antibiotic drug concentrations. It can automatically adapt the used drug concentration to the growth rate of the liquid bacterial culture (Toprak *et al.* 2011). Beforehand, culture devices were not able to guarantee a constant selection pressure with similar conditions over a long period of time. Thus, in comparison to other culture devices the morbidostat allows a cultivation at a consistent growth rate while still challenging the bacteria at the same time (Rosenthal *et al.* 2011) (Figure 4).

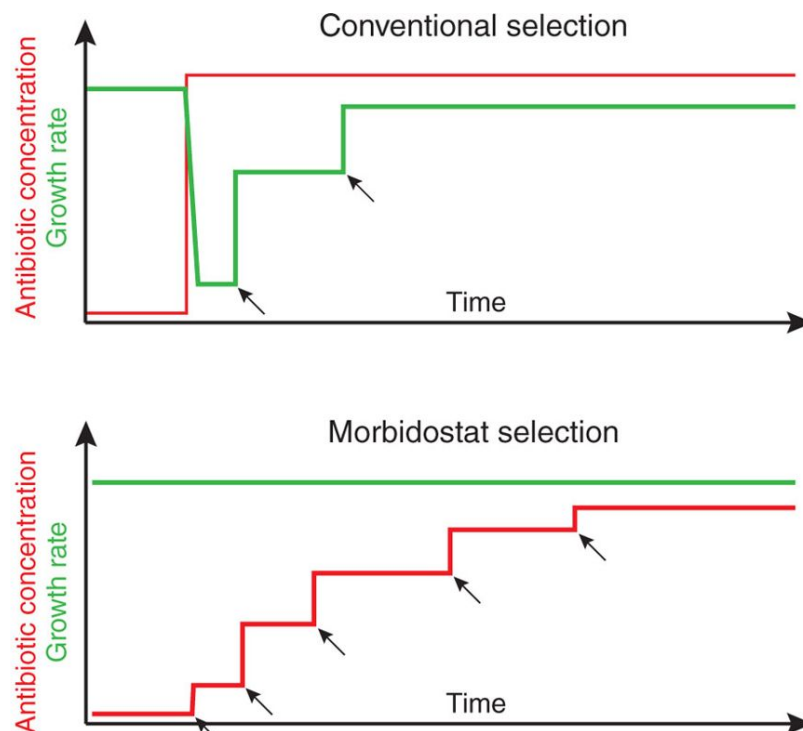


**Figure 4: Comparison of conventional culture devices to morbidostat culture.** Conventional antibiotic selection is performed by adding high antibiotic pressure. This initially reduces the growth rate until resistance emerges and the bacterial population regains growth. In the morbidostat the bacterial growth rate is maintained constant with automatically adjusted antibiotic concentrations. Black arrows indicate alterations in the bacterial culture leading to higher antibiotic resistance. (Rosenthal *et al.* 2011)

This applied selection pressure forces the bacteria to quickly evolve and develop resistance against the antibiotic drug (Toprak *et al.* 2011). Such a construction can simulate a medical situation in which the antibiotic concentration in the body does not reach the lethal dosage required to eliminate the source of infection. The exposure to these sublethal antibiotic concentrations are then likely to result in the evolution of antibiotic resistance (Andersson *et al.* 2014).

By tracing the distinct steps of acquired resistance it is possible to further investigate the associated phenotypic evolution. Hence, the morbidostat setup is ideal for the examination of evolutionary pathways.

Previously, our group was able to perform a morbidostat run using colistin against clinical *P. aeruginosa* isolates from bloodstream infections. Colistin resistance increased up to 100-fold within 20 days in the morbidostat. Sequencing of the morbidostat derived strains revealed that mutations leading to colistin resistance frequently occurred in genes involved in the modulation of L-Ara4N including mutations in *pmrA/pmrB*. Thus, mutations that result in colistin resistance in *P. aeruginosa* acquired in the morbidostat culture device are very similar to those found in colistin resistant clinical isolates (Dößelmann *et al.* 2017).

## 1.9 Objective of this study

The aim of this study is to investigate the connection between the evolution towards antibiotic resistance against colistin and phenotypical changes in biofilm formation and virulence in *P. aeruginosa*.

Colistin is a last resort antibiotic against *P. aeruginosa* interacting with the bacterial cell wall (Storm *et al.* 1977, Falagas *et al.* 2005). Alterations in the composition of the lipid A moiety limit the interaction of colistin with the outer membrane of the bacteria resulting in antibiotic resistance (Raetz *et al.* 2007, Fernández *et al.* 2010, Lee *et al.* 2016). It is still unknown, whether these mutations would also lead to phenotypical changes that also depend on the LPS structure of the outer membrane, such as biofilm formation and virulence.

Moreover, evolution towards colistin resistance as well as the phenotypical changes in *P. aeruginosa* might be enhanced by a combination therapy with metronidazole, a drug presumably increasing the mutation frequency in the bacteria (Cirz *et al.* 2006, Hocquet *et al.* 2013).

To further investigate these relationships, a morbidostat is the ideal culture device to develop colistin resistant *P. aeruginosa* strains under the exposure to different antibiotic compositions: plain colistin, colistin with the addition of metronidazole and pure metronidazole as a control. With these generated resistant and non-resistant strains, it is subsequently possible to explore their phenotypic characteristics for alterations in their ability to form biofilm and in their virulence. Thus, this setup allows the performance of phenotypic assays for different stages of the evolution towards colistin resistance.

Investigating these evolutionary pathways may help predict the development of resistance and assess the clinical impact of an infection after such evolution.

## 2 Material & Methods

### 2.1 Material

#### 2.1.1 Laboratory equipment

Device	Manufacturer
BioPhotometer® D30	Eppendorf (Hamburg, Germany)
Centrifuge 5415 R	Eppendorf (Hamburg, Germany)
Clean Bench – Maxisafe 2020	Thermo Scientific (Waltham, USA)
Incubator – Hera Therm	Thermo Scientific (Waltham, USA)
Shaking incubator – Innova-44	New Brunswick Scientific (Edison, USA)
Epoch2 microplate reader	BioTek (Vermont, USA)
Spectrophotometer CLARIOstar plate reader	BMG Labtech (Ortenberg, Germany)
Vortex-shaker	VWR International GmbH (Radnor, USA)
RS-RD10 Rocking table	Phoenix Instrument (Garbsen, Germany)
Sonorex™ RK100 ultrasonic bath	Bandelin (Berlin, Germany)
Eddy Jet 2 spiral plater	IUL Instruments (Barcelona, Spain)
Flash & Go colony counter	IUL Instruments (Barcelona, Spain)
Ultrapure water system – PureLab Chorus	ELGA LabWater (Lane End, UK)
Morbidosat	Built by Richard Neher (Biozentrum Basel)

### 2.1.2 Plastic devices

Device	Manufacturer
Falcon tubes (15 ml, 50 ml)	Corning (Corning, USA)
Eppendorf tubes (1.5 ml, 2 ml)	Eppendorf (Hamburg, Germany)
Petri dishes	Sarstedt AG (Nümbrecht, Germany)
96-well plate U-bottom	Greiner (Kremsmünster, Austria)
96-well plate flat-bottom	Greiner (Kremsmünster, Austria)
96-well plate	Corning (Corning, USA)
48-well plate	Corning (Corning, USA)
Nunc-Immuno™ TSP Lids, MaxiSorp™ nontreated	Thermo Scientific (Waltham, US)
Nunc MicroWell™ 96-well MaxiSorp™ flat bottom plates	Thermo Scientific (Waltham, US)
2.5 l Anaerobic jar	Merck (Darmstadt, Germany)

### 2.1.3 Bacterial strains

Species	Strain	Characteristics	Reference
<i>P. aeruginosa</i>	PA77	Clinical isolate	Diagnostics
<i>P. aeruginosa</i>	PA83	Clinical isolate	Diagnostics
<i>P. aeruginosa</i>	ID4	Clinical isolate	VARPA study (Willmann <i>et al.</i> 2018)
<i>P. aeruginosa</i>	ID21	Clinical isolate	VARPA study (Willmann <i>et al.</i> 2018)
<i>P. aeruginosa</i>	ID40	Clinical isolate	VARPA study (Willmann <i>et al.</i> 2018)



### 2.1.4 Antibiotics

Antibiotic	Manufacturer	Stock solution	Solvent
Colistin	Fagron GmbH (Rotterdam, Netherlands)	10 mg/ml	Sterile, distilled water
Metronidazole	Braun (Melsungen, Germany)	5 mg/ml	Sterile, distilled water
Vancomycin	Hikma Pharma (Terrugem, Portugal)	0.04 mg/ml (1g of powder in 25ml of solvent)	Sterile, distilled water

### 2.1.5 Chemicals

Chemical	Concentration	Manufacturer
Acetic acid	5 %	Sigma-Aldrich (St. Louis, USA)
Crystal violet	0.1 %	Sigma-Aldrich (St. Louis, USA)
Ethanol	80 %	VWR Chemicals (Radnor, USA)
Glucose		Merck (Darmstadt, Germany)
Phosphate buffered saline (PBS)	1 M	Carl Roth (Karlsruhe, Germany)
Anaerocult A		Merck (Darmstadt, Germany)
H <sub>2</sub> O <sub>bidest</sub>		
Poly-L-Lysin solution	0.1 % (w/v) in H <sub>2</sub> O	Sigma-Aldrich (St. Louis, USA)
Ethylenediaminetetraacetic acid (EDTA)	0.1 M from 0.5 M Stock	Carl Roth (Karlsruhe, Germany)

3-[(3-Cholamidopropyl) dimethylammonio]-1-propanesulfonate (CHAPS)	0.1 M solubilized in ultrapure water, stored at -8°C	Sigma-Aldrich (St. Louis, USA)
Sodium hypochlorite	3 %	Merck (Darmstadt, Germany)

### 2.1.6 Growth media for bacterial cultivation

The Lysogeny Broth (LB) medium for bacterial growth was prepared using deionized water (dH<sub>2</sub>O), then autoclaved at 121°C and 2.1 bar and stored at room temperature. Solid Tryptic Soy Broth (TSB) agar plates (TSA) were prepared by adding 15 g agar to 1 l of liquid medium. For TSA plates with 5% sheep blood 50 ml of sterile, defibrinated sheep blood and 15 g agar was mixed with 1 l of TSB medium. After autoclaving and cooling, media were poured into Petri dishes. For antibiotic agar plates 0.2 ml, 0.8 ml, 1.6 ml, 3.2 ml or 6.4 ml out of the 10 mg/ml colistin stock solution was added to the medium before pouring out. Plates were stored at 4°C.

Medium	Composition
LB-Medium (Lennox) (Carl Roth, Karlsruhe, Germany)	40 g 1 l dH <sub>2</sub> O
TSB (Thermo Scientific, Waltham, USA)	30 g 1 l dH <sub>2</sub> O
TSB 5 % sheep blood (Thermo Scientific, Waltham, USA)	100ml sheep blood 30 g TSB, 1l dH <sub>2</sub> O
Mueller Hinton II Broth (Cation-Adjusted) (CAMHB) (Thermo Scientific, Waltham, USA)	21 g 1 l dH <sub>2</sub> O

### 2.1.7 Animals

*Galleria mellonella* larvae

Bio Systems Technology | **TruLarv™**  
(Exeter, UK)

### 2.1.8 Others

Device	Manufacturer
Microbanks	Bestbion dx (Köln, Germany)
500 µl Instrumental Syringe	Hamilton (Bonaduz, Switzerland)
PB600-1 Repeating Dispenser	Hamilton (Bonaduz, Switzerland)
Sterican® 27G x 3/4, Gr. 20 disposable hypodermic needle	Braun (Melsungen, Germany)
PTFE coated stirring magnets	Neolab (Heidelberg, Germany)

## 2.2 Bacterial strains

The five baseline strains (PA77, PA83, ID4, ID21, ID40) used in this study are clinical isolates from patients with *P. aeruginosa* bloodstream infections. The species were identified using MALDI-TOF MS (Bruker, Billerica, USA) and the VITEK 2 (bioMérieux, Marcy-l'Étoile, France) system. Later, the isolates were screened for their resistance status by conducting a standard diagnostic Etest for the most common antibiotics used against *P. aeruginosa*. Etests were analysed in the diagnostics laboratory according to the manufacturer's guidelines (bioMérieux, Marcy-l'Étoile, France) and resistance against multiple antibiotics was evaluated by EUCAST (European Committee On Antimicrobial Susceptibility Testing) standards (EUCAST 2019). All five baseline strains showed MDR antibiotic resistance with all of them being susceptible to colistin.

## 2.3 Morbidostat

### 2.3.1 General principal

The construction of the morbidostat was previously set up by Richard Neher and colleagues as described in (Döbelmann *et al.* 2017) and ready to use. Each strain was inoculated in three vials with 20 ml of LB as growth medium. Vial number one was connected to two bottles containing either 50 µg/ml of colistin which is 25-times higher than its previous minimal inhibitory concentration (MIC) or later

100 µg/ml of colistin which is equal to 50x MIC. The second vial was connected to the same colistin bottles as well as to a 50 µg/ml solution of metronidazole. The last vial was only connected to the metronidazole solution. The bacterial liquid cultures were placed in an incubator and constantly kept at 37°C.

The morbidostat measures the optical density of the bacterial cultures in each vials every 30 seconds. Out of this data it calculates the growth rate of the bacteria every 10 minutes and depending on this it adds either pure medium to stimulate the growth, or one of the colistin solutions to inhibit the growth. The growth rate was set to doubling time of 90 minutes and a target optical density (OD) at 600nm of 0.1.

Thus, the bacteria were constantly exposed to sublethal antibiotic concentrations which stimulated the development of resistance against these antibiotics.

Given that setup, all of the five clinical isolates of *P. aeruginosa* were exposed to three different conditions over the time period of 21 days: these are colistin only, a colistin-metronidazole combination, and metronidazole only. A small magnet was included in each vial, and all vials placed on a magnetic stirrer in order to avoid biofilm from forming in the vial.

A 16-channel peristaltic pump was set up to remove all surplus liquid and waste from the vials. The waste was stored in a jerrycan, inactivated with Sekusept™PLUS (Ecolab, St. Paul, USA) and autoclaved before dumping it.

Two independent morbidostat runs were completed as described above. Samples were taken three times a week, resulting in a large number of strains with different levels of resistance against colistin.

### **2.3.2 Control run using LB medium**

A morbidostat run over a time period of three weeks as previously stated was performed with only LB medium as basis for cultivation without the addition of any antibiotic drugs. In this case, bacterial solutions grew very fast and could only be diluted with the LB medium by the morbidostat. This was performed as a negative control, and in order to measure the effect of the morbidostat setup on the strains.

### **2.3.3 Sample collection**

Samples were taken every two to three days. Therefore, 1 ml of the bacterial cultures from every vial was transferred to a Microbank™. After mixing with the beads, all liquid was removed and the Microbanks™ were stored at -80°C. For purity control approximately 1 µl of the bacterial culture was streaked out on a blood agar plate and grown overnight at 37°C.

A problem in this setup could be the collection of dormant cells that sustain antibiotic susceptibility even under high colistin concentrations. Such cells could subsequently overgrow the metabolically active but antibiotic resistant bacteria. Thus, an alternative method was employed for the second run: The cultures of the morbidostat were streaked out on TSA blood plates containing various concentrations of colistin (2 mg/l, 8 mg/l, 16 mg/l, 32 mg/l or 64 mg/l) and incubated overnight. Then, one colony from the colistin plate was picked and grown overnight on a plain TSA blood plate. These colonies were then transferred to the Microbanks™ and frozen as described above.

To resume the morbidostat run after sample collection and to ensure the same population was used for inoculation each time, sterile vials with 19 ml of fresh LB medium were reinoculated with 1 ml of the continuous bacterial culture and reconnected to the vial lids of the morbidostat again.

### **2.3.4 Cleaning**

After every run of 21 days the morbidostat was completely cleaned with disinfectants and the vials were autoclaved. The optimum method to get rid of remaining bacteria and potential biofilm in the tubes was to flush them out with different chemical agents: 80 % ethanol, 3 % sodium hypochlorite and Vancomycin (40 mg/l). The hygiene procedures were discussed with the hospital infection control director beforehand.

## **2.4 Cultivation of bacteria**

To grow liquid cultures from the Microbanks™ generated from the first morbidostat run and the medium run, 1-3 beads were given to 10-15 ml of LB

medium in a sterile Erlenmeyer flask and incubated overnight at 37°C and 140 rpm in a shaking incubator.

To further ensure the purity of the resistant population and to avoid the persistence of dormant bacteria, another method was implemented. For the second morbidostat run, one Microbanks™-bead was streaked onto a TSA blood agar plate with different concentrations of colistin solution (between 2 mg/l and 32 mg/l) depending on their MIC or plain TSA blood agar plates in case of strains from the metronidazole conditions and incubated overnight at 37°C. Consequently, before executing one of the phenotypic assays, colonies of these TSA blood plates had to be picked using a cotton swap, and the bacteria were dissolved into a solution of LB medium or PBS, depending on the assay's standards.

## **2.5 Susceptibility tests**

Each strain was tested for the level of colistin-resistance using broth microdilution (BMD) and Micronaut-S. The Micronaut-S is a repeatable standardized commercial BMD method which was used according to the manufacturer's instruction (MERLIN Diagnostika GmbH, Bornheim, Germany). Its detection of resistance levels is comparable to the gold standard BMD, but with some weakness for strains with low resistance as reported by Javed *et al.* (Javed *et al.* 2018).

BMDs were performed according to ISO 20776-1 standard. A colistin stock solution was diluted to a variety of concentrations from 128 µg/ml to 0.125 µg/ml with Mueller-Hinton Broth (CAMHB). 50 µl of each concentration was added in 96-well microtiter plate wells in an ascending sequence, except for one row of wells as positive control. Next, the bacterial inocula were adjusted to an OD 0.1 at 625 nm wavelength, and further diluted by the factor 1:60 (33.3 µl of inoculum added into an Eppendorf tube with 2 ml of CAMHB). 50 µl of this dilution were then added to each of the wells, except a row of three wells as negative control, and incubated at 37°C for 18 h. The minimal inhibitory concentration (MIC) is the lowest concentration that completely inhibits visual bacterial growth. The BMDs

were performed in triplicates for each strain and the mean was considered as the final MIC value.

According to EUCAST guidelines, the MIC for “colistin-susceptible” was defined to be  $\leq 2$   $\mu\text{g/ml}$ , with *P. aeruginosa* strain ATCC 27853 being the control and reference strain (EUCAST 2019).

## **2.6 Biofilm formation**

### **2.6.1 Principle of assay**

To assess the ability of *P. aeruginosa* strains to adhere to a surface and form a biofilm at different time points during the morbidostat run, two different methods were used. The first method quantifies the mass of cells in the biofilm in the wells of a Microtiter plate by staining the biofilm matrix and the cell walls with crystal violet.

The other method uses a transferable 96-peg solid phase plate (TSP) lid that fits into the wells of a 96-well plate. This allows the biofilm to grow on the pegs and quantify the number of viable cells in the biofilm by counting the colony forming units (CFU) after removing the adherent cells from the pegs.

### **2.6.2 Crystal violet staining method**

This assay was performed following the protocol “O’Toole, G. A. Microtiter Dish Biofilm Formation Assay. *J. Vis. Exp.* (47), e2437, doi:10.3791/2437 (2011)” (O’Toole 2011).

Liquid cultures or blood agar plates of the strains were prepared as described above. The overnight liquid cultures were then diluted to an  $\text{OD}_{600\text{nm}}$  of 0.1 in LB medium, whereas for bacterial cultures grown on colistin blood agar plates first some colonies had to be picked with a cotton swab, dissolved in fresh LB medium and diluted to an  $\text{OD}_{600\text{nm}}$  of 0.1. Then, 100  $\mu\text{l}$  of each dilution was added to the wells of a round-bottom 96-well plate in triplicates. The 96-well plate was covered and incubated at 37°C for 24 h. As a negative control and to indicate the background staining, three wells were filled with LB medium without any bacteria.

Then, planktonic bacteria were removed out of the wells by shaking out the plate, rinsing the wells with water, and drying the plate until no liquid remained in the wells. Next, all wells were stained with 125  $\mu$ l of 0.1 % crystal violet for 10 min at room temperature. After removing the crystal violet, the wells were rinsed three to four times by submerging the 96-well plate in water and shaking it out until no excess stain was left. The plate was left to dry for 3-5 hours before dissolving the biofilm-bound crystal violet by adding 200  $\mu$ l of 5 % acetic acid to the wells. To mix the acetic acid with the crystal violet, the solution was resuspended 2-3 times and incubated for 10 min at room temperature.

After transferring 125  $\mu$ l of the solution to a clean flat-bottom 96-well plate the absorbance was read at OD<sub>600nm</sub>. Nevertheless, the raw data of absorbance were not suitable for the comparability between the experiments, especially to evaluate significance between the morbidostat-derived strains and medium run strains or baseline isolates. Therefore, we calculated the ratios for all morbidostat-derived strains compared to their baseline isolate. Subsequently, the calculated values of the morbidostat-derived strains with antibiotic exposure were put in relation to the calculated values of medium run strains corresponding to the same day, giving us the final ratio used for the analysis.

Each assay was performed three times in triplicates. Statistical analysis of the ratios was implemented between values from the same condition and the same days of a morbidostat run performing a two-tailed, unpaired t-test using GraphPad Prism 7 (GraphPad Software, Sun Diego, USA).

### **2.6.3 Peg-lid method biofilm assay**

The *Nunc-Immuno*<sup>™</sup> transferable 96-peg solid phase plate (TSP) lid was dipped into a 0.1 % Poly-L-lysine solution at 37°C for 30 min. Coating the pegs in Poly-L-lysine helps the bacteria to attach to the surface in the first place and to keep the biofilm stabilized on the pegs.

Liquid cultures or blood agar plates of the strains were prepared as described in 2.6.2. After that, 150  $\mu$ l of each dilution was added to the wells of a Nunc MicroWell<sup>™</sup> 96-well MaxiSorp<sup>™</sup> flat bottom plate in triplicates and the prepared TSP was put on top so that the pegs were immersed into the bacterial solution.



As a negative control three wells were filled with only LB medium. The plate was incubated at 37°C for 2 h allowing the bacteria to adhere to the pegs. Then the TSP was removed from the liquid culture, washed with PBS, and transferred to a new Nunc MicroWell™ 96-well MaxiSorp™ flat bottom plate with 200 µl of fresh LB medium. The plate was incubated at 37°C for 48 h under anaerobic conditions, allowing the formation of biofilm on the pegs. Anaerobic conditions were created using a 2.5 l anaerobic jar with Anaerocult® A by pouring 35 ml of water on top of the Anaerocult® A and putting it along with the plate inside the anaerobic jar and sealing the jar immediately.

Next, the TSP was removed from the bacterial solution again, washed with PBS, transferred to a Nunc MicroWell™ 96-well MaxiSorp™ flat bottom plate filled with 75 µl 0.1 M EDTA and 75 µl 0.1% CHAPS and incubated at room temperature for 1h on a rocking table to detach and solubilize the biofilm from the pegs.

To make sure that the majority of the biofilm was detached from the peg, the plate was tightly sealed with parafilm and put into an ultrasonic bath for 10 min.

After the ultrasonic bath the biofilm solution was further diluted in PBS in a new 96-well plate as diluent (dilution factor between 1:10 to 1:1000 depending on the amount of biofilm produced by the strains).

The hereby produced dilution was then plated out on TSA plates in a standardized spiral formation using the *Eddy Jet* and incubated overnight at 37°C.

The number of CFU on the plate was counted and the number of viable cells that were in the original solution and therefore in the biofilm was calculated with the *Flash&Go* colony counter.

For better comparability ratios of CFU counts were formed as with the OD<sub>600nm</sub> values from the crystal violet staining method described in 2.6.2.

Each assay was performed three times in triplicates. Statistical analysis of the ratios was conducted between values from the same condition and the same days of a morbidostat run performing a two-tailed, unpaired t-test using GraphPad Prism 7.

## 2.7 Virulence

### 2.7.1 The *Galleria mellonella* infection model

To quantify virulence, *Galleria mellonella*, the greater wax moth or honeycomb moth, was used as an animal model. The larvae of the moths can be used as an infection model, because “their innate immune response shows remarkable similarities with the immune response in vertebrates” (Tsai *et al.* 2016). Their immune system consists of a complement system, various cytokines, antimicrobial peptides, reactive oxygen species and phagocytes. Thus, it can be used as a reliable high-throughput model to compare different strains (Pereira *et al.* 2018).

*Galleria mellonella* were acquired from TruLarv who provided similar sized and healthy larvae. After the larvae arrived the experiments were carried out within 1-2 days to make sure the larvae stayed motile and agile.

### 2.7.2 Preparation

For each experiment, the corresponding baseline strains (before incubation in the morbidostat) were used alongside the strains from the three different time points (days 7, 14 and 21) of one condition from the first or second morbidostat run or the medium run. The strains were prepared as described in 2.4 and 2.6.2. For second run strains, a few colonies were picked from the agar plates and solubilized in PBS. Further dilution steps with PBS were carried out to create the intended concentration of 1000 CFU/ml.

### 2.7.3 Injection

The injection was performed with a Hamilton 500  $\mu$ l Instrumental Syringe and 27G x  $\frac{3}{4}$  Sterican® disposable hypodermic needles that are just small enough to penetrate and inject into the larvae’s hemolymph without harming them too much. By injecting 10  $\mu$ l of the prepared dilution into each larva a total amount of 8 to 16 bacteria were inserted into the *Galleria mellonella*. This was managed with the Hamilton PB600-1 Repeating Dispenser that is set to press 10  $\mu$ l per push out of the syringe. 30 larvae per strain were used and the amount of CFU

in the dilution was controlled by plating out 10 µl of the solution on agar plates. In general, the range of CFU in the solution with which *Galleria mellonella* larvae were infected was set at 8 to 16 CFU per 10 µl. Every experiment with CFU values outside that range had to be repeated.

For every experiment, a negative control was carried out with the injection of 10 µl of PBS.

The larvae were put into petri dishes and incubated at 37°C.

#### **2.7.4 Survival control**

The survival of the larvae was checked on certain time points after the injection. To determine a larva's death the *Galleria mellonella* were turned around onto their back. If there was no detectable movement the larvae were classified as dead and removed from the petri dish.

The first control took place after 12h. From there on the larvae's survival was controlled every 2h until most of them died, which was in general after 24h. The last control was 36h after the injection.

To assess the virulence from the infection model, the survival was analyzed by creating Kaplan Meier curves. For a better comparison of the different curves of the strains and the different experiments, the hazard ratio for each strain was calculated. This is a measure of how rapidly subjects are dying and it is calculated as a quotient of death rates. In this case, the hazard ratio of the different morbidostat strains was calculated by dividing its death rate by the death rate of the baseline strain for each individual experiment using GraphPad Prism 7. Observing the overall effect between hazard ratios from the morbidostat run and the medium run from the equivalent days a frailty model was performed in Stata version 12.1 (StataCorp, College Station, USA). To improve comparability and to enable statistical evaluation between the morbidostat runs with antibiotics and the medium run, the percentage of their hazard ratio was calculated and presented in column bar graphs.

### **2.7.5 Growth curve**

For each strain of the experiment a growth curve in LB was conducted to monitor the strains' ability to replicate and whether some of the strains might have a general deficit in growth, which could explain a loss of virulence in the infection model.

The strains were cultivated overnight as described in 2.4. The inocula were brought to an OD<sub>600nm</sub> 0.05 using LB as diluent. Then, 500 µl each in triplicates were transferred into the wells of a 48-well microtiter plate and the bacteria were grown at 37°C in the Epoch2 microplate reader measuring the OD<sub>600nm</sub> every 15 minutes for 24h.

Growth curves were illustrated using GraphPad Prism 7, showing the OD<sub>600nm</sub> plotted against time. For statistical analysis, Stata version 12.1 was used to calculate the linear regression for the individual growth curves, which help us to create a better comparability for the large quantity of strains and determine the differences between the curves. The linear regression indicates how strongly the OD<sub>600nm</sub> has increased as a function of time and is therefore a measure for the kinetics of growth.

### **2.8 Correlation analysis**

Additionally, for every phenotypic assay the correlation between the calculated ratios and the MIC for the individual strains was determined. This was achieved by assessing the nonparametric Spearman correlation coefficient  $\rho$  out of the values and the logarithmic MIC as a test for association between paired samples. The calculations and statistical analysis were performed by a cor.test-function using the method "spearman" between two variables, implemented using the software R (The R Foundation for Statistical Computing, Vienna, Austria) as a programming language for statistical computing and graphical illustration.

The interpretation of the  $\rho$ -values was performed as follows: Values from -1 to -0,7 were considered a strong negative correlation, values from -0,7 to -0,5 a moderate negative correlation, values from -0,5 to -0,1 a weak negative correlation, values from -0,1 to 0,1 no linear relationship, values from 0,1 to 0,5 a

weak positive correlation, values from 0,5 to 0,7 a moderate positive correlation and values from 0,7 to 1 a strong positive correlation between the variables.

For this analysis, a  $p$ -value of  $\leq 0,1$  was considered significant.

## **2.9 Statistical analysis**

Statistical analyses were carried out using GraphPad Prism version 7 (GraphPad Software, Sun Diego, USA) and Stata version 12.1 (StataCorp, College Station, USA) for the analysis of the growth curves and the hazard ratios.

For both biofilm methods, a two-tailed, unpaired t-test was performed between the calculated ratios from the same condition and the same days of a morbidostat run as described in 2.6.2. Thus, it was possible to directly measure the actual increase in biofilm production on distinct days compared to the baseline isolates as well as the medium run strains.

For the *Galleria mellonella* infection model, the hazard ratio was calculated as a measure of virulence and the percentage compared to the medium run was calculated as described in 2.7.4. Statistical analysis of the hazard ratios of strains exposed to antibiotics and medium was carried out by a frailty model using Stata version 12.1.

For all assays apart from the correlation analysis, a  $p$ -value of  $\leq 0,05$  was considered significant.

## **2.10 Ethics**

The overall approach of generating resistant isolates was approved by our local ethics review committee.

Ethics review number: 677/2013BO1

### 3 Results

All morbidostat-derived strains were examined for their ability to form biofilm and for their virulence potential. In addition, these phenotypes were compared with the individual baseline isolate – that was not cultured in the morbidostat - and the medium run strains.

#### 3.1 Sample collection from the morbidostat and growth failure

A morbidostat culture device was used to expose the *P. aeruginosa* isolates to the antibiotic drugs and to examine the evolutionary pathways throughout the development of colistin resistance (1.8 and 2.3). Two replicates of morbidostat runs for a time period of 21 days were performed for each baseline strain (PA77, PA83, ID4, ID21, ID40) and condition (colistin, colistin + metronidazole, metronidazole). Furthermore, for every baseline isolate a third run was performed, in which only LB medium instead of antibiotics was used for the three-week period. These strains as well as the baseline strains are the references for all evaluations of the following results of the phenotypical tests.

Collecting samples every two to three days the morbidostat runs provided us with a total of 315 strains of which 105 have been used for the phenotypic experiments. Strains were used from samples taken after 7, 14 and 21 days of morbidostat cultivation. This was done for all five baseline isolates (PA77, PA83, ID4, ID21, ID40) and the four conditions of cultivation (colistin, colistin + metronidazole, metronidazole, medium).

Growth failure occurred for two strains in the initial morbidostat run due to the cultivation process. Specifically, Day 21 strains from the combination condition (colistin + metronidazole) from PA77 as well as ID40 were affected. For those two strains, recovery was not possible from the Microbanks. Thus, no phenotypic characterization is available for those strains.

#### 3.2 Colistin resistance development under antibiotic exposure

Throughout the morbidostat runs, the concentration of colistin needed to keep the bacterial culture on approximately the same OD increased heavily, which implies an enhanced resistance against the antibiotic drug. Thus, all *P. aeruginosa*

strains were tested for their susceptibility to the antibiotic colistin using BMD and Micronaut-S.

The MIC for “colistin-susceptible” was defined as a maximum of 2 µg/ml, whereas a MIC between 4 to 8 µg/ml was considered as “intermediate antibiotic resistant” and a MIC greater than or equal to 16 µg/ml as “highly antibiotic resistant” to colistin.

Table 1 shows the MICs for the baseline isolates (Table 1 A) before their incubation in the morbidostat and the morbidostat-derived strains from day 7, 14 and 21 (Table 1 B, C, D). As expected, the level of resistance against colistin increased considerably in the conditions that were exposed to colistin. At the end of the three-week run most of these strains were highly colistin resistant (Table 1 B, C Col., Col.+Met.). However, resistance was reached even more rapidly in the second run which could be due to the potentially cleaner selection of resistant colonies in this run: On day 14, in the first morbidostat run only two out of ten strains exposed to colistin could be classified as highly colistin-resistant and only three were intermediate colistin-resistant, while in the second run at this point in time seven out of ten strains were already highly resistant and the remaining three were intermediate colistin-resistant. After 21 days almost all the strains exposed to colistin were highly antibiotic resistant.

Nearly every colistin-treated strain and all the strains in the combination condition were already highly antibiotic resistant on day 14 (Table 1 C Col., Col+Met.). Nevertheless, especially in the second morbidostat run, the strains gained high levels of colistin-resistance even faster in the combination condition, with all strains reaching MICs equal to or above 16 µg/ml already after 14 days, whereas only two out of five strains in the colistin condition could be classed as highly antibiotic resistant at this point in time.

In contrast, there were some exceptional cases that were not following that pattern and even had a decrease in their MIC during the experiment (Table 1 C ID40 Col+Met, ID4 Col).

As expected, there were no changes in resistance against colistin in the metronidazole condition as well as in the LB-medium run, because the bacteria were not exposed to colistin at all.

**A – MICs baseline isolates**

Day 0	
PA77	1
PA83	2
ID4	2
ID21	1
ID40	1

<span style="background-color: #ADD8E6; border: 1px solid black; display: inline-block; width: 20px; height: 10px;"></span>	≤ 2 µg/ml
<span style="background-color: #FFD700; border: 1px solid black; display: inline-block; width: 20px; height: 10px;"></span>	4-8 µg/ml
<span style="background-color: #FF6347; border: 1px solid black; display: inline-block; width: 20px; height: 10px;"></span>	≥ 16 µg/ml

**B – MICs first run**

**C – MICs second run**

**D – MICs Medium run**

Day 7										
	Col.	Col.+Met.	Met.		Col.	Col.+ Met.	Met.			Medium
PA77	1	1	1		2	4	1			1
PA83	4	1	1		4	2	2			1
ID4	1	4	1		>64	64	2			2
ID21	8	2	0,5		8	32	1			1
ID40	2	1	1		4	8	1			2
Day 14										
PA77	0,5	1	1		>64	>64	1			2
PA83	4	32	1		4	>64	2			1
ID4	2	8	2		>64	64	1			2
ID21	16	2	1		8	64	1			1
ID40	4	1	2		4	16	1			1
Day 21										
PA77	4	/	1		>64	>64	1			2
PA83	16	> 64	2		>64	>64	2			2
ID4	64	> 64	2		4	128	1			2
ID21	32	16	1		16	>64	1			1
ID40	8	/	2		2	4	2			1

**Table 1: MICs for baseline isolates and morbidostat-derived strains.** Minimal inhibitory concentrations (MICs) were measured with broth microdilution (BMD) and Micronaut-S for baseline isolates (A), morbidostat-derived strains from the first (column B) and second run (column C) and from the medium run (column D) on day 7, 14 and 21. Col. = colistin condition, Col.+Met. = colistin and metronidazole combination condition, Met. = metronidazole condition. The level of resistance against colistin is illustrated in different colors: ≤2 µg/ml = colistin-susceptible (blue), 4-8 µg/ml = intermediate resistant (yellow), ≥16 µg/ml = highly antibiotic resistant (red).



### **3.3 Alterations in biofilm formation ability after antibiotic exposure**

Next, we studied the changes in the phenotypic characteristics of *P. aeruginosa* under antibiotic drug pressure, one of which was the biofilm formation. The ability of *P. aeruginosa* to adhere to surfaces and form biofilms is one of the major problems of hospital- and community-acquired infections. Forming biofilm allows bacteria to survive and maintain infection despite aggressive antibiotic therapy. A combination of colistin and other antimicrobial peptides has been suggested to be highly effective against biofilm-associated infections caused by MDR *P. aeruginosa* (Jorge *et al.* 2017, Tan *et al.* 2017). However, it is not known whether resistance to colistin with its associated changes in the outer membrane of *P. aeruginosa* leads to alterations in characteristics of biofilm formation. We conducted two biofilm assays, each focusing on other aspects of the biofilm.

#### **3.3.1 Irregular production of biofilm biomass under antibiotic influence**

In this experiment, biofilm grew in a 96-well plate. By staining it with crystal violet, the amount of biofilm could be measured. Crystal violet mainly binds to the biofilm matrix and additionally to cell walls of both dead and living bacteria in the biofilm. Thus, using this method, conclusions can primarily be drawn about the quantity of biomass in the biofilm (Wilson *et al.* 2017).

After staining the biofilm, it was possible to quantify the biomass by measuring the absorbance at OD<sub>600</sub> (graphs shown in Supplementary 7.1). For better comparability, we calculated the ratios for all morbidostat-derived strains compared to their baseline isolate and then put the calculated ratios of the morbidostat-derived strains with antibiotic exposure in relation to the calculated ratios of medium run strains. Thus, it was possible to combine all values in one diagram and to evaluate them more effectively (Figure 5). A value of “1” indicates that there is no difference between the strains that were exposed to the antibiotics and medium run strains. Thus, values above “1” show an increase, whereas values below “1” display a reduction in the overall biomass of the biofilm in the antibiotic exposed morbidostat-derived strains.

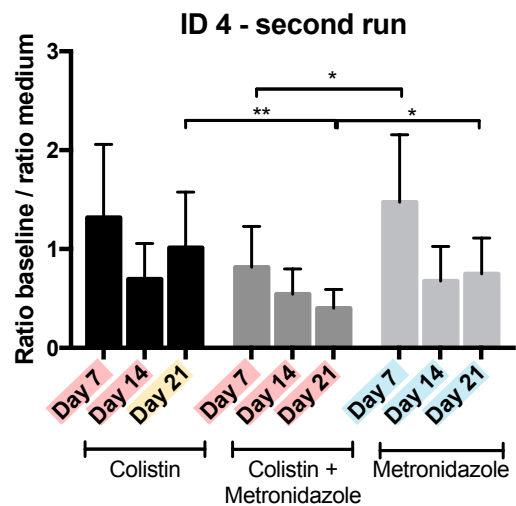
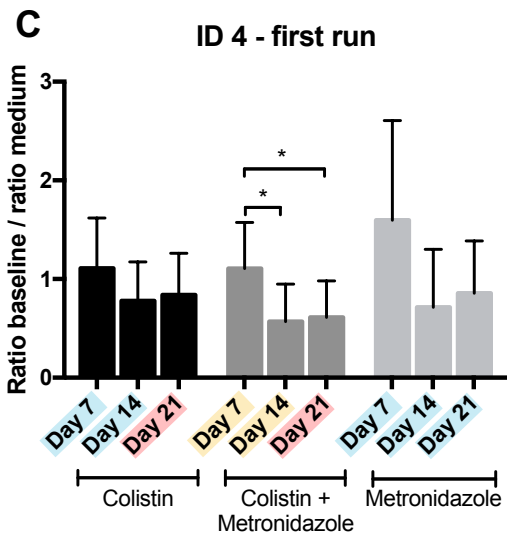
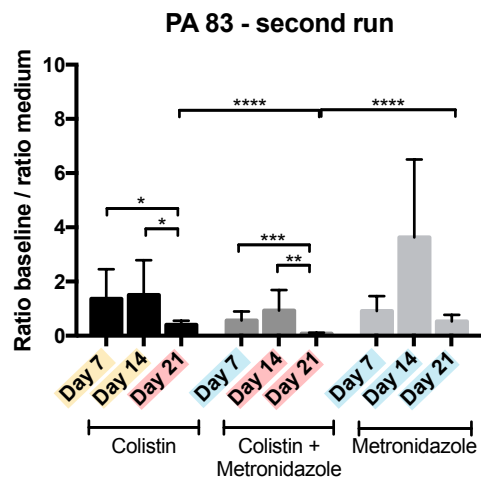
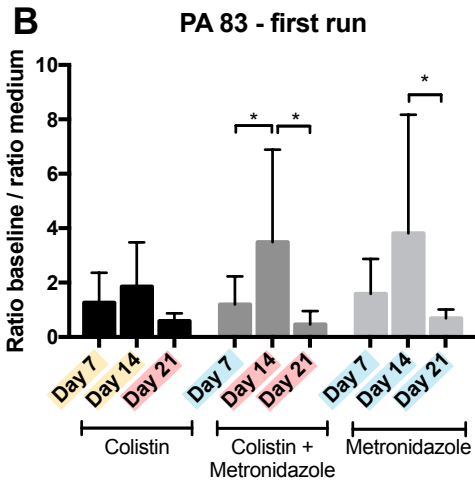
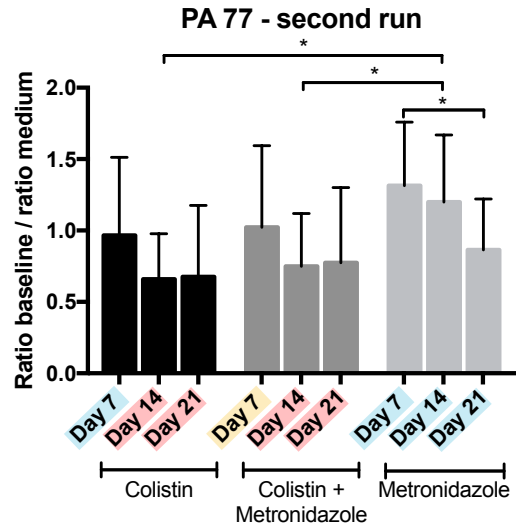
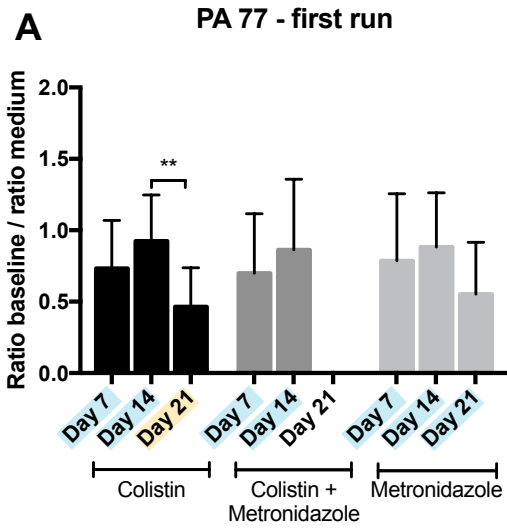
Figure 5 illustrates the results for all five baseline strains. PA77 (Figure 5 A) and ID4 (Figure 5 C) in general showed no changes at all in their amount of biofilm

when compared to the medium run strains, which is represented by a ratio around 1. PA83 (Figure 5 B) showed in both runs a remarkable increase at day 14 in nearly all conditions, followed by a sharp and significant decrease at day 21. A similar pattern can be seen for the first run of ID21 (Figure 5 D). However, for ID21 the second run did not show significant changes at all, with ratios around 1. Concerning ID40 (Figure 5 E), a comparable trend as described for PA83 was discovered in the first run, while the ratios for the second run were clearly below 1, especially in the metronidazole condition. As mentioned in 3.1, there are no values available for PA77 and ID40 at day 21 from the colistin and metronidazole combination condition from the first morbidostat run.

Generally, at least for three of the five strains (PA83, ID21, and ID40) a pattern was observed regarding changes of biofilm formation. They all showed an increased biofilm production in the middle of the incubation period, each with values dropping again on day 21. Furthermore, this development of biofilm production was reproducible in both morbidostat runs.

For the other two strains neither the described pattern nor any other clear trend could be detected.

In summary, it can be assumed that the exposure to colistin and the development of resistance against the antibiotic did lead to irregular changes in the biomass formed in the biofilm with ascending values after 14 days of incubation and descending values on day 21 within the individual strains and discrepancies among the different stains.



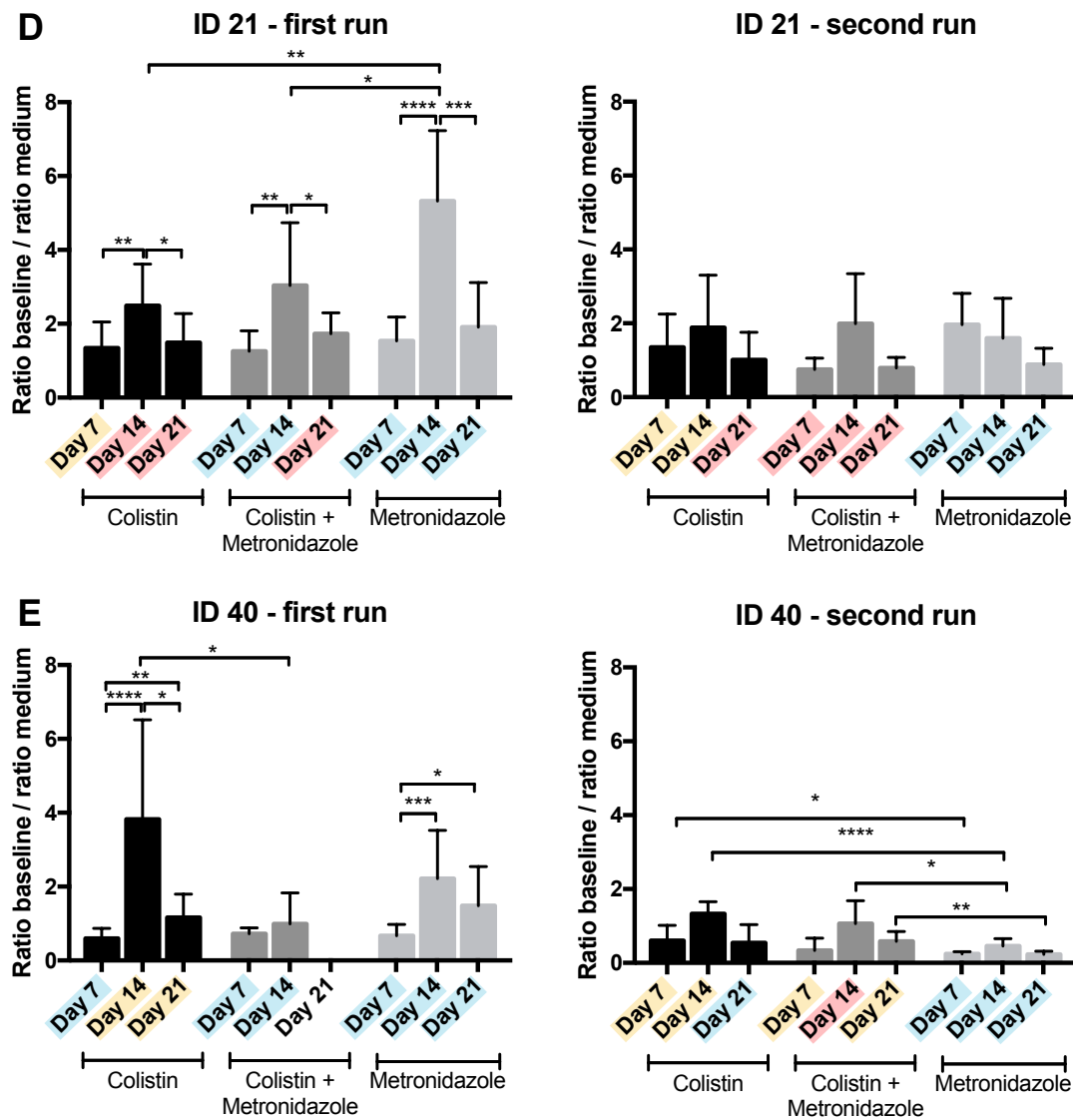


**Figure 5: Results for crystal violet staining biofilm assay.** Biofilm was grown a 96-well plate and stained using crystal violet.  $OD_{600nm}$  was measured to quantify the amount of biofilm. Ratios of  $OD_{600nm}$  values from morbidostat-derived strains compared to baseline strain values and then put in relation to the equivalent, calculated medium run ratios are shown. Values are means representing three independent experiments with three replicates each, error bars display standard deviation. Level of resistance against colistin is illustrated in different colors (blue: colistin-susceptible, yellow: intermediate antibiotic resistant, red: highly antibiotic resistant). A) PA77 first and second run B) PA83 first and second run C) ID4 first and second run D) ID21 first and second run E) ID40 first and second run. Statistical analysis was performed by two-tailed, unpaired t-test and significant differences are indicated with asterisks ( $p < 0.05$ : \*,  $p < 0.01$ : \*\*,  $p < 0.001$ : \*\*\*,  $p < 0.0001$ : \*\*\*\*).

### 3.3.1.1 Less biomass with increasing levels of colistin resistance

Additionally, for every strain a Spearman correlation between the calculated ratios and the MIC for the individual strains was performed (Figure 6). This allowed us to get an idea of how acquired antibiotic resistance affects our phenotypic findings, whereas previously statements on this could only be made with regards to the antibiotic exposure. In the graph the MIC is displayed on the x-axis in a logarithmic form for better visualization. For clarification, if the Spearman correlation coefficient  $\rho$  is positive it shows a positive linear relationship, while a negative  $\rho$  indicates an anticorrelation between the two variables. Values around 0 imply no correlation at all.

The graph shows that most strains present no strong connection or even present an anticorrelating connection between the two variables, with ID40 that was exposed to pure colistin and the second run of ID21 from the combination condition being the only exceptions. This is expressed by the fact that the Spearman correlation provides negative  $\rho$  values for most of the strains. Most  $\rho$  values are within the range of -0,5 to -0,1, which can be considered a moderate to weak anticorrelation. These results suggest that the more resistant the strains are to colistin, the lower the total biomass produced by the bacteria in most cases. However, for the majority of strains, this correlation is weak, indicating that there is no distinct relationship between these two variables.

An evaluation of the Spearman correlation for strains in the metronidazole condition is not relevant as none of the bacteria exposed only to metronidazole have acquired colistin resistance.

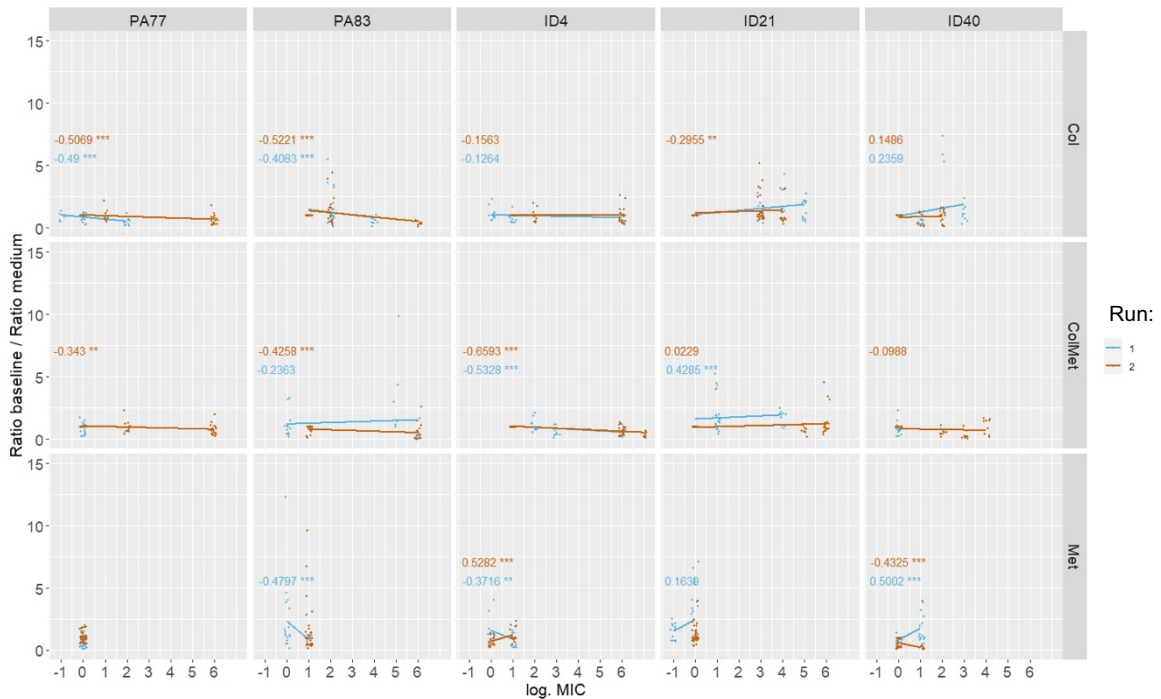


**Figure 6: Spearman correlation between ratios and MIC (violet staining biofilm assay).** Association between calculated ratios comparing OD<sub>600nm</sub> from morbidostat-derived strains to baseline and medium run strains and the MIC of the strains was statistically tested by calculating the Spearman's correlation coefficient  $\rho$ . X-axis displays a logarithmic form of the strains MIC (3.2); y-axis shows the calculated ratios from 3.3.1. Numbers in the boxes represent the corresponding Spearman's correlation coefficient  $\rho$ . Selected data points were randomly "jittered" by small amounts for better visualization to prevent overplotting of data points. Few data points outside the range are not displayed in order not to reduce the scale of the images too much. Different morbidostat runs for the individual strains are illustrated in different colors (blue: first run; red: second run). Significant differences are indicated with asterisks ( $p < 0.1$ : \*,  $p < 0.05$ : \*\*,  $p < 0.01$ : \*\*\*).

### 3.3.2 Increased quantity of viable cells in biofilm under colistin exposure

In this assay, biofilm was grown on the pegs of a transferable 96-peg solid phase plate (TSP). The TSP were immersed into liquid bacterial culture. After biofilm formation on the pegs, the biofilm was detached, plated out on agar plates and CFUs were counted (graphs shown in Supplementary 7.2). Hence, in contrast to the crystal violet staining method, this assay enabled us to investigate primarily the number of viable cells in the biofilm.

As explained in 2.6.3 and 3.3.1, also for this assay ratios of the CFUs from morbidostat-derived strains compared to the baseline isolate were calculated and then put into relation to the corresponding medium run ratios.

Figure 7 illustrates the results for all five baseline strains. The number of viable cells detected in the biofilm produced by PA77 (Figure 7 A) increased significantly over time in each condition, especially for the strains exposed to colistin. Interestingly, for the colistin and the combination conditions, the largest changes were observed between time points when resistance against colistin increased as well (see coloring). Remarkably, in the second run were also significantly more viable cells in day 14 and day 21 strains of the colistin and metronidazole combination condition compared to the same days of the colistin only condition. The trend towards increased viable cells in the biofilm produced by *P. aeruginosa* over time in the morbidostat could also be detected for the metronidazole condition but with considerably lower ratios. Hence, there were significantly higher ratios in the strains exposed to colistin than in the metronidazole condition. In the first run of PA83 (Figure 7 B) a gradually increasing ratio of CFU in the biofilm could be observed for the antibiotic combination condition but not for the colistin condition. Again, all strains exposed to colistin showed a higher ratio than strains from the metronidazole condition. The metronidazole condition did not indicate an increase in viable cells in the biofilm having ratios of only around 1. In contrast, the second run indicated a noticeable up to 20-fold increase in the metronidazole condition compared to the medium run on day 21. However, there were no substantial changes between any days and condition of the morbidostat run.

A similar pattern as PA77 was observed for ID4 (Figure 7 C). The first run of ID4 specifically resembled the alterations in ratios outlined for PA77, but with no differences between the antibiotic combination and the colistin condition. The second run showed not many significant changes over time in the morbidostat, except an increased ratio on day 21 of the combination condition. the metronidazole condition again showed significantly lower ratios compared to equivalent strains exposed to colistin.

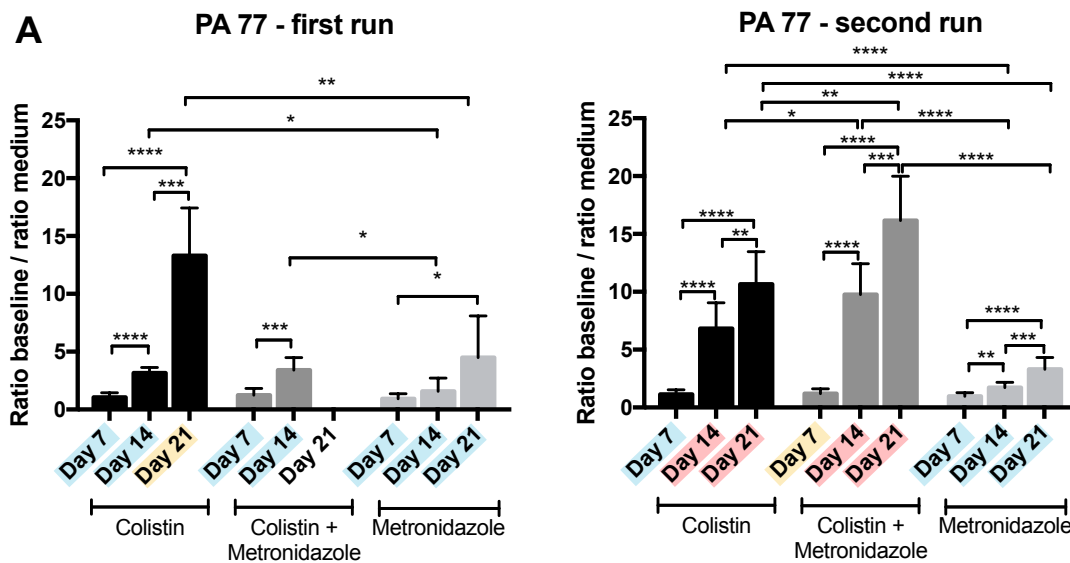
Both runs of ID21 (Figure 7 D) did not display the gradual increase described for PA77 and showed considerably lower ratios than most of the strains derived from the other baseline isolates. However, both runs still showed a clearly higher ratio

of CFU in the biofilm for the strains exposed to colistin compared to the metronidazole condition.

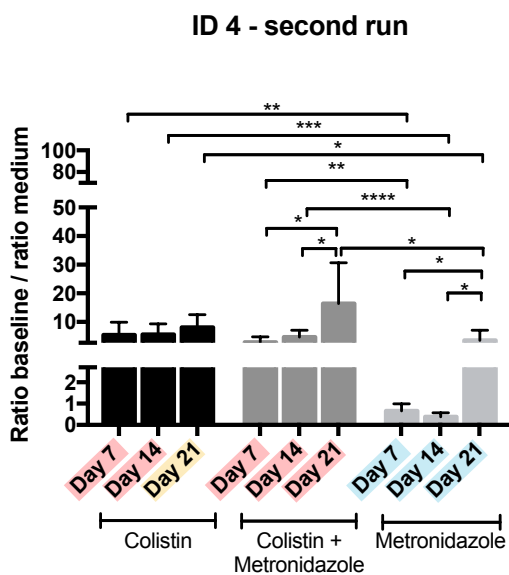
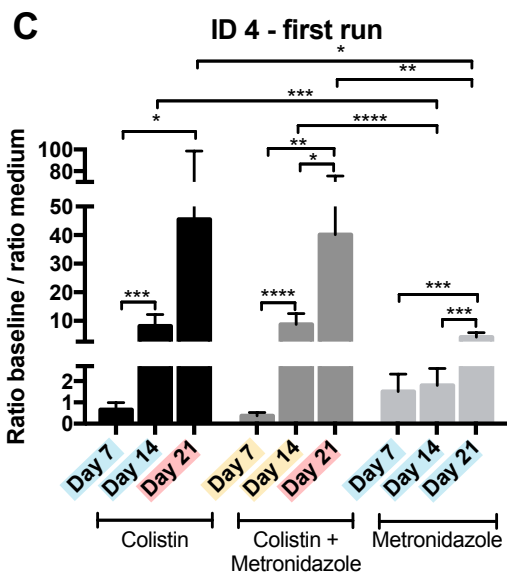
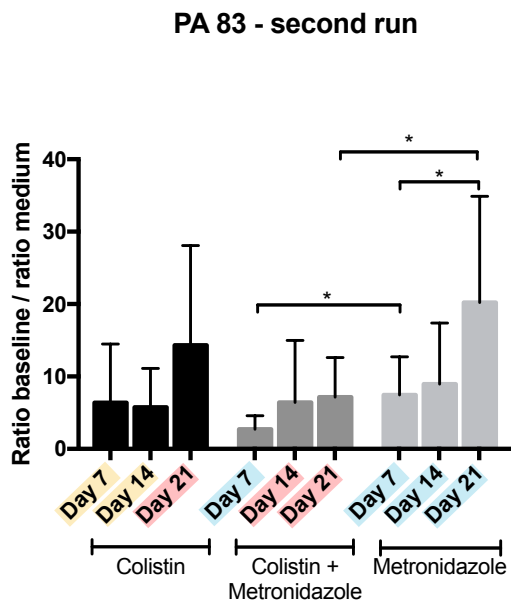
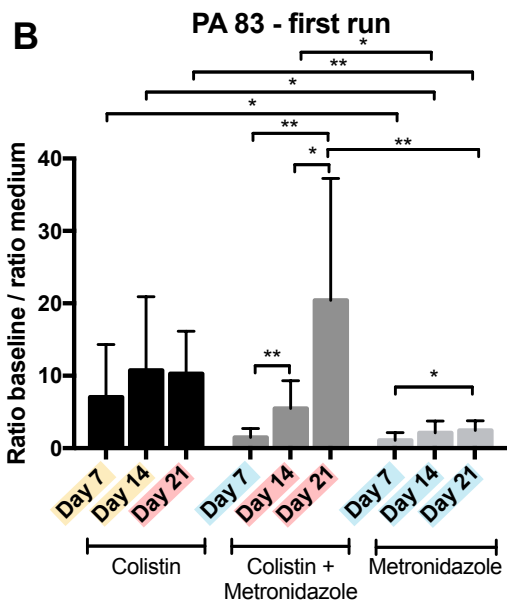
Looking at ID40 (Figure 7 E), especially the second run displayed a comparable pattern to PA77. However, the first run was difficult to interpret due to the missing value.

Thus, most of the strains exposed to colistin indicated a strong increase in the ratio of viable cells in the biofilm compared to the baseline isolate and the medium run strains. This increase was almost always significantly lower for strains from the metronidazole condition. In most cases, significant alterations corresponded to an increase in resistance against colistin, with a few exceptions in the strains with irregular decline in resistance mentioned in 3.2.

In summary, the abundance of viable cells in the biofilm produced by *P. aeruginosa* increased with the exposure to antibiotics.







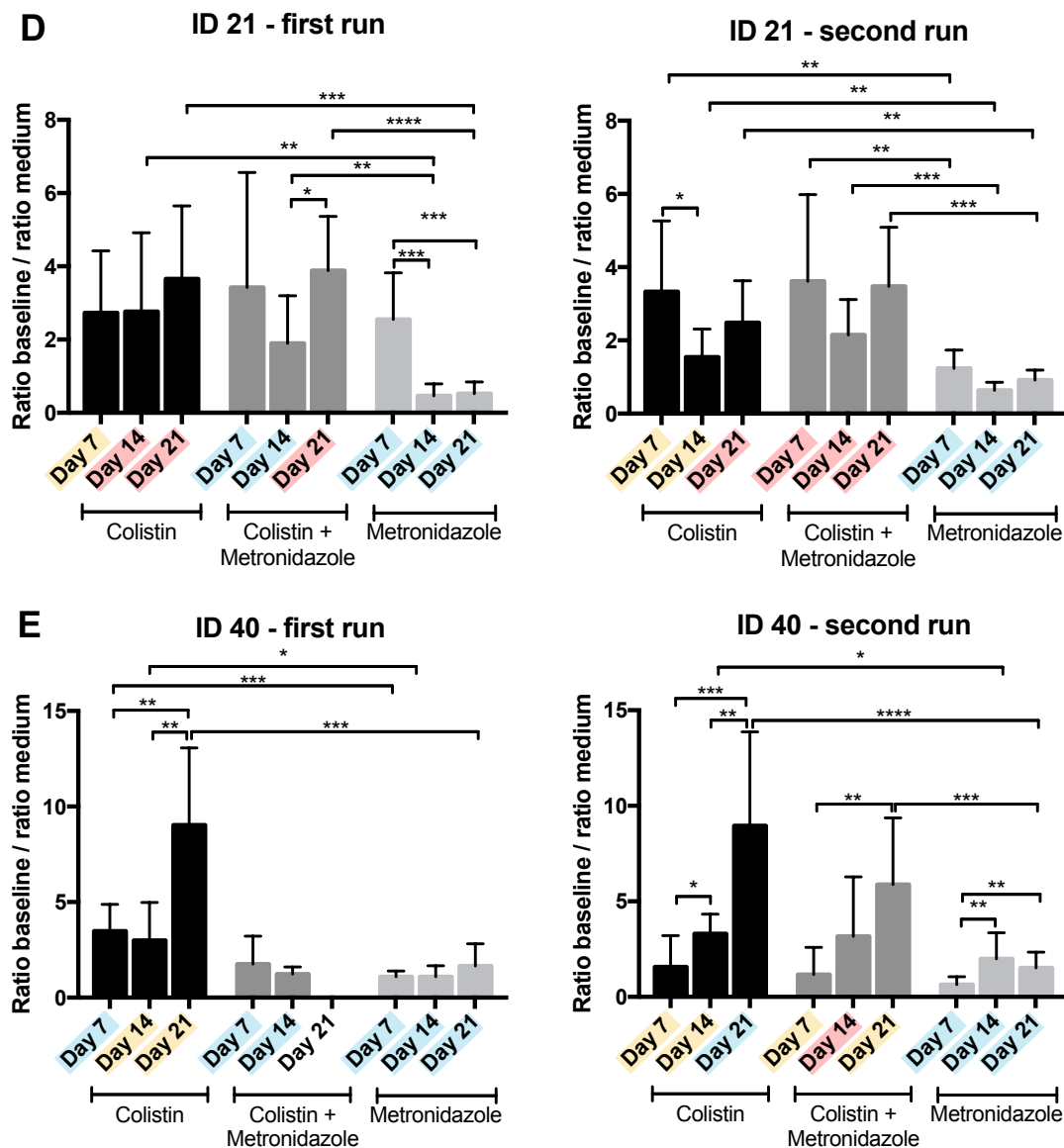


**Figure 7: Results for peg-lid method biofilm assay.** Biofilm was grown on TSP pegs immersed into 96-well microtiter plate wells filled with liquid culture of bacteria with  $OD_{600nm}$  0.1. Then, biofilm was dissolved from the pegs using 0.1 M EDTA and 0.1% CHAPS. The solution was plated on agar plates and CFUs were counted. The figure shows the ratio of CFU values from morbidostat-derived strains compared to baseline strain values and then put in relation to the equivalent, calculated medium run ratios. Values are means representing three independent experiments with three replicates each, error bars display standard deviation. Level of resistance against colistin is illustrated in different colors (blue: colistin-susceptible, yellow: intermediate antibiotic resistant, red: highly antibiotic resistant). A) PA77 first and second run B) PA83 first and second run C) ID4 first and second run D) ID21 first and second run E) ID40 first and second run. Statistical analysis was performed by two-tailed, unpaired t-test and significant differences are indicated with asterisks ( $p < 0.05$ : \*,  $p < 0.01$ : \*\*,  $p < 0.001$ : \*\*\*,  $p < 0.0001$ : \*\*\*\*).

### 3.3.2.1 Positive correlation between CFU in biofilm and colistin MIC

As for the crystal violet staining biofilm assay, the Spearman correlation coefficient  $\rho$  was calculated for every strain, correlating the increase in produced biofilm forming cells to the MIC, as described in 3.3.1 (Figure 8).

Interestingly, investigating this biofilm assay there seems to be a positive correlation between the number of viable cells in the biofilm and the level of colistin resistance in all our strains. As most of the  $\rho$  values lie in the range 0,5-0,8, this relationship can be considered a moderate correlation for most of the strains. The only exception in our variety of strains was the second runs of ID40 in both the colistin and the combination condition with  $\rho$  values around 0,1, indicating only a weak positive correlation. These findings are congruent to the irregular pattern of decreasing levels of colistin resistance after an initial increase in this strain during the cultivation in the morbidostat. As displayed in Figure 7 despite this exceptional development in their colistin MIC, the strain still gained in CFU along the exposure to colistin.

Thus, the quantity of viable cells in the biofilm of our *P. aeruginosa* strains not only increased with the exposure to colistin, but also particularly with the development of resistance against colistin.

Again, an evaluation of the Spearman correlation for strains in the metronidazole condition is not considered relevant as none of the bacteria exposed to metronidazole have become resistant to colistin.

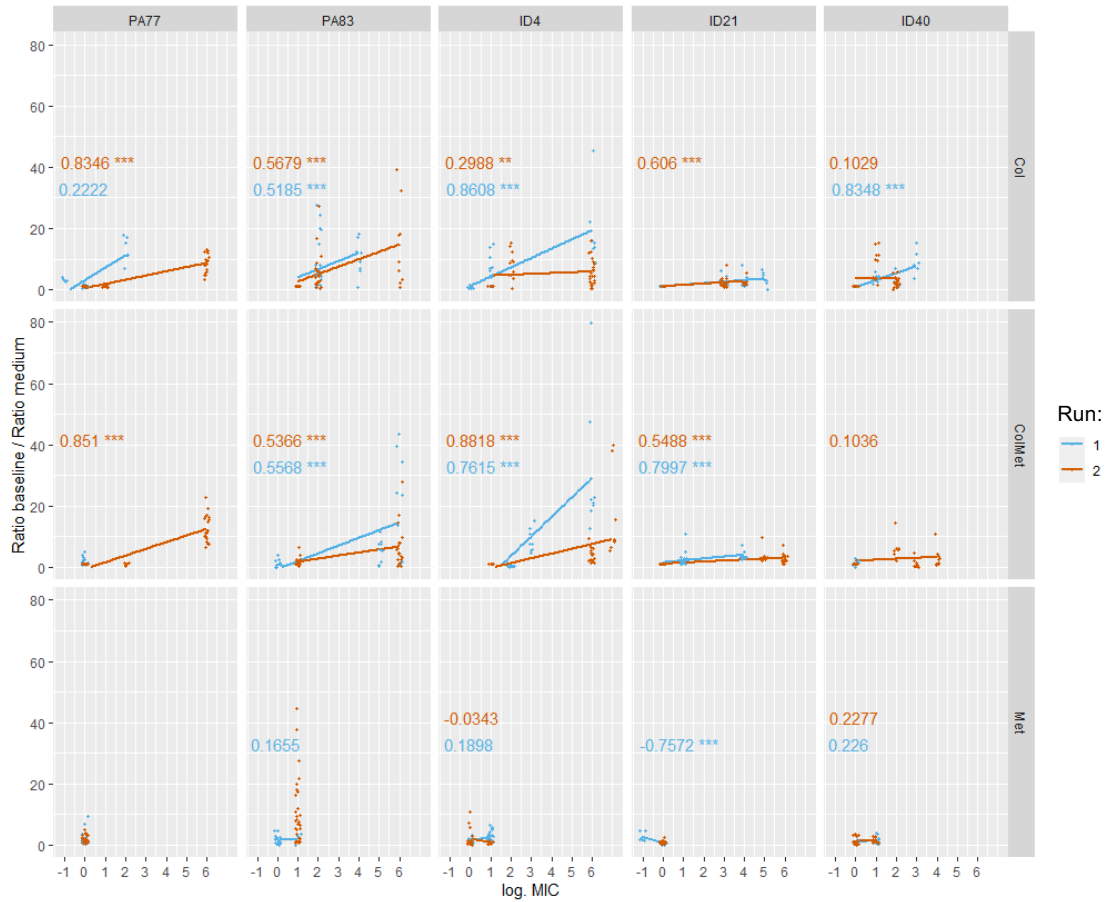


**Figure 8: Spearman correlation between ratios and MIC (peg-lid method biofilm assay).** Association between calculated ratios comparing CFU from morbidostat-derived strains to baseline and medium run strains and the MIC of the strains was statistically tested by calculating the Spearman's correlation coefficient  $\rho$ . X-axis displays a logarithmic form of the strains MIC (3.2); y-axis shows the calculated ratios from 3.3.23.3.1. Numbers in the boxes represent the corresponding Spearman's correlation coefficient  $\rho$ . Selected data points were randomly "jittered" by small amounts for better visualization to prevent overplotting of data points. Few data points outside the range are not displayed in order not to reduce the scale of the images too much. Different morbidostat runs for the individual strains are illustrated in different colors (blue: first run; red: second run). Significant differences are indicated with asterisks ( $p < 0.1$ : \*,  $p < 0.05$ : \*\*,  $p < 0.01$ : \*\*\*).

### 3.4 Exposure to colistin leads to loss of virulence

As a further phenotypic characteristic of *P. aeruginosa*, we investigated the virulence of the bacteria regarding the exposure to the antibiotics in the morbidostat. To investigate virulence, *Galleria mellonella* larvae were used as an animal infection model. As described in 2.7.1 it is a reliable high-throughput model as an alternative to mammalian infection models with which the many strains can be compared to each other. Hence, the assay does not allow absolute but relative statements about the virulence of the different strains.

Because of the missing strains in the morbidostat runs for PA77 and ID40 mentioned in 3.1, we decided to perform the experiment only with the strains PA83, ID4 and ID21.

For each experiment, a baseline isolate was used alongside the corresponding strains from the three different time points (days 7, 14 and 21) of one condition from the first or second morbidostat run or the medium run. The virulence of each strain was examined by infecting 30 larvae, each of them with 8 to 16 CFU of the bacteria, and their survival was investigated over 36 h after injection. For each assay, Kaplan Meier curves could be generated from the data of the larvae dying in the course of time. Figure 9 shows the results for the second run of ID21 as a representative example. Death rates declined the longer strains were exposed to colistin (Figure 9 A) or to colistin/metronidazole (Figure 9 B) in the morbidostat. On the other hand, there were no noticeable death rate changes under metronidazole exposure (Figure 9 C). Similar results could be seen for most of the other morbidostat runs and baseline isolates (graphs shown in Supplementary 7.3).

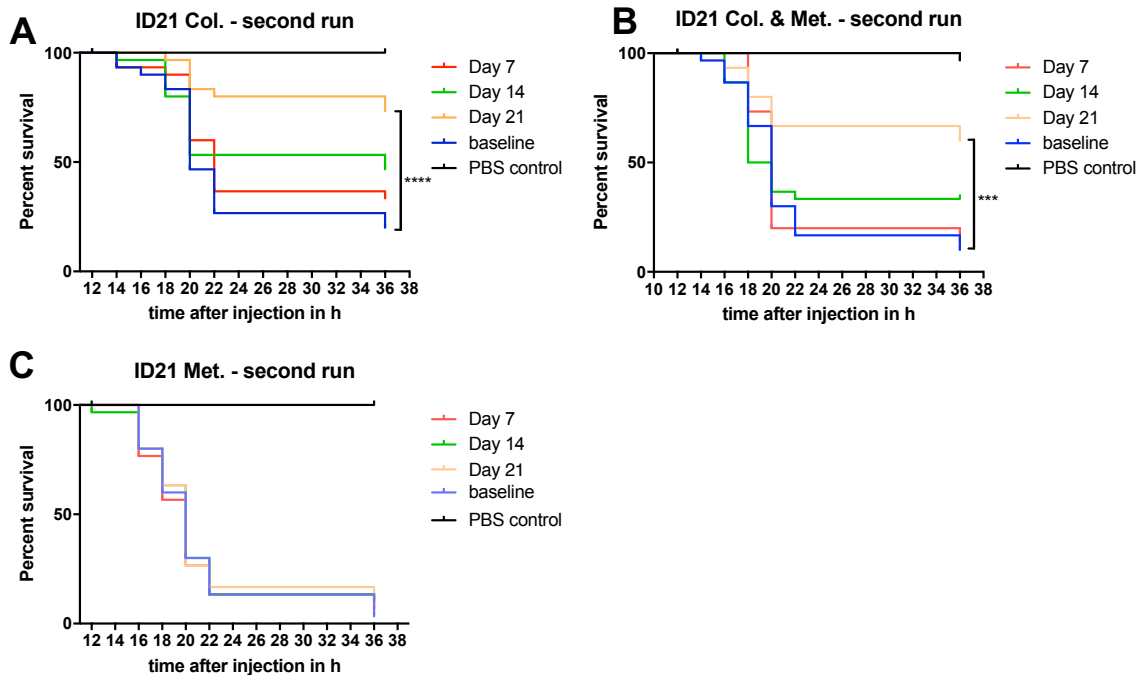


**Figure 9: Kaplan Meier curves monitoring the survival of *G. mellonella* larvae after infection with ID21.** *Galleria mellonella* larvae were infected with about 10 CFU of *P. aeruginosa* strains and survival was controlled for 36h. Kaplan Meier curves were created for baseline strain next to day 7, 14 and 21 strains from one condition of a morbidostat run with 30 larvae each. A) Col. = colistin condition, B) Col.+Met. = colistin and metronidazole combination condition, C) Met. = metronidazole condition. Statistical analysis was performed by Log-rank test and significant differences are indicated with asterisks ( $p < 0,05$ : \*,  $p < 0,01$ : \*\*,  $p < 0,001$ : \*\*\*,  $p < 0,0001$ : \*\*\*\*).

As described before, with these values it is difficult to compare the different single experiments with each other. Moreover, there is no guarantee that the observed effect is really attributed to the exposure to the antibiotic. Lower death rates could also simply be due to the long incubation in the morbidostat. Thus, for every morbidostat-derived strain the hazard ratios were determined as the quotient of death rates relative to the baseline isolate (shown in Supplementary 7.4). In addition, to determine the true impact of the antibiotic exposure to the virulence, percentages of these hazard ratios were formed by dividing the hazard ratios of the antibiotic exposed strains by the medium run hazard ratios (shown in Supplementary 7.4) of the equivalent days (Figure 10). This means that in case of a percentage of 100% there would be no difference in death rates between the strains that were exposed to colistin and the medium run strains. Hence, percentages below 100% indicate lower, and percentages above 100% show increased death rates in the antibiotic exposed strains.

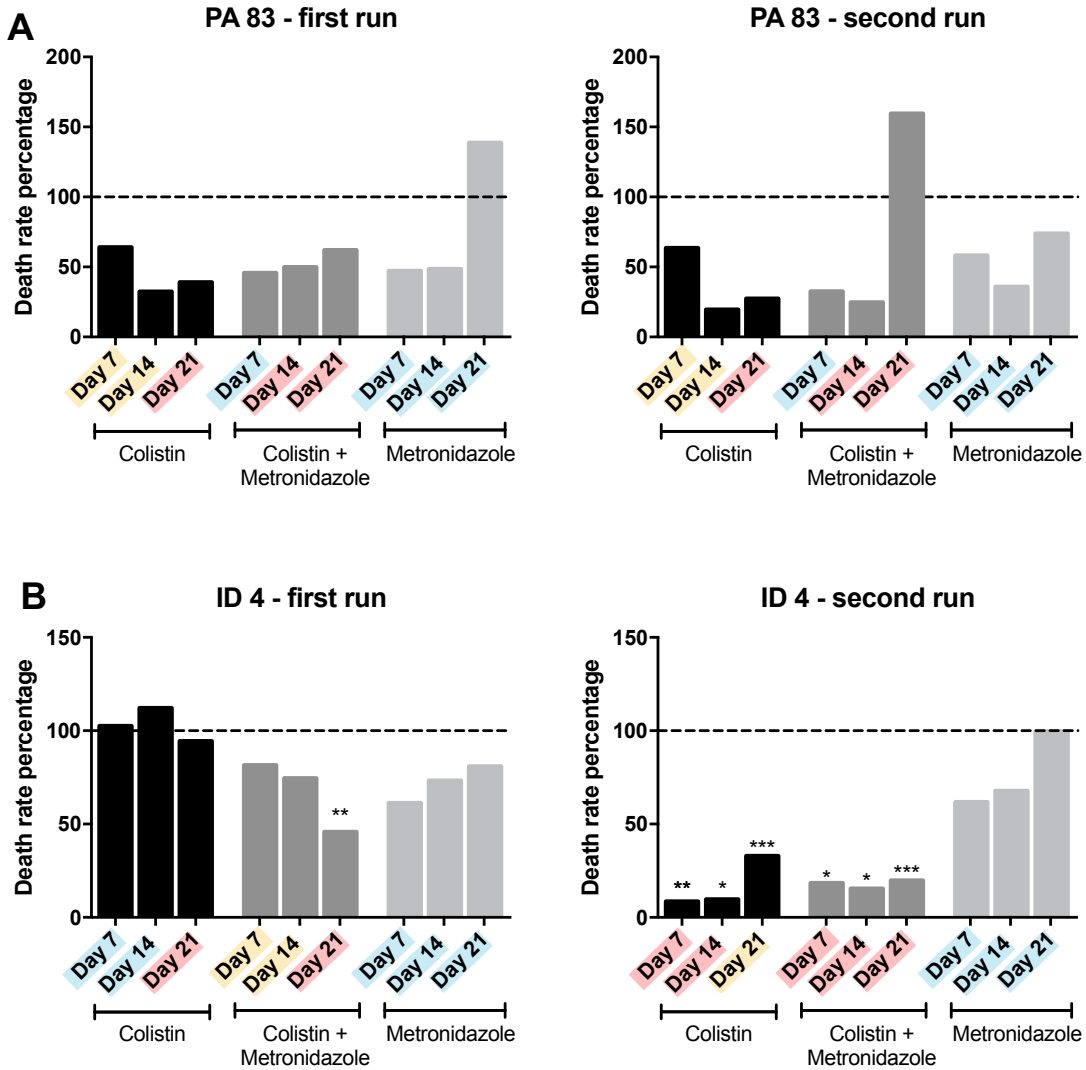
PA83 (Figure 10 A) showed reduced death rates in all conditions compared to the medium run strains, with decreases of up to 80%. Despite this distinct decrease, there were no statistically significant differences in any strain for both runs of this strain in comparison to the medium run strains. Two strains (day 21 of the metronidazole condition from the first run and day 21 of the combination condition from the second run) even showed percentages above 100% (139% and 160% respectively), which, however, were not significantly different to the medium run strains.

In contrast, there were statistically significant alterations for ID4 (Figure 10 B). In the first run, there was a gradual decrease of death rates in the colistin and metronidazole combination condition, with day 21 being the only value significantly lower than the medium run strains, at 45% of the initial value of virulence. There were no changes in the colistin only and the metronidazole only condition. However, all strains in the colistin only and the combination condition showed a strong reduction of 80% to 91% in hazard ratios relative to the medium run strains in the second run, whereas there were no variations in the metronidazole condition.

A comparable pattern could be observed for the second run of ID21 (Figure 10 C). There was a gradual virulence reduction over time when exposed to colistin, with day 21 strains of the colistin condition (28% of the medium run value) as well as the combination condition (45% of the medium run value) being significantly lower compared to the medium run strains. However, there were no changes and no trend of virulence decrease induced by the effect of the antibiotics in the strains of the first run.

In general, it can be said that most of the strains exposed to the antibiotics showed reduced virulence compared to the medium run condition. Our observations for ID4 and ID21 showed some decrease in virulence when exposed to colistin in the morbidostat, but not with metronidazole alone. This phenomenon has not been observed for PA83, with a trend towards lower levels of virulence in all conditions, but no significant alterations compared to the medium run. Comparing the two morbidostat runs, it can be suggested that the loss of virulence was more prominent in the second run, with the clear exception of PA83

whose evolution in virulence modification seems not to be driven by exposure to antibiotics.





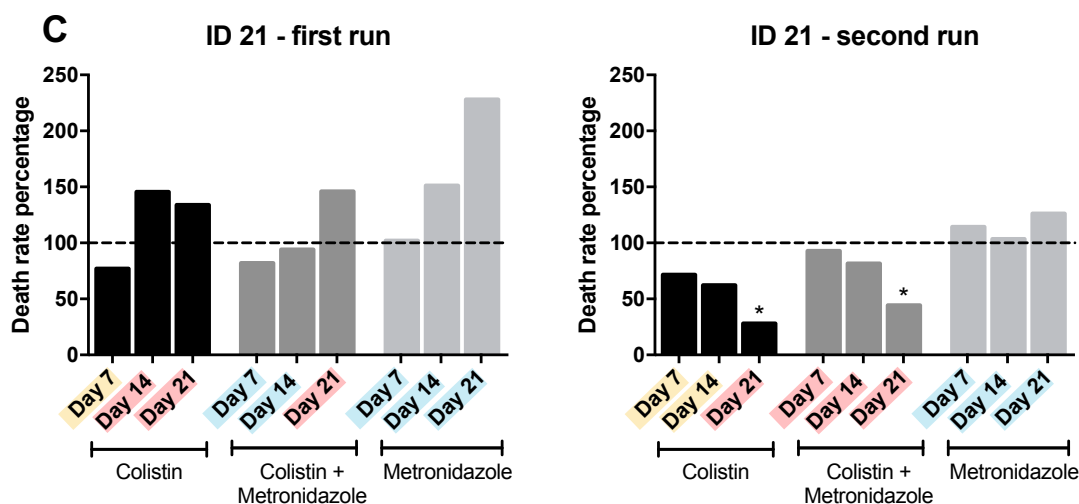


**Figure 10: Results for *Galleria mellonella* infection model.** Hazard ratio for morbidostat-derived strains was calculated out of Kaplan Meier curves in relation to baseline isolates. The figure shows percentages formed out of hazard ratios from antibiotic exposed strains compared to values from medium run strains. Level of resistance against colistin is illustrated in different colors (blue: colistin-susceptible, yellow: intermediate antibiotic resistant, red: highly antibiotic resistant). A) PA83 first and second run B) ID4 first and second run C) ID21 first and second run. Statistical analysis was performed by a frailty model and significant differences are indicated with asterisks ( $p < 0,05$ : \*,  $p < 0,01$ : \*\*,  $p < 0,001$ : \*\*\*).

### 3.4.1 Partly clear connection between loss of virulence and increasing MIC

As previously performed for the biofilm assays, the relationship between the death rate percentages and the strain's MIC was investigated using a Spearman correlation (Figure 11).

As expected, a strong negative correlation between the death rate percentages and the level of resistance to colistin could be determined for most strains, in line with the observed trend of virulence loss the longer the strains were exposed to colistin. This is represented by the Spearman correlation coefficient  $\rho$  that displays values from -1 to 0,3162, with 8 out of the 12 strains exposed to colistin ranging from -1 to -0,3162. This negative correlation indicates that the strains loose virulence the higher their colistin-MIC is.

Nevertheless, there were inconsistencies in this correlation looking at the different runs of ID 21 in particular: In the first run the death rate percentages even increase ( $\rho = 0,3162$ ) with rising MICs for both the colistin and the colistin and metronidazole condition. This pattern is consistent with observations of no

trend towards reduced virulence on prolonged exposure to colistin in this specific run of ID 21, described in 3.4 and visible in Figure 10 C.

Thus, although there were only a few significant decreases in virulence during the exposition to colistin, most strains showed a substantially reduced virulence the more colistin resistant they were, but with inconsistencies in the replicability of this development.

Again, a further analysis of the Spearman correlation for strains in the metronidazole condition was not implemented as none of the bacteria exposed to metronidazole have become resistant to colistin.

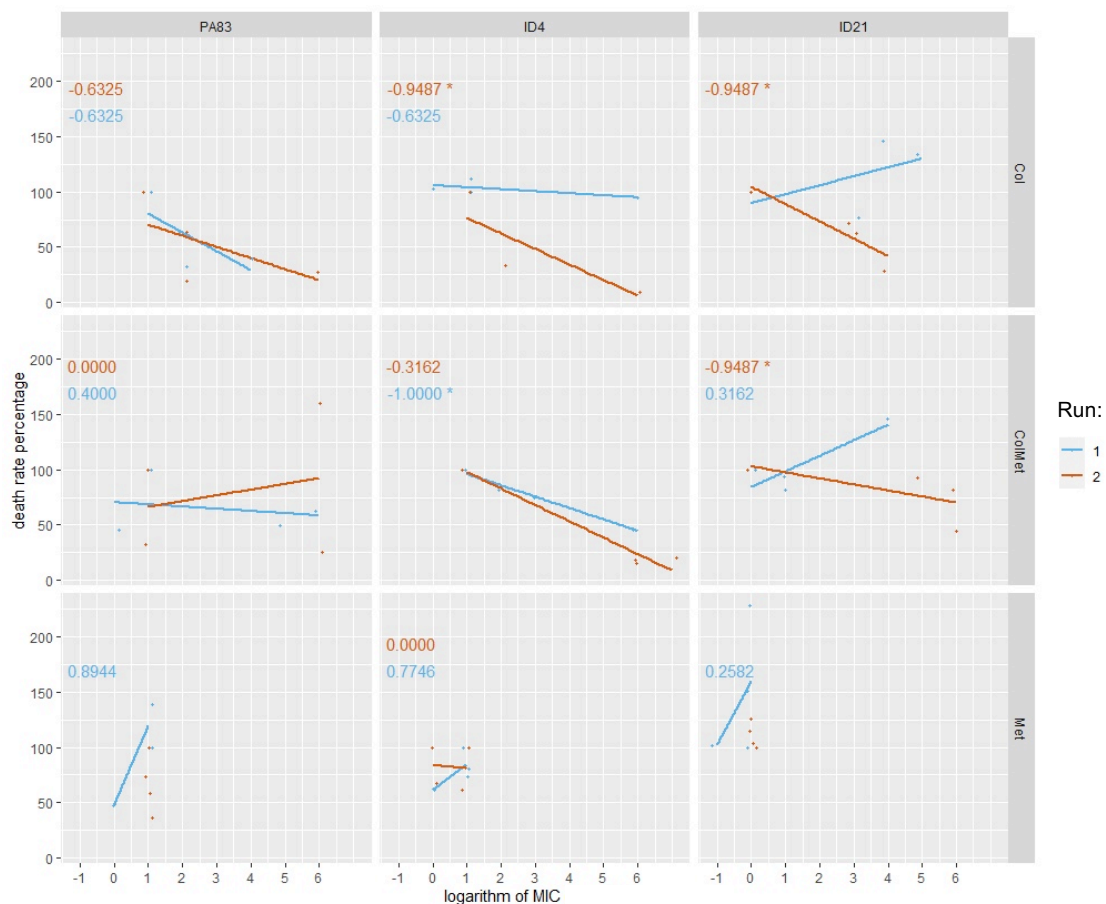


**Figure 11: Spearman correlation between ratios and MIC (*G. mellonella* infection model).**

Association between death rate percentages and the MIC of the strains was statistically tested by calculating the Spearman's correlation coefficient  $\rho$ . X-axis displays a logarithmic form of the strains MIC (3.2); y-axis shows the calculated ratios from 3.4. Numbers in the boxes represent the corresponding Spearman's correlation coefficient  $\rho$ . Selected data points were randomly "jittered" by small amounts for better visualization to prevent overplotting of data points. Few data points outside the range are not displayed in order not to reduce the scale of the images too much. Different morbidostat runs for the individual strains are illustrated in different colors (blue: first run; red: second run). Significant differences are indicated with asterisks ( $p < 0.1$ : \*,  $p < 0.05$ : \*\*,  $p < 0.01$ : \*\*\*).

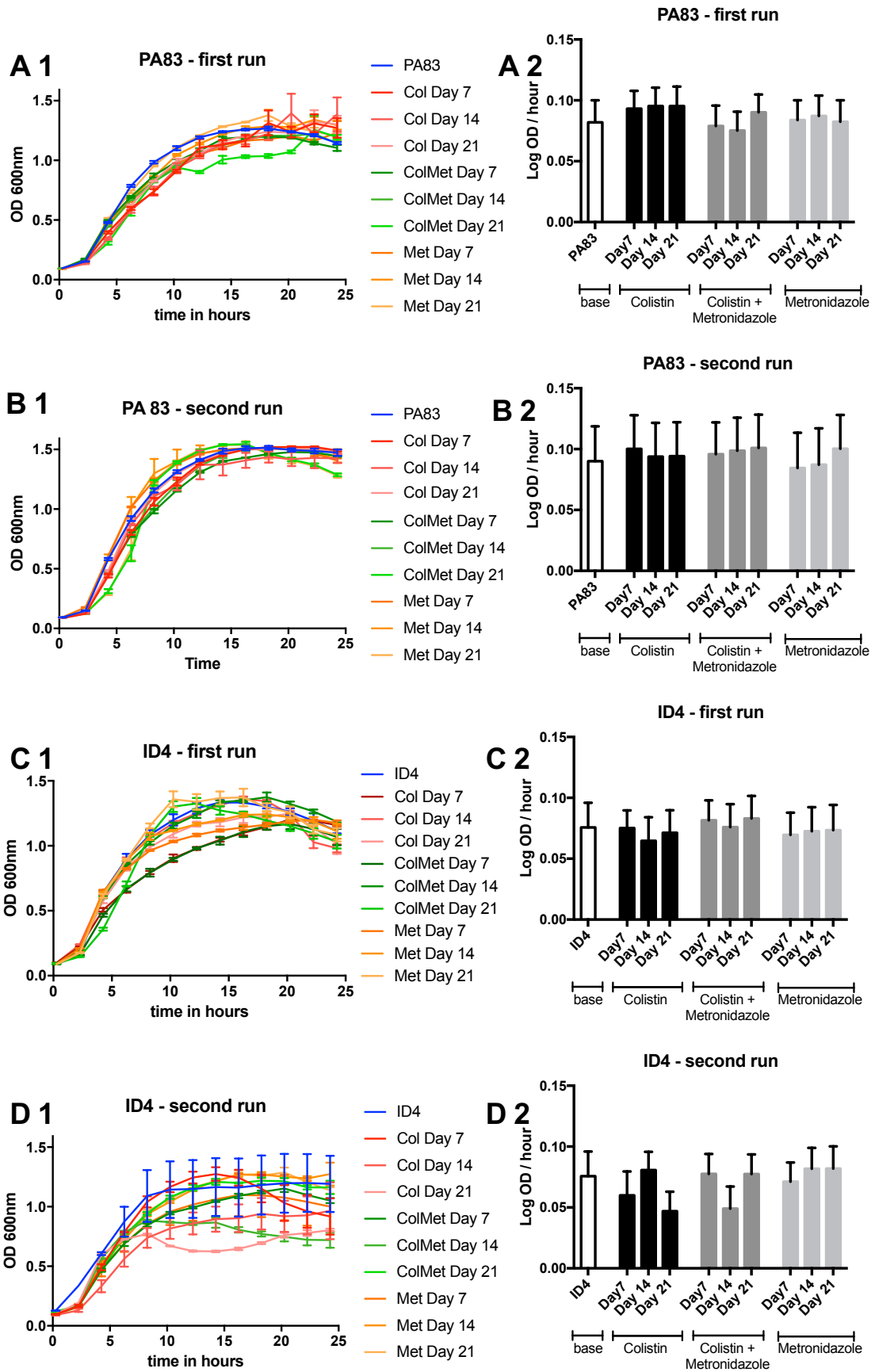
### **3.4.2 No growth restriction due to antibiotic exposure**

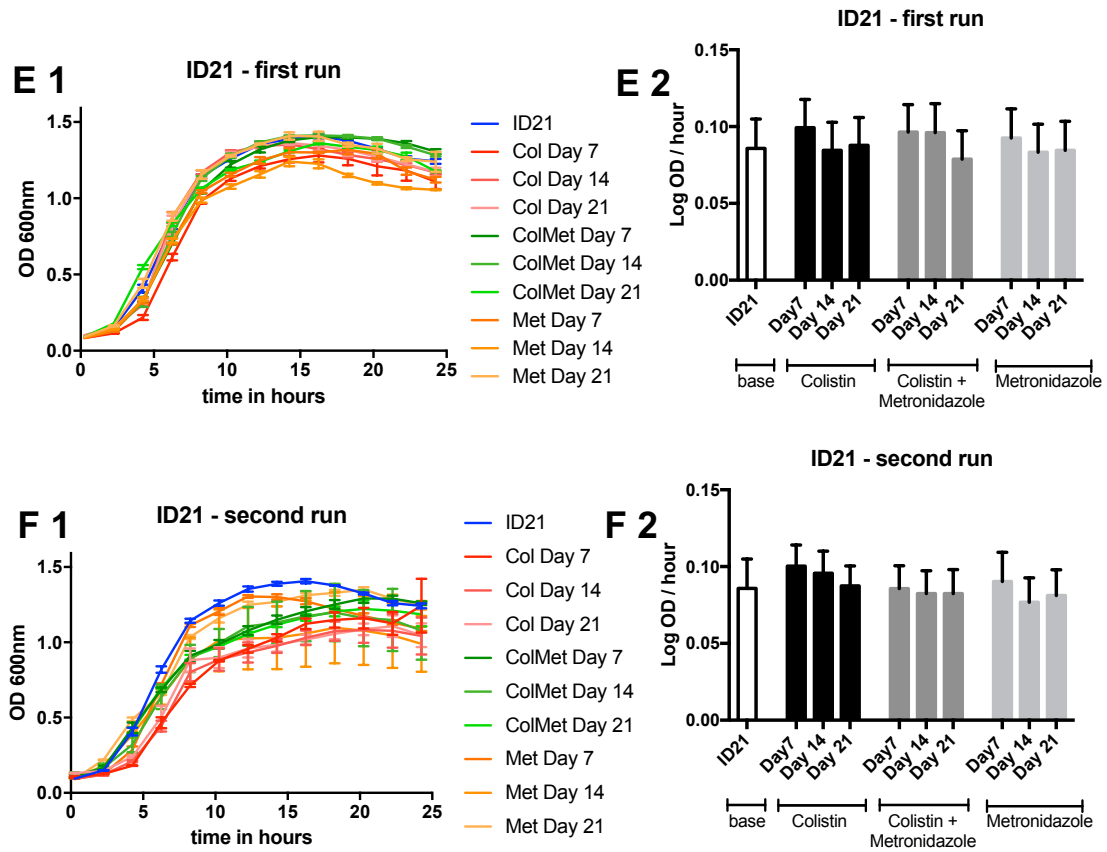
For each strain used in the *Galleria mellonella* infection model, growth potential was investigated in LB medium to determine whether evolution in the morbidostat results in fitness level reduction, which could - in parts - explain the observed loss of virulence.

Figure 12 shows the observed growth curves (Figure 12 A-F 1) alongside the corresponding kinetics of growth (Figure 12 A-F 2). The kinetic of growth is displayed as the linear regression of the growth curves which indicates how strongly the OD<sub>600nm</sub> has increased as a function of time. This has been added for a better comparison between the different growth curves and to detect modest differences.

The observations suggest that no strain changed substantially in its growth characteristic over time and under different conditions.

Thus, variations in virulence observed in the *Galleria mellonella* infection model are not likely due to reduced strain fitness.





**Figure 12: Growth curves and corresponding linear regression.** Growth curves were performed for every strain in LB. OD<sub>600nm</sub> was measured every 15 min for 24h (A-F 1). Kinetics of growth is displayed as linear regression of the growth curves (A-F 2). Values are means representing three replicates each, error bars display standard deviation. Col = colistin condition, ColMet = colistin and metronidazole combination condition, Met = metronidazole condition. A) PA83 first run, B) PA83 second run, C) ID4 first run, D) ID4 second run, E) ID21 first run, F) ID21 second run.

## 4 Discussion

In view of the increasing resistance of bacterial pathogens to antibiotic drugs and the impending post-antibiotic era, we will face challenges with infectious diseases that we were not used to before. Thus, understanding evolutionary pathways leading to resistance and the associated changes of phenotypic patterns leading to potentially differential clinical outcomes is of great importance. For this purpose, we investigated the impact of the last resort antibiotic colistin on the phenotypic evolution of clinical MDR *P. aeruginosa* strains.

Increased numbers of MDR- and XDR-*P. aeruginosa* related infections (Buhl *et al.* 2015) and the lack of novel antimicrobial agents (Livermore 2004) lead to the revival of the old antibiotic drug colistin as one of the last treatment options (Falagas *et al.* 2005). At present, emerging colistin-resistant Gram-negative pathogens leave clinicians dealing with limited or even no treatment options (Antoniadou *et al.* 2007) as well as uncertainty about the suspected changes of bacterial behavior during an infection.

A widespread phenomenon is the fitness loss after development of resistance as it has been shown, for example, in colistin-resistant *A. baumannii* (López-Rojas *et al.* 2011). However, the impact of the exposure to colistin on virulence and other clinically relevant phenotypic characteristics such as biofilm formation of *P. aeruginosa* in particular is largely unknown. These phenotypes are primarily dependent on the composition of the bacterial cell wall, which is influenced and altered during the development of colistin-resistance (Lee *et al.* 2016).

We exposed five different colistin-susceptible clinical isolates from *P. aeruginosa* bloodstream infections to an increasing concentration of colistin and acquired a total of 315 strains with a broad spectrum of colistin-resistance. Subsequently, we were able to investigate the biofilm formation and virulence for the strains during the development of resistance.

This was achieved by the morbidostat, a culture device that continuously puts the bacteria under pressure with constantly rising, subinhibitory antibiotic drug concentrations (Toprak *et al.* 2011). For instance, this setup could simulate a medical scenario in which the focus of a bacterial infection is in a compartment

of the body where the required antibiotic dose is not reached due to the pharmacokinetics or wrong dosage of the antibiotic drug, but bacteria are still exposed to sublethal concentrations. These sublethal antibiotic concentrations are a decisive element in the evolution of antibiotic resistance (Andersson *et al.* 2014) and has been shown several times to be a phenomenon occurring in *P. aeruginosa* in general (Jørgensen *et al.* 2013, Nair *et al.* 2013, McVicker *et al.* 2014). Although the morbidostat obviously does not accurately reflect reality, it is nevertheless a good approximation of an in vitro experiment to the true processes in the human body.

The frequency of mutations leading to resistance in the bacteria is increased by the induction of the SOS response, which is a cellular DNA repair mechanism activated by DNA damage (Cirz *et al.* 2006). One of the substances activating the SOS response and leading to a higher incidence of antibiotic resistance is metronidazole, as it has been shown in a combination therapy with ciprofloxacin and amikacin in *P. aeruginosa* (Hocquet *et al.* 2013). In addition to the phenotypic alternations, we investigated whether the same effect can be found for colistin by incubating clinical MDR *P. aeruginosa* strains with single colistin, a combination of colistin/metronidazole and single metronidazole.

For colistin, high antibiotic resistance emerged for nearly every strain within 21 days in the morbidostat. These findings correspond to the results of a morbidostat run with colistin previously performed by our group, in which colistin-resistance increased up to 100-fold within 20 days (Dößelmann *et al.* 2017). A similar pattern is found for strains from the combination condition, but with even higher MICs compared to the colistin condition. Furthermore, especially in the second morbidostat run, high levels of colistin-resistance were reached faster in the combination condition, with all strains reaching MICs equal to or above 16 µg/ml already after 14 days (compared to two out of five in the colistin condition). Thus, colistin-resistance developed slightly faster and to a higher extent by the addition of metronidazole, which is comparable but not as significant as the findings for ciprofloxacin and amikacin suggested (Hocquet *et al.* 2013). These results imply that the mutational frequency with respect to the development of antibiotic resistance may be enhanced in strains exposed to the combination of colistin and

metronidazole. However, this statement is not directly apparent from our analysis, in which we did not look for mutations at all, but only for the kinetics of certain phenotypes, in this case resistance to colistin.

Some of the strains showed a different development of resistance against colistin with an initial increase but a noticeable decline in resistance levels after 21 days. This could be explained by measurement errors in the BMDs or the Micronaut-S, considering that a high colistin concentration was required to maintain bacterial cultures in a stable growth state. Another explanation would be the persistence of susceptible dormant cells that survived the morbidostat run and were re-cultivated while performing the assay.

Since we could obtain a large number of strains with varying colistin exposure time and resistance from different clinical *P. aeruginosa* isolates, we were now able to analyze the impact on the phenotypic characteristics such as biofilm formation. *P. aeruginosa* biofilms are frequently associated with causing device related bloodstream infections and pneumonia. Thereby, within a biofilm bacteria are not only difficult to access by antibiotics, but also the resulting continuous bacteremia leads to more severe infection with severe clinical outcome (Bekaert *et al.* 2011, Mulcahy *et al.* 2014, Maurice *et al.* 2018).

We conducted two different biofilm assays. One staining the biofilm with crystal violet focusing on the biomass in the biofilm (Wilson *et al.* 2017). The other one using the pegs of a TSP and counting the number of viable cells in the biofilm. While the crystal violet staining method showed irregular alterations of the biomass formed in the biofilm with a clear trend towards a peak value after 14 days and a subsequent decline, the peg-lid method evidently demonstrated a significant increase of viable bacterial cells the longer they were incubated in colistin enriched medium. There was no distinct difference comparing the colistin to the colistin and metronidazole condition. Moreover, investigating the relationship between the produced biofilm and the level of colistin resistance, there is also a clear increase in the number of viable cells produced in the biofilm with increasing colistin resistance, while there is no clear correlation or even rather a decreasing relationship between the total biomass and the colistin MIC.



However, the wide dispersion of the values in the crystal violet assay makes it difficult, especially for the correlation analysis, to make reliable statements.

To our knowledge, the correlation between antibiotic exposure and biofilm formation in *P. aeruginosa* is currently unclear. In the past years, several studies on both *P. aeruginosa* and related Gram-negative bacteria have led to contradictory results. Whereas Gurung *et al.*, Abidi *et al.*, and Karami *et al.* reported about the significantly high prevalence of multi drug-resistance among strong biofilm producing *P. aeruginosa* (Abidi *et al.* 2013, Gurung *et al.* 2013, Karami *et al.* 2020) and *A. baumannii* respectively (Gurung *et al.* 2013), Qi *et al.*, Rodriguez-Bano *et al.*, and Kamali *et al.* presented contrary results for *P. aeruginosa* (Kamali *et al.* 2020) and *A. baumannii* (Rodríguez-Baño *et al.* 2008, Qi *et al.* 2016). Furthermore, the role of colistin in particular is even less understood. Similar to our results of the peg-lid method suggesting an increase in biofilm producing cells, Sato *et al.* showed a positive correlation between biofilm formation in MDR *A. baumannii* and the exposure to sub-MIC concentrations of colistin and polymyxin B (Sato *et al.* 2018). However, other studies found a significant defective biofilm produced by colistin-resistant *A. baumannii* (Dafopoulou *et al.* 2015) and *P. aeruginosa* respectively (Azimi *et al.* 2019) compared to colistin-susceptible strains. It must be noted, that Azimi *et al.*'s study only conducted a crystal violet-based assay, which is comparable to our crystal violet experiment, in which we were at least not able to see a significant increase in biomass of the biofilm correlating to colistin-resistance either.

A possible explanation for the divergent results in the literature in general terms might be the different mechanisms of colistin-resistance, with some strains acquiring resistance through LPS-deficiency, whereas most strains obtain it through LPS-mutations and modifications as Farshadzadeh *et al.* speculated for *A. baumannii* (Farshadzadeh *et al.* 2018). In addition, the great advantage of our study design is the fact that we followed the phenotypic evolution during the development of colistin-resistance of the individual clinical isolates, while most of the studies mentioned above looked at snapshots in the behavior of different bacterial strains.

A major difference between Sato *et al.*'s and Azimi *et al.*'s studies is the fact that Sato *et al.* investigated the biofilm formation after exposure to colistin, while Azimi *et al.* analyzed the biofilm formation of colistin-resistant *P. aeruginosa* strains. A difference between pure exposure to colistin and the development of colistin-resistance can also be found in our results: The second run of ID 40 presents the same pattern of significant increased viable cells in the biofilm produced by the bacteria as almost all our strains show, although resistance tests showed decreasing levels of colistin-resistance after 21 days after an initial MIC-increase. This finding is reflected in the correlation analysis, which revealed only a weak correlation between living cells in the biofilm and the colistin-MIC, as an exceptional case for this strain.

This singular result does not guarantee for a definite conclusion but suggests that it is not the acquisition of colistin resistance itself, but the exposition to colistin might be the underlying cause of the changes in the biofilm observed in the peg-lid biofilm assay. Yet, if this presumption is confirmed, it would mean that *P. aeruginosa* could exhibit altered phenotypic characteristics through contact with sublethal concentrations of colistin alone, even without the emergence of resistance.

Additionally, the observation of irregular alterations of the biomass formed in the biofilm with increasing values after 14 days and a subsequent decline in combination with the weak correlation between biomass and MIC in the crystal violet assay indicates that not only changes in the LPS could be the cause of colistin resistance, because if that would be the case, a linear relationship between the variables would be expected. This supports the assumption that other mechanisms apart from the development of resistance may also occur under the influence of colistin, which can lead to phenotypic changes in *P. aeruginosa*.

On the other hand, we can only make definite statements about the relationship between the phenotypic changes that we observed in the bacteria and colistin exposure, as the Spearman correlation analysis is not the main focus of our study and only provides a rough estimation of the true link between colistin-resistance and the phenotype of *P. aeruginosa*. For more precise statements on that

relationship, further experiments would have to be carried out that can detect the changes on a genetic level. Such an analysis could, for example, be carried out via Next Generation Sequencing (NGS), in which certain mutations are sought during evolution in the bacteria, that could explain both the phenotypic changes and the development of resistance against colistin.

However, considering we discovered divergent results in the two different assays, we speculate that the composition of the biofilm might have changed during colistin exposure. While the overall biomass of the biofilm was not affected, there may be more viable cells in biofilm that produce relatively less matrix. If this is the case, this would have a remarkable influence on the clinics, as bacteria from a biofilm could detach and manage to spread more easily in the bloodstream, possibly causing bacteremia and sepsis.

In order to really confirm that the alterations in biofilm production of *P. aeruginosa* during colistin exposure and the development of colistin resistance are indeed clinically relevant and important for the patients' outcome further investigations need to be carried out. Thus, biofilm formation should be tested in a flow model in urinal or central venous catheters in order to simulate an even more accurate scenario of one of the major risk factors of biofilm formation leading to bloodstream infections. Furthermore, the experiments conducted in this study involve only a small number of clinical isolates and therefore have limited information on the general behavior of the bacteria under the influence of the antibiotics.

Another important aspect regarding the biofilm experiments is the use of Poly-L-Lysine in the peg-lid assay (2.6.3). Poly-L-Lysine is a cationic polymer that helps different types of cells to bind to negatively charged surfaces like plastic polymers or glass (Huang *et al.* 1983, Takahashi *et al.* 1992, Morga *et al.* 2015). To date, it has been widely used as a standard tool to enhance the attachment of bacterial cells to multiple surfaces and therefore improve biofilm formation on the coated region (McEachran *et al.* 1986, Cowan *et al.* 2001). Yet, it has been established that Poly-L-Lysine can also have antimicrobial effects on the bacteria, especially if applied as thick coating (Shima *et al.* 1984, Colville *et al.* 2010) and may even be used as a treatment for *P. aeruginosa* biofilms (Guillon *et al.* 2018).

In that respect, the use of Poly-L-Lysine in this biofilm experiment can be considered as novel and effective, but irregular results between the different assays and strains could be attributed to its antimicrobial activity.

Considering the importance of virulence, the degree of virulence in *P. aeruginosa* is multifactorial and may be variable from one strain to the other (Lee *et al.* 2006), which makes it extremely difficult to estimate the outcome of an infection.

As mentioned above, the acquisition of antibiotic resistance is often connected to a fitness cost or loss of virulence and has even been displayed in colistin-resistant *A. baumannii* (López-Rojas *et al.* 2011). However, to our knowledge it has never been shown following the evolution of clinical *P. aeruginosa* isolates during long-term exposure to colistin.

We decided to quantify virulence using *G. mellonella* larvae as an animal infection model. In recent years, the introduction of the *G. mellonella* infection model has become widespread, as it provides a great *in vivo* test with well-known immune response mechanisms. It has been used effectively in testing novel therapeutics and the characterization of host-pathogen interaction for multiple microbial organisms (Pereira *et al.* 2018, Cutuli *et al.* 2019). This gave us the opportunity of a semiquantitative, high-throughput model, that was ideal for the comparison of the large number of strains obtained during the morbidostat runs. As explained in 3.4, the assay was only performed with the strains PA83, ID4 and ID21.

Although almost all strains showed the expected trend of an impaired virulence the longer they were exposed to the antibiotics in the morbidostat, there were only a few with significant reductions. Again, there was no difference comparing the colistin and the colistin and metronidazole combination condition. Nevertheless, taking the correlation analysis into account, most strains showed considerably lower virulence the more colistin-resistant they were, but with inconsistencies in the reproducibility of this development between the different runs.

In general, these results roughly reflect the common perception of a trend towards reduced virulence associated with the acquisition of antibiotic resistance. Apart from the fitness cost, impaired virulence and reduced expression of virulence

factors that has been shown several times for colistin-resistant *A. baumannii* (Fernández-Reyes *et al.* 2009, López-Rojas *et al.* 2011, Rolain *et al.* 2011) and *Klebsiella pneumoniae* (Choi *et al.* 2015), Gomez-Zorrilla *et al.* also displayed a similar behavior for MDR *P. aeruginosa* in murine models (Gómez-Zorrilla *et al.* 2016). Furthermore, in a competition assay Lee *et al.* presented that fitness was decreased when *P. aeruginosa* strains developed resistance to colistin (Lee *et al.* 2016). However, in our experiment only few highly antibiotic resistant strains (especially ID4) showed a significantly impaired virulence, with some strains (PA83 and the first run with ID21) indicating no significant changes in their performance in the infection model at all. This observation may be explained by the different resistance mechanisms that affect the LPS of the outer membrane in other ways. This theory is based on the findings of Wand *et al.* and Beceiro *et al.*, who detected a significantly reduced virulence in some of the colistin-resistant *A. baumannii* compared to their baseline strains, but not in the strains that developed resistance through mutations in *prmB* (Beceiro *et al.* 2014, Wand *et al.* 2015). Thus, this might be an indication for strain-specific differences in evolution under antibiotic exposure, which lead to individual adaptations in terms of virulence. Such individual evolutionary paths would also provide an explanation for the sometimes even ascending virulence values that do not fit the pattern of a steady decrease. To further investigate these strain-specific evolutionary trajectories and identify the connection to the different mechanisms of resistance against colistin it would be necessary to sequence all the strains and examine their genome for the corresponding mutations.

Moreover, the inconsistencies in the reproducibility between the different runs might be an indication of different evolutionary trajectories the strains could have. Although the strains became equally resistant in both runs after 21 days, their phenotypic behavior (in this case virulence) did not change to the same extent. Sequencing of the strains might help to find accompanying mutations, which explain the phenotypic changes without a direct connection to the antibiotic resistance.

However, it is difficult to draw definite conclusions out of our results, and the study would benefit from a higher number of strains and replicates in order to confirm

the phenotypic effects we have seen so far. The smaller number of strains used may be an explanation for the lack of significant results.

In addition, the virulence of selected strains could be further analyzed by a murine model or an *in vitro* phagocytic assay, both are superior in the transfer to the immune reactions of the human body compared to the *G. mellonella* model.

Furthermore, the strains' fitness was assessed using standard cell growth assay in LB medium. In contrast to virulence, which is a quantitative term describing the severity of an infection caused by an organism (Steinhaus *et al.* 1970, Shapiro-Illan *et al.* 2005), bacterial fitness displays the reproductive success in a given environment (Elena *et al.* 2003). During the long-term incubation in the morbidostat and the acquisition of antibiotic resistance, it could be assumed that the general thrive of the bacteria to replicate is lowered, as it has been shown in multiple studies (Levin *et al.* 1997, Melnyk *et al.* 2015). Considering we did not observe any significant reductions in growth rates in the LB-medium of the strains over time and under different conditions, there is no substantial evidence of a fitness cost in our *P. aeruginosa* strains under the antibiotic pressure in the morbidostat. Hence, the variations in virulence observed in the *Galleria mellonella* infection model are not caused by a reduced strain fitness.

In view of our results, the extent to which virulence or fitness is attenuated via the evolution of colistin-resistance could be less predictable than previously assumed. Thus, to transfer this to clinical application, the emergence of colistin-resistant *P. aeruginosa* could be an even more important threat for hospitals and patients. In fact, some of the pathogens would be untreatable and just as dangerous as before. In order to be able to predict such an evolution in the individual bacteria, it would be necessary to investigate the bacterial genome and detect parameters such as biomarkers that correlate with their phenotypic development. This would potentially allow us to assess the outcome of an infection on a case-by-case basis.

Metronidazole currently belongs to the first-line antibiotic treatment options against infections of all kinds caused by anaerobic bacteria (Freeman *et al.* 1997, Brook 2016, Dingsdag *et al.* 2017) and is part of the therapy against *H. pylori*

(Löfmark *et al.* 2010). Thus, there is a considerable probability that patients with *P. aeruginosa* infections may also require metronidazole as a therapy of a co-infection with anaerobic bacteria or to prevent gastrointestinal infections during surgery (Giske *et al.* 2017). However, despite having no antimicrobial effect on aerobic *P. aeruginosa* Hocquet *et al.* found increased and faster resistance emerging against ciprofloxacin and amikacin in *P. aeruginosa* if combined with metronidazole (Hocquet *et al.* 2013). This results from the induction of the SOS response by metronidazole, which increases the mutational frequency in the bacteria (Cirz *et al.* 2006, Hocquet *et al.* 2013).

We investigated whether this phenomenon also applies to and influences the phenotypical changes in *P. aeruginosa* during the development of colistin-resistance. First of all, the addition of metronidazole led to faster and higher antibiotic resistance against colistin. Especially in the second run, high levels of antibiotic resistance were reached in all strains by day 14 in the combination condition, while only two out of the five strains obtained this in the colistin condition. However, neither the biofilm assays nor the *G. mellonella* infection model showed significant differences between the colistin condition and the colistin and metronidazole combination.

Therefore, we assume that metronidazole may lead to alterations in the mutational activity in the bacteria, but this effect may only be recognizable if there is a certain selection pressure that drives this process. This would explain the (at least somewhat) faster development of antibiotic resistance under the pressure of colistin, while there is no selection advantage for the bacteria in the evolution of biofilm formation or virulence. However, this analysis is purely descriptive and requires further detailed experiments on a genetic basis and statistical analysis to make a definitive statement on this issue.

Comparing the two morbidostat runs, the main difference between them was the approach of re-cultivation after taking samples from the morbidostat: While the bacteria were grown in liquid culture using LB medium for the first run, they were cultivated on blood agar plates containing different concentrations of colistin for the second run, depending on the level of resistance for each individual strain.

The second method was implemented to guarantee the selection of the generated *P. aeruginosa* strains and ensure the purity of the resistant population. In contrast to the first run, resistance emerged particularly faster in the second run, with seven out of ten highly colistin resistant strains compared to two out of ten in the first run after 14 days of exposure to colistin. After 21 days nearly all strains exposed to colistin were classified as highly antibiotic resistant. In terms of the phenotypic assays, the basic message and the conclusions that can be drawn from the experiments do not vary between the two runs. This suggests that the evolutionary trajectories of the strains are more or less replicable and individually characteristic for most strains. However, the results were even more distinct and also more often significant in the strains acquired from the second run, for both the biofilm (particularly for the peg-lid method) and the virulence experiments. This could be attributed to the intended and expected effect that by cultivating the strains on an antibiotic-containing medium, only a selection of the desired resistant bacteria remained in the morbidostat and potential non-resistant persister cells were eliminated. In order to confirm this theory, it might be useful to assess the metabolic activity in the strains under the influence of sublethal colistin concentrations, e.g. by adding metabolites, which can be detected via fluorescence-activated cell sorting (FACS) analysis after metabolisation, as a reduced metabolism seems to be decisive for persister cells (Wood *et al.* 2013).

Concluding, the morbidostat culture device enabled us to simulate a clinical scenario in which *P. aeruginosa* strains spread from a compartment within the human body where the dosage of the antibiotic colistin does not exceed sublethal concentrations. The constant antimicrobial pressure led not only to the emergence of colistin resistance, but also to specific alterations in other phenotypic features. Those, in particular, were irregular changes in the biomass with significantly more viable cells in the biofilm formed by the bacteria. While in most cases virulence declined with colistin exposure, not all strains displayed the same pattern and extent of attenuation. The addition of metronidazole as a drug which presumably affects the mutational frequency in the bacteria caused faster antibiotic resistance, without this being statistically verifiable with our analysis and



without distinct variations in other phenotypes. In view of the results in this study, we suppose that antibiotic treatment with colistin may result in strain-specific, changing bacterial features in the course of an infection.

Thus, the next essential step would be to sequence all of our collection of strains and to compare the genetic variations between the different isolates as well as the strains in the course of time during the acquisition of colistin-resistance. This may explain the varying evolutionary trajectories of the isolates in the morbidostat on a genetic level. As a result, it may be possible to find specific mutations or distinct genetic preconditions in some *P. aeruginosa* that correlate with the probability of a certain evolution during the exposure to colistin, for example resistance development and the extent of phenotypic changes. In consequence, such biomarkers could be key to predict a strain's evolution under a certain antibiotic treatment, allowing doctors to optimize the treatment from the very start in consideration of what we call a "personalized medicine".

## 5 Summary

*Pseudomonas aeruginosa* is one of the most dangerous opportunistic bacteria in hospital acquired infections and ICU patients in recent times. With its variety of virulence factors and its ability to maintain in moist environments and to form biofilms it can cause wound infections, pneumonia and septicemia.

Especially the rising number of multi-drug-resistant (MDR) strains poses a threat to healthcare facilities, which is why *P. aeruginosa* is listed as one of the critical priority pathogens with by the WHO. For this reason, colistin, an antibiotic that had almost disappeared as a form of treatment, requires increasing use as a last-resort antibiotic.

The impact of subinhibitory concentrations of colistin on bacterial traits like virulence and biofilm formation in clinical *P. aeruginosa* isolates is largely unexplored. Moreover, the effect of metronidazole, a drug with no bactericidal effect on *Pseudomonas* but has been shown to induce mutagenesis, could be important for the phenotypic evolution of the bacteria.

We applied a morbidostat as a culture device, that can automatically adapt the required concentrations of antibiotics to allow consistent growth while still challenging the bacteria, with the three conditions colistin, metronidazole and a combination of the two antibiotics.

Over a time period of 21 days of incubation performed in two replicates we were able to acquire a total of 315 strains of which 105 have been used for the phenotypic experiments. Most strains exposed to colistin became highly antibiotic resistant after 21 days of incubation, even though the majority in the combination condition reached this threshold already by day 14.

A series of assays were performed to elucidate the changes in bacterial phenotype. Exposure to colistin resulted in irregular alterations in the overall biomass of the biofilm with rising and falling amounts along the incubation, but also a significant increase in viable cells in the biofilm. Correlating the cell density of the biofilm to the level of colistin resistance mainly showed positive correlation, although one exceptional development indicates that exposure to colistin may be key to phenotypic changes not resistance alone. This suggests that the exposure to colistin might lead to changes in the composition in the biofilm with more cells

in relatively less biomatrix. While in most cases virulence decreased with colistin exposure, not all strains displayed the same pattern and extent of attenuation, which makes it very difficult to predict the strains' development in individual cases. The loss in virulence could not be attributed to an impaired growth potential of the strains, as there was no noticeable difference in growth kinetics before and after the incubation. The addition of metronidazole caused faster antibiotic resistance, without this being statistically verifiable with our analysis and without distinct variations in other phenotypes.

Concluding, the morbidostat culture device enabled us to simulate a clinical scenario in which *P. aeruginosa* strains spread from a compartment within the human body where the dosage of the antibiotic colistin does not exceed sublethal concentrations. The constant antimicrobial pressure led not only to the emergence of colistin resistance, but also to specific alterations in other phenotypic features. In view of our results in this study, we suppose that antibiotic treatment with colistin may result in strain-specific, variable bacterial features in the course of an infection, which might make it extremely difficult to treat the individual infection.

Further investigation of these strains' specific evolutions on a genetic level and the search for potential biomarkers that could help predict the bacterial behavior, could be key to an optimized treatment of a severe infection with *P. aeruginosa*.

## 6 Zusammenfassung auf Deutsch

*Pseudomonas aeruginosa* wurde in den letzten Jahren zu einem der gefürchtetsten opportunistischen Bakterien für Krankenhausinfektionen, insbesondere für Patienten auf der Intensivstation. Mit seiner Vielfalt an Virulenzfaktoren und seiner Fähigkeit, sich in feuchter Umgebung zu vermehren und Biofilme zu bilden, kann es Wundinfektionen, Lungenentzündungen oder Sepsen verursachen.

Insbesondere die steigende Zahl multiresistenter Stämme stellt eine Bedrohung für Gesundheitseinrichtungen dar, weshalb *P. aeruginosa* von der WHO als einer der kritischen Erreger gelistet wird. Daher muss zunehmend Colistin, ein Antibiotikum, das fast vom Markt verschwunden war, als Reserveantibiotikum eingesetzt werden.

Der Einfluss von subinhibitorischen Konzentrationen von Colistin auf bakterielle Eigenschaften wie Virulenz und Biofilmbildung bei klinischen *P. aeruginosa*-Isolaten ist weitgehend unerforscht. Darüber hinaus könnte die Wirkung von Metronidazol, einem Medikament, das selbst keine bakterizide Wirkung auf *Pseudomonas* hat, aber nachweislich deren Mutagenese induziert, wichtig für die phänotypische Evolution der Bakterien sein.

Wir setzten einen Morbidostat als Kultivierungsgerät ein, das automatisch die erforderlichen Antibiotikakonzentrationen so anpassen kann, dass ein gleichmäßiges Wachstum trotz dauerhaftem Stress für die Bakterien möglich ist. Dabei verwendeten wir drei verschiedene Ansätze an Antibiotika: Colistin, Metronidazol und eine Kombination der beiden Antibiotika.

In zwei Inkubationsdurchläufen über je 21 Tage konnten wir insgesamt 315 Stämme gewinnen, von denen 105 für die phänotypischen Experimente verwendet wurden. Die meisten Stämme, die Colistin ausgesetzt waren, wurden nach 21 Tagen Inkubation hochgradig antibiotikaresistent, wobei die Mehrheit aus der Kombinationsgruppe diese Schwelle bereits an Tag 14 erreichte.

Anschließend wurde eine Reihe von Versuchen durchgeführt, um die Veränderungen der bakteriellen Phänotypen zu ermitteln. Die Exposition gegenüber Colistin führte zu unregelmäßigen Veränderungen in der Gesamtbiomasse des Biofilms mit zunächst steigenden und anschließend wieder

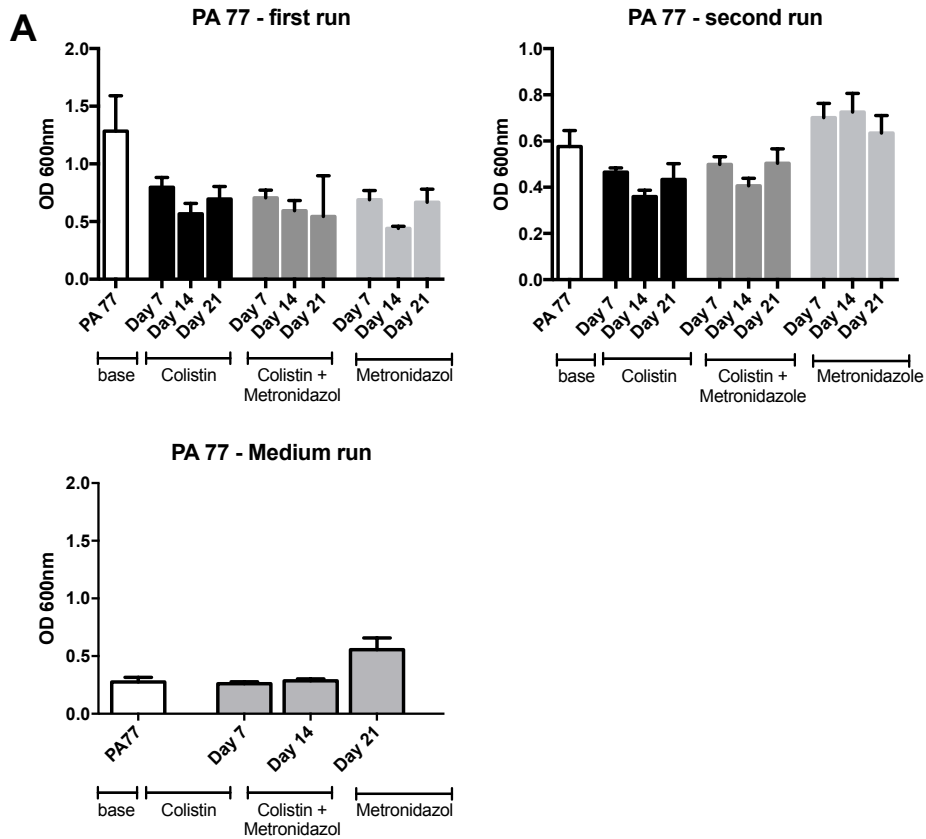
fallenden Mengen bei längerer Inkubation, aber auch zu einer signifikanten Zunahme der lebensfähigen Zellen im Biofilm. Die Zelldichte des Biofilms korrelierte weitestgehend positiv mit dem Grad der Colistinresistenz. Eine abweichende Entwicklung in einem Stamm weist jedoch darauf hin, dass der Schlüssel zu den phänotypischen Veränderungen nicht die Resistenz allein, sondern die Exposition gegenüber Colistin sein könnte. Diese Ergebnisse deuten darauf hin, dass die Exposition gegenüber Colistin zu Veränderungen in der Zusammensetzung des Biofilms mit mehr Zellen in verhältnismäßig weniger Biomatrix führen könnte. Während überwiegend die Virulenz mit der Colistinexposition abnahm, zeigten nicht alle Stämme das gleiche Muster und das gleiche Ausmaß an Abschwächung. Dies macht es sehr schwer, die Entwicklung der Stämme im Einzelfall vorherzusagen. Der Virulenzverlust konnte dabei nicht auf ein vermindertes Wachstumspotenzial der Stämme zurückgeführt werden, da kein merklicher Unterschied in der Wachstumskinetik vor und nach der Inkubation zu beobachten war. Die Zugabe von Metronidazol bewirkte eine schnellere Antibiotikaresistenz, wobei dies mit unserer Analyse statistisch nicht auswertbar war. Es zeigten sich aber keine signifikanten Veränderungen in anderen Phänotypen.

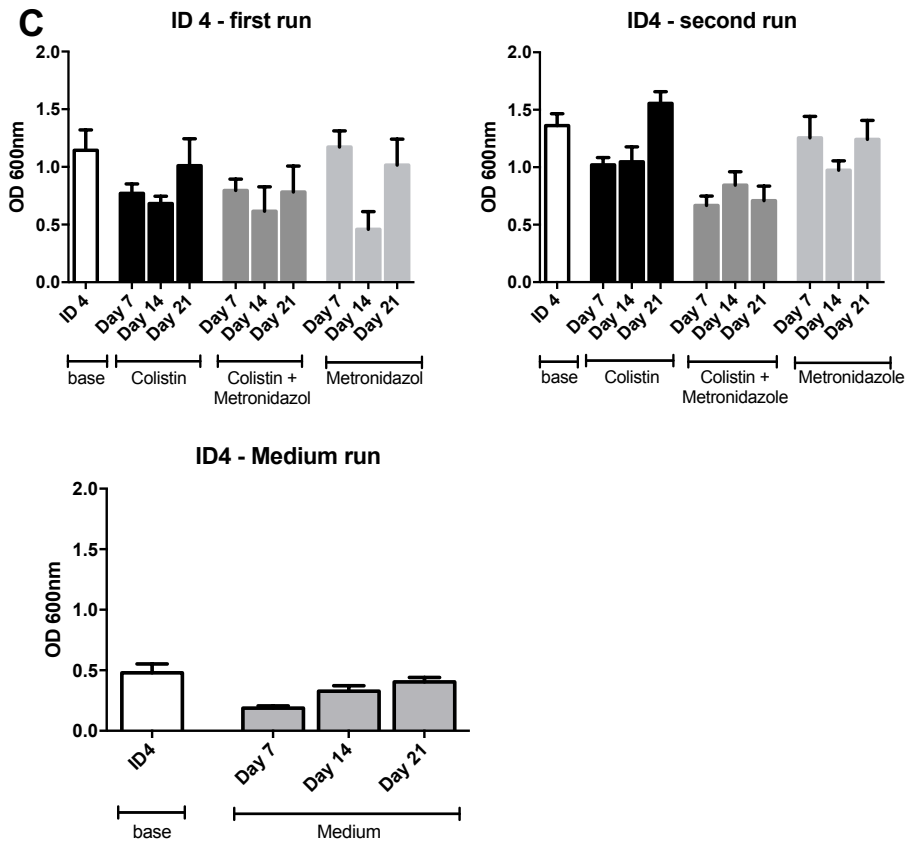
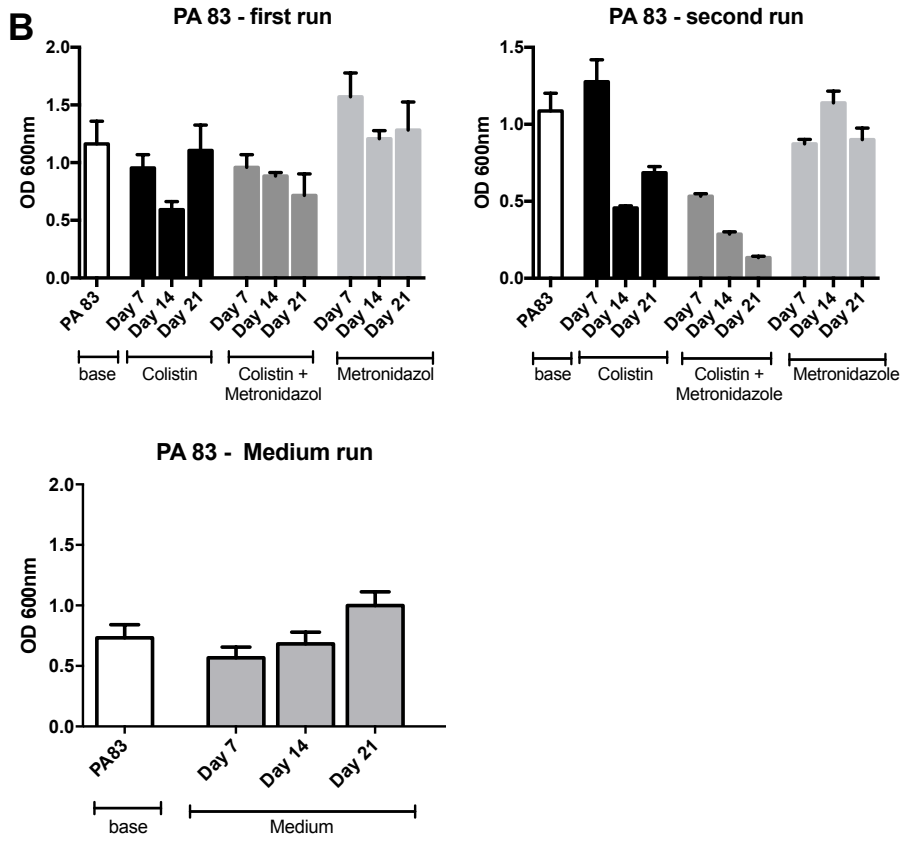
Zusammenfassend lässt sich sagen, dass wir mit dem Morbidostat ein klinisches Szenario simulieren konnten, in dem sich *P. aeruginosa*-Stämme in einem Kompartiment im menschlichen Körper ausbreiten, in dem die Dosierung des Antibiotikums Colistin subletale Konzentrationen nicht überschreitet. Der konstante antimikrobielle Druck führte nicht nur zur Entstehung einer Colistinresistenz, sondern auch zu spezifischen Veränderungen anderer phänotypischer Merkmale. In Anbetracht unserer Studienergebnisse vermuten wir, dass eine antibiotische Behandlung mit Colistin zu stammspezifisch variablen bakteriellen Eigenschaften im Verlauf einer Infektion führen kann. Dies könnte die Behandlung der individuellen Infektion deutlich erschweren.

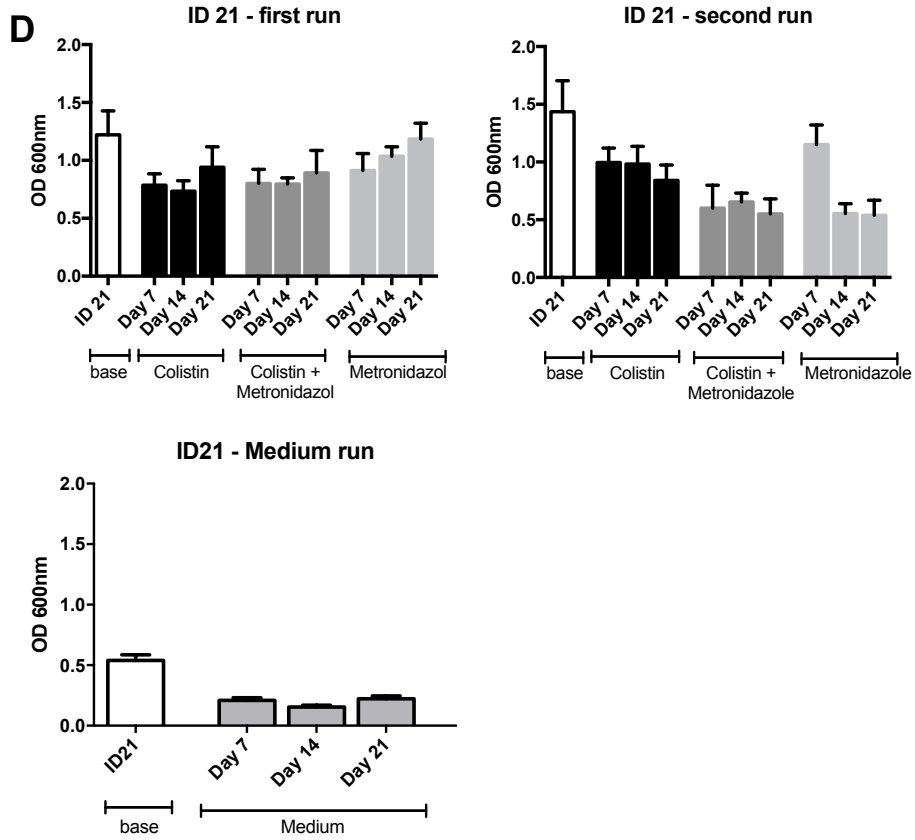
Es bedarf weiterer Untersuchungen der spezifischen Entwicklung dieser Stämme auf genetischer Ebene und die Suche nach potenziellen Biomarkern, die dabei helfen könnten, das bakterielle Verhalten vorherzusagen, um die Behandlung schwerer Infektionen mit *P. aeruginosa* optimieren zu können.

## 7 Supplementary

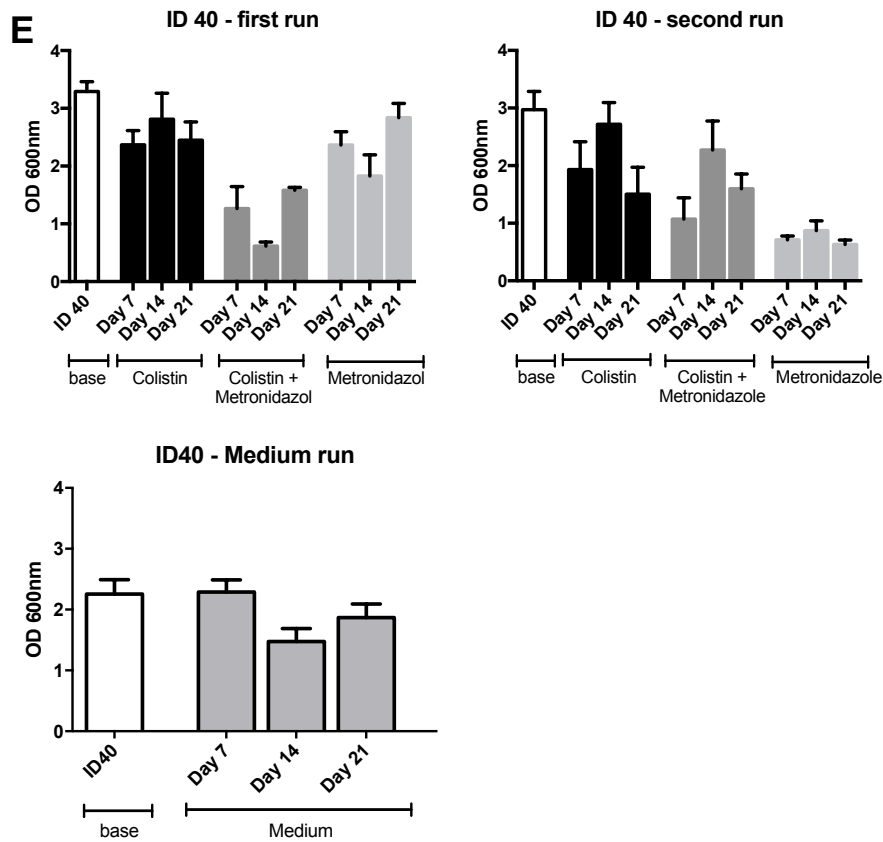
### 7.1 Crystal violet staining method - OD<sub>600nm</sub> values





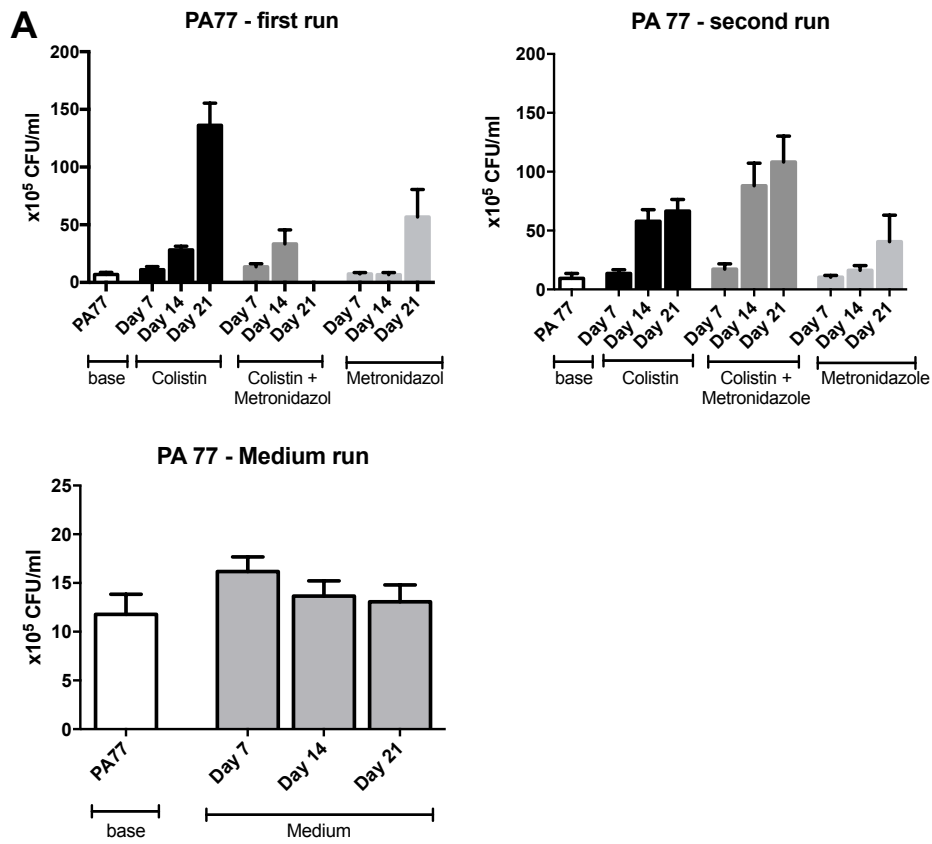


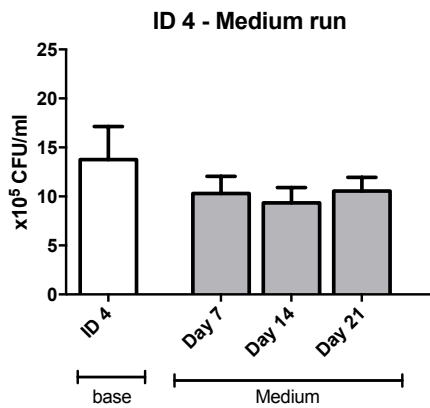
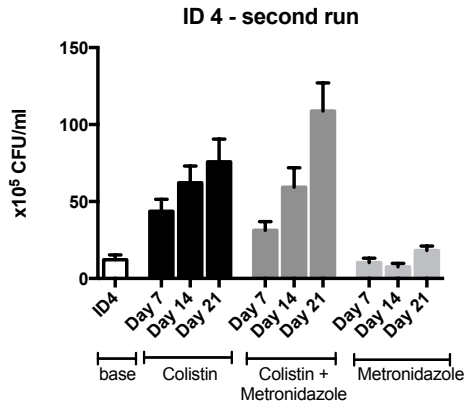
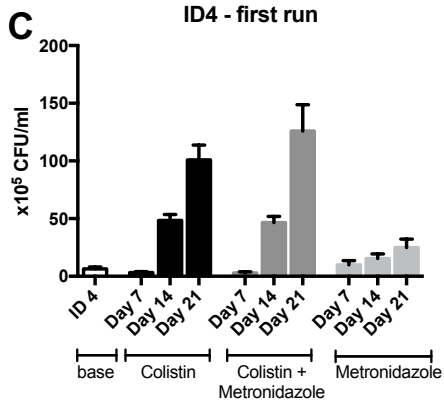
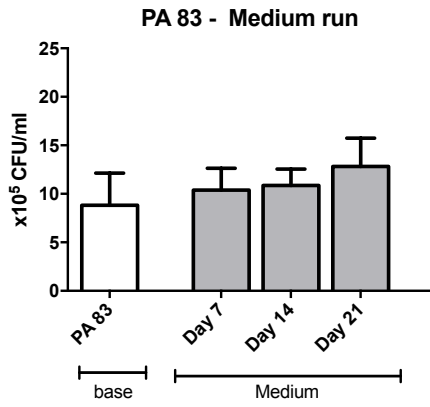
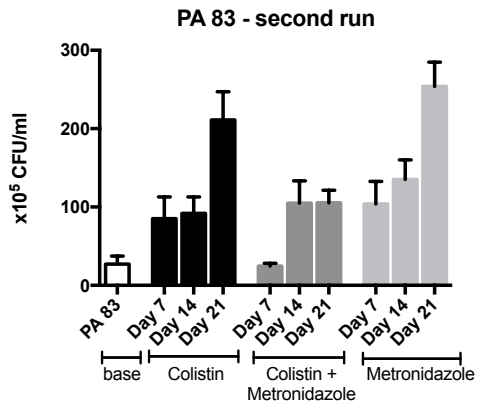
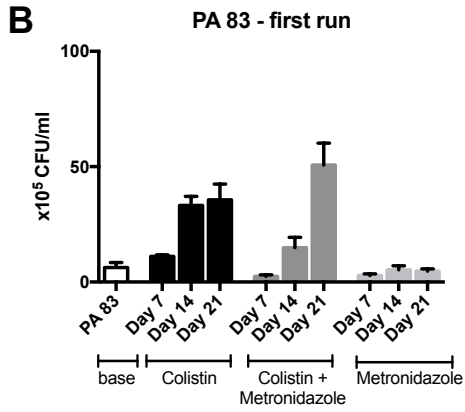


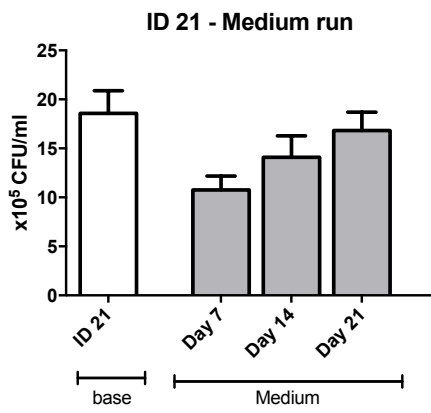
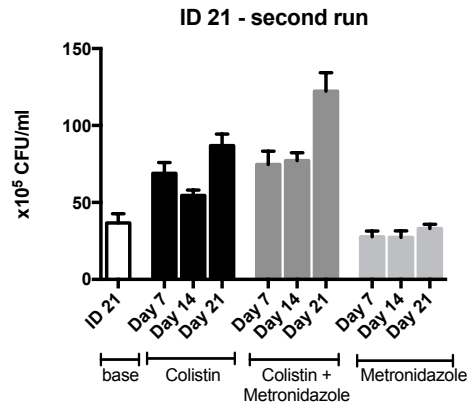
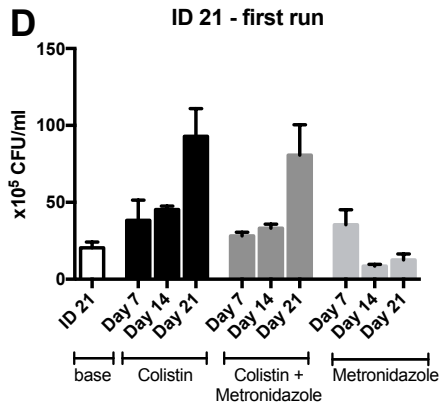


**Figure 13: Results for crystal violet staining biofilm assay.** Biofilm was grown a 96-well plate and stained using crystal violet. The figure shows the OD<sub>600nm</sub> that was measured to quantify the amount of biofilm. A) PA77 first -, second - and medium run B) PA83 first -, second - and medium run C) ID4 first -, second - and medium run D) ID21 first -, second - and medium run E) ID40 first -, second - and medium run.

## 7.2 Peg-lid method – CFU count







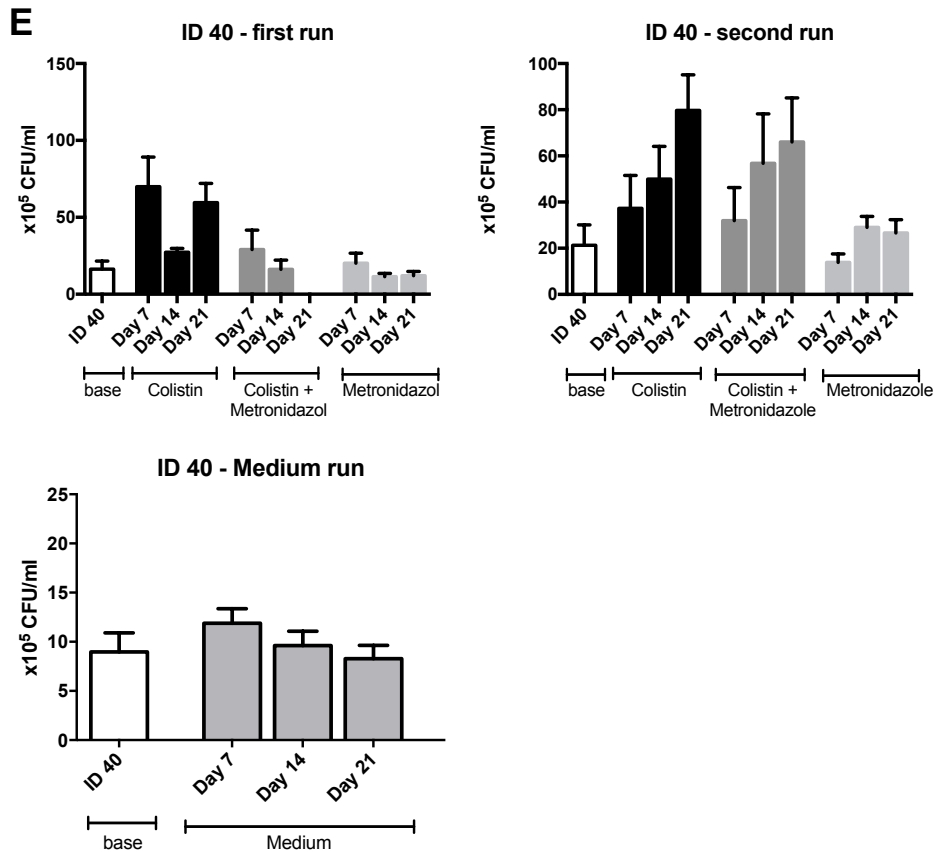
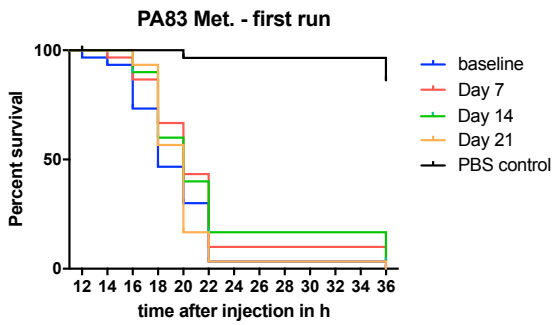
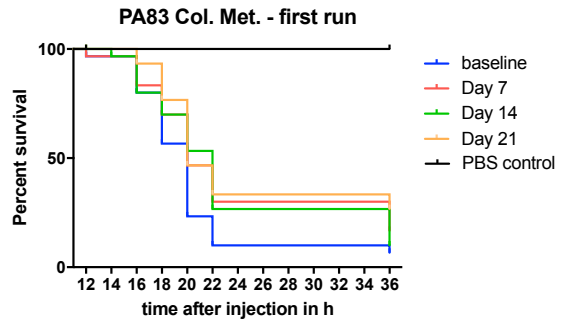
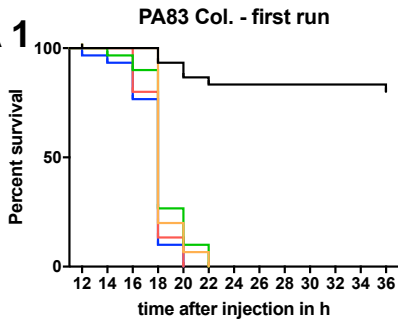


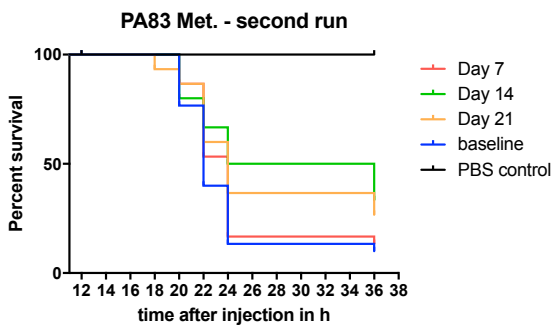
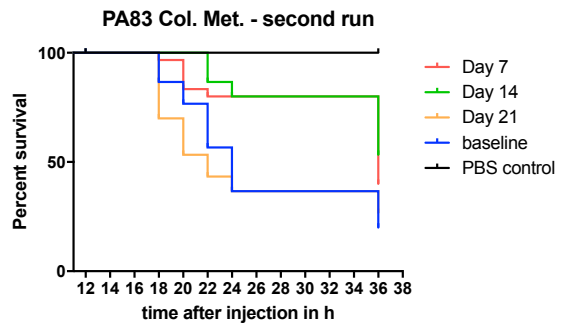
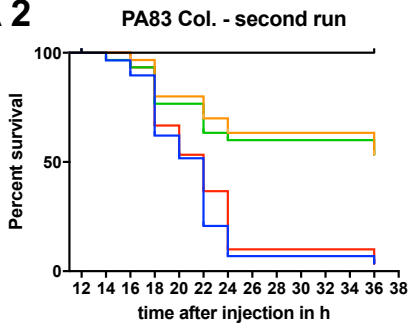
**Figure 14: Results for peg-lid method biofilm assay.** Biofilm was grown on TSP pegs immersed into 96-well microtiter plate wells filled with liquid culture of bacteria with OD<sub>600nm</sub> 0.1. Then, biofilm was dissolved from the pegs using 0.1 M EDTA and 0.1% CHAPS. The solution was plated on agar plates and CFUs were counted. The figure shows the number of CFUs counted on the agar plates. A) PA77 first -, second - and medium run B) PA83 first -, second - and medium run C) ID4 first -, second - and medium run D) ID21 first -, second - and medium run E) ID40 first -, second - and medium run.

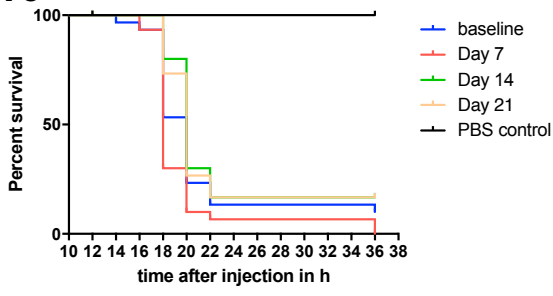
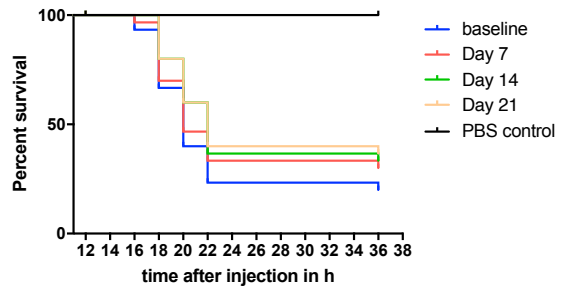
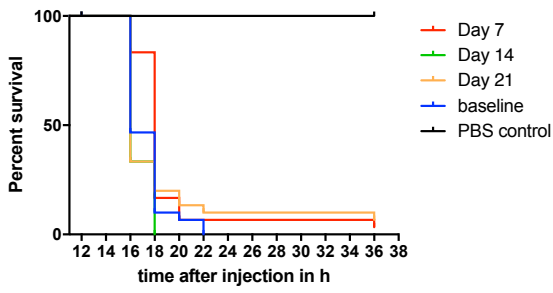
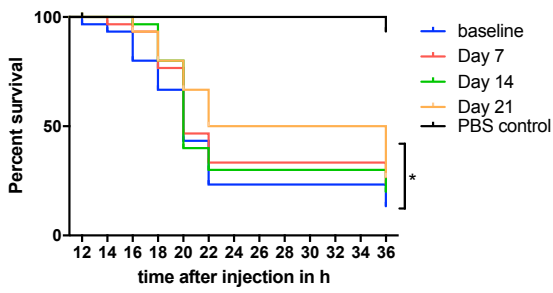
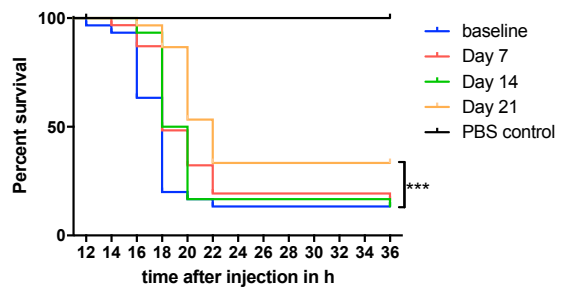
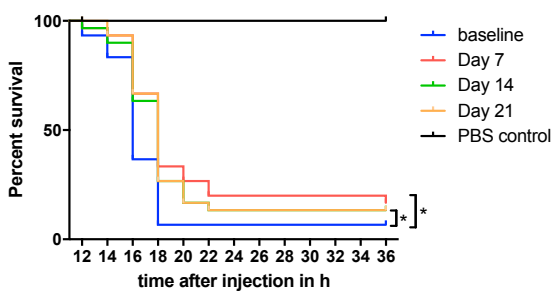
### 7.3 *Galleria mellonella* infection model – Kaplan Meier curves

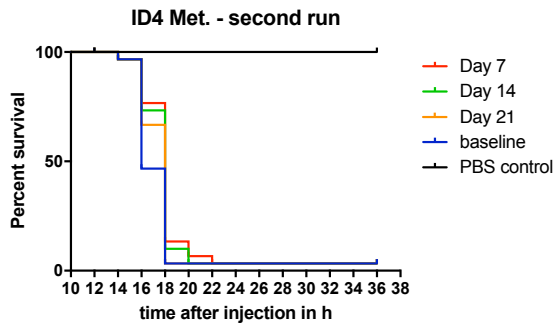
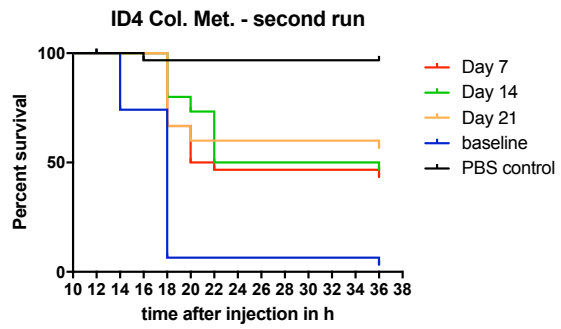
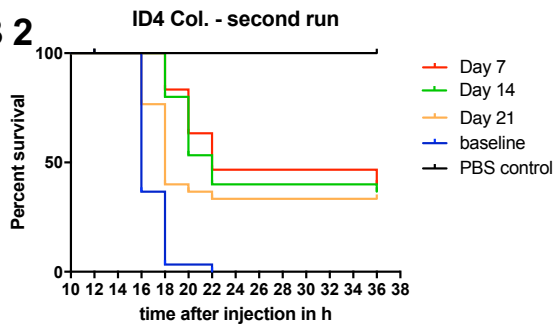
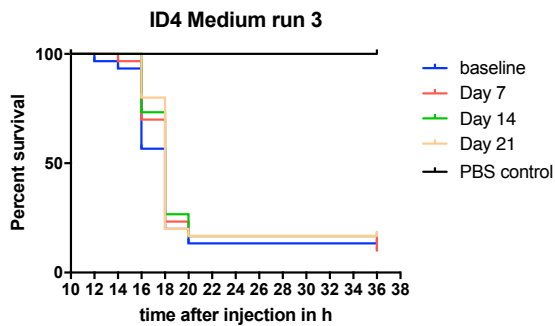
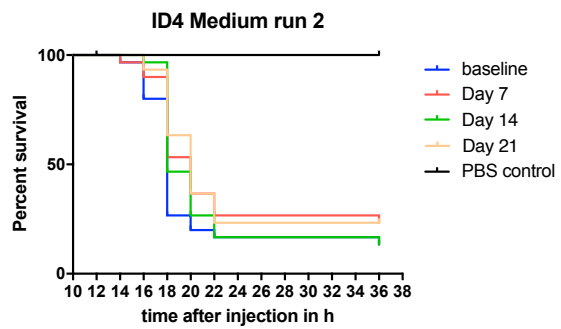
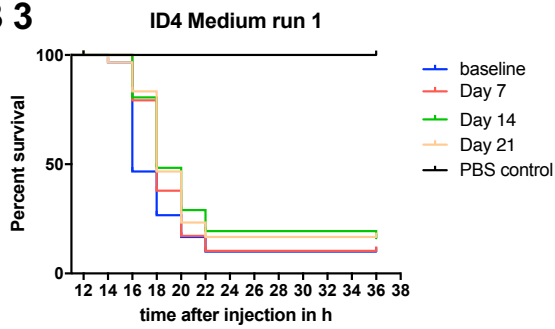
**A 1**



**A 2**

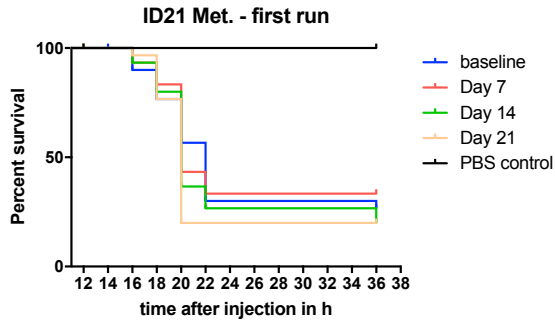
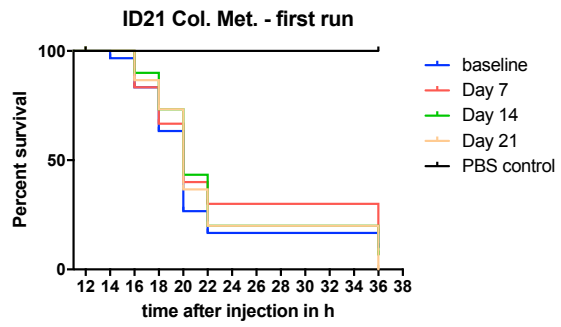
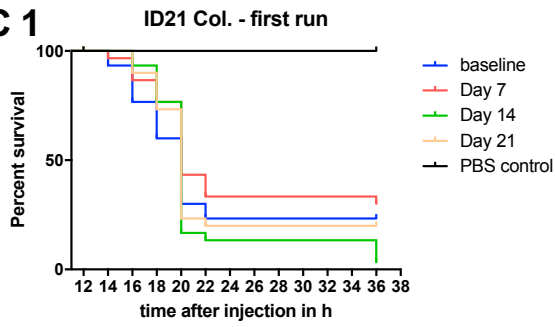


**A 3****PA83 Medium run 1****PA83 Medium run 2****PA83 Medium run 3****B 1****ID4 Col. - first run****ID4 Col. Met. - first run****ID4 Met. - first run**

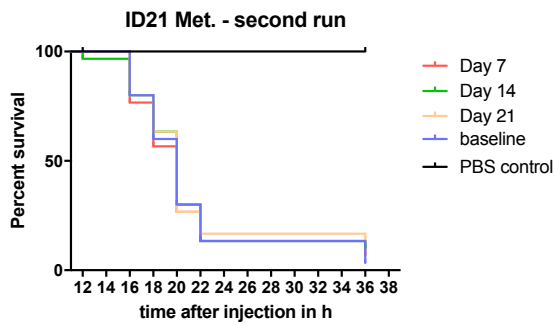
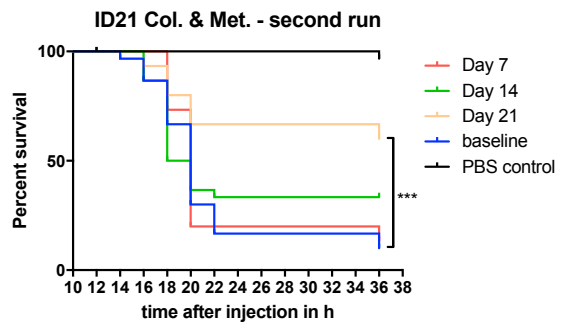
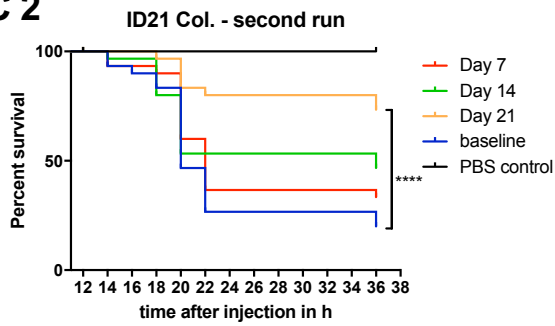
**B 2****B 3**

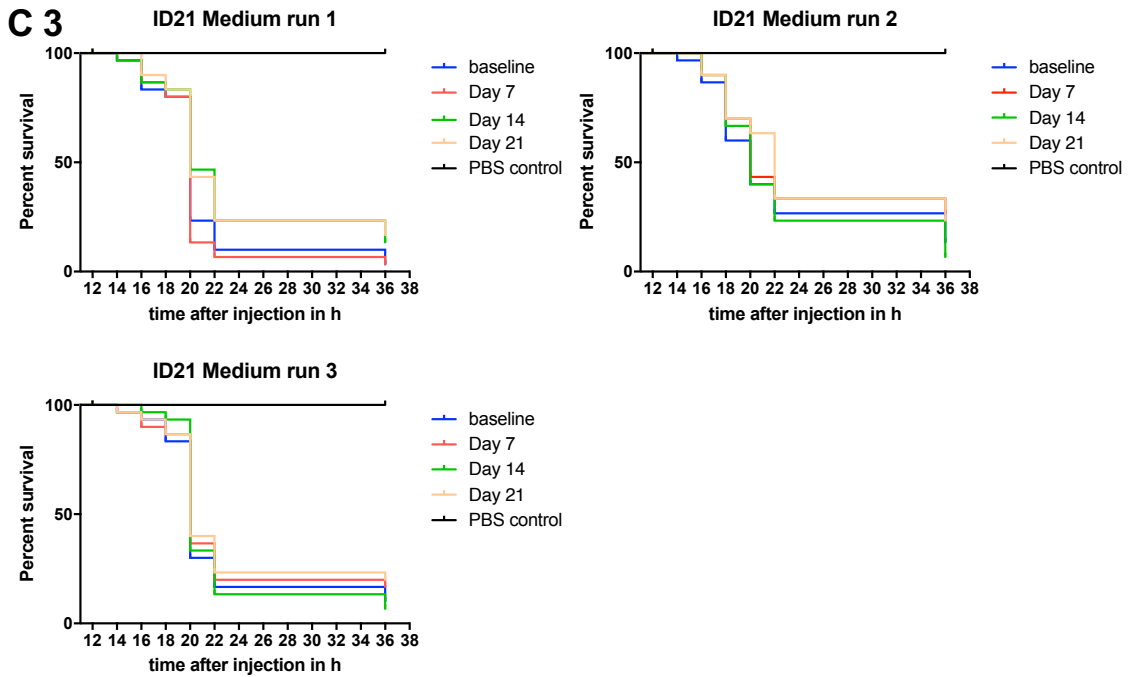


**C 1**



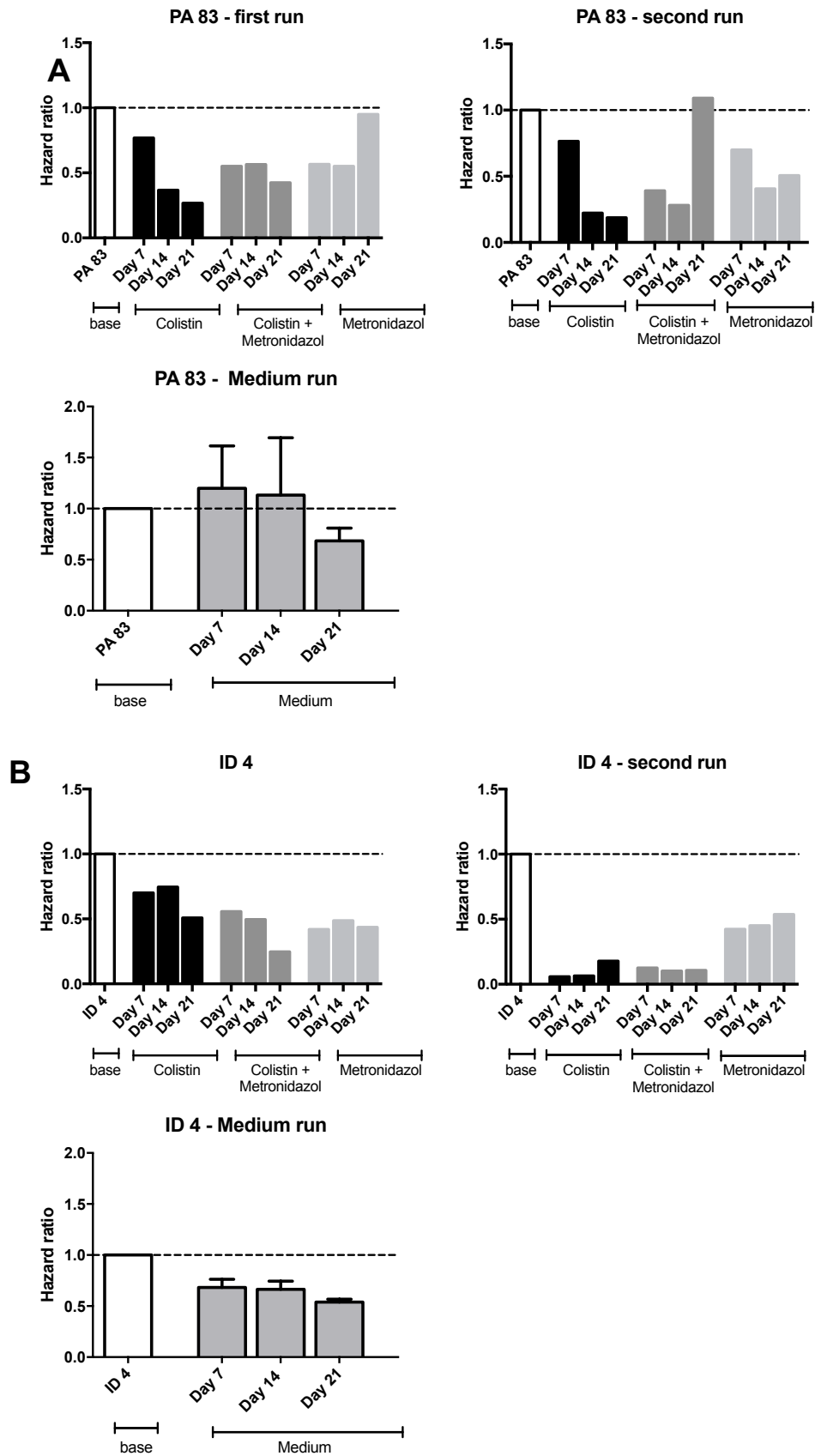
**C 2**





**Figure 15: Kaplan Meier curves monitoring the survival of *G. mellonella* larvae after infection.** *Galleria mellonella* larvae were infected with about 10 CFU of *P. aeruginosa* strains and survival was controlled for 36h. Kaplan Meier curves were created for baseline strain next to day 7, 14 and 21 strains from one condition of a morbidostat run with 30 larvae each. A 1) PA83 first run, A 2) PA83 second run, A 3) PA83 medium run (performed in triplicates), B 1) ID4 first run, B 2) Id4 second run, B 3) ID4 medium run (performed in triplicates), C 1) ID21 first run, C 2) ID21 second run, C 3) ID21 medium run (performed in triplicates) Col. = colistin condition, Col.+Met. = colistin and metronidazole combination condition, Met. = metronidazole condition. Statistical analysis was performed by Log-rank test and significant differences are indicated with asterisks ( $p < 0,05$ : \*,  $p < 0,01$ : \*\*,  $p < 0,001$ : \*\*\*,  $p < 0,0001$ : \*\*\*\*).

## 7.4 *Galleria mellonella* infection model – Hazard ratios



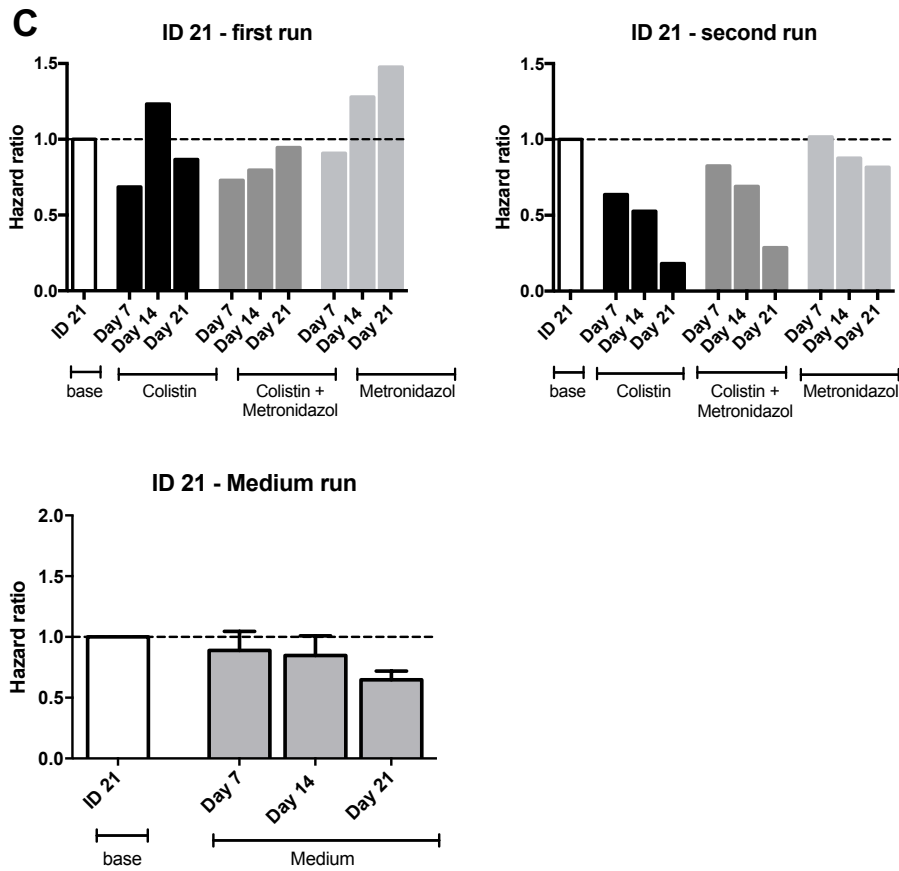


**Figure 16: Hazard ratios for *Galleria mellonella* infection model.** The figure shows Hazard ratios for morbidostat-derived strains calculated out of Kaplan Meier curves in relation to baseline isolates. A) PA83 first -, second - and medium run B) ID4 first -, second - and medium run C) ID21 first -, second - and medium run.

## 8 References

- Abidi, S. H., *et al.* (2013). "Drug resistance profile and biofilm forming potential of *Pseudomonas aeruginosa* isolated from contact lenses in Karachi-Pakistan." *BMC Ophthalmol* **13**: 57.
- Al-Tahhan, R. A., *et al.* (2000). "Rhamnolipid-induced removal of lipopolysaccharide from *Pseudomonas aeruginosa*: effect on cell surface properties and interaction with hydrophobic substrates." *Appl Environ Microbiol* **66**(8): 3262-3268.
- Andersson, D. I., *et al.* (2014). "Microbiological effects of sublethal levels of antibiotics." *Nature Reviews Microbiology* **12**(7): 465-478.
- Antoniadou, A., *et al.* (2007). "Colistin-resistant isolates of *Klebsiella pneumoniae* emerging in intensive care unit patients: first report of a multiclonal cluster." *Journal of Antimicrobial Chemotherapy* **59**(4): 786-790.
- Azimi, L., *et al.* (2019). "Colistin-resistant *Pseudomonas aeruginosa* clinical strains with defective biofilm formation." *GMS Hyg Infect Control* **14**: Doc12.
- Beceiro, A., *et al.* (2014). "Biological cost of different mechanisms of colistin resistance and their impact on virulence in *Acinetobacter baumannii*." *Antimicrob Agents Chemother* **58**(1): 518-526.
- Bekaert, M., *et al.* (2011). "Attributable Mortality of Ventilator-Associated Pneumonia." *American Journal of Respiratory and Critical Care Medicine* **184**(10): 1133-1139.
- Bodey, G. P., *et al.* (1983). "Infections Caused by *Pseudomonas aeruginosa*." *Clinical Infectious Diseases* **5**(2): 279-313.
- Brook, I. (2016). "Spectrum and treatment of anaerobic infections." *Journal of Infection and Chemotherapy* **22**(1): 1-13.
- Buhl, M., *et al.* (2015). "Prevalence and risk factors associated with colonization and infection of extensively drug-resistant *Pseudomonas aeruginosa*: a systematic review." *Expert Review of Anti-infective Therapy* **13**(9): 1159-1170.
- Caiazza, N. C., *et al.* (2004). "SadB Is Required for the Transition from Reversible to Irreversible Attachment during Biofilm Formation by *Pseudomonas aeruginosa* PA14." *Journal of Bacteriology* **186**(14): 4476.
- Caselli, E., *et al.* (2018). "Spread of mcr-1-Driven Colistin Resistance on Hospital Surfaces, Italy." *Emerg Infect Dis* **24**(9): 1752-1753.
- Choi, M.-J., *et al.* (2015). "Loss of Hypermucoviscosity and Increased Fitness Cost in Colistin-Resistant *Klebsiella pneumoniae* Sequence Type 23 Strains." *Antimicrobial Agents and Chemotherapy* **59**(11): 6763.
- Cirz, R. T., *et al.* (2006). "Defining the *Pseudomonas aeruginosa* SOS response and its role in the global response to the antibiotic ciprofloxacin." *J Bacteriol* **188**(20): 7101-7110.
- Colville, K., *et al.* (2010). "Effects of Poly(L-lysine) Substrates on Attached *Escherichia coli* Bacteria." *Langmuir* **26**(4): 2639-2644.
- Costerton, J. W., *et al.* (1999). "Bacterial biofilms: a common cause of persistent infections." *Science* **284**(5418): 1318-1322.
- Cowan, S. E., *et al.* (2001). "Development of engineered biofilms on poly- L-lysine patterned surfaces." *Biotechnology Letters* **23**(15): 1235-1241.

Cryz, S. J., Jr., *et al.* (1984). "Role of lipopolysaccharide in virulence of *Pseudomonas aeruginosa*." Infect Immun **44**(2): 508-513.

Cutuli, M. A., *et al.* (2019). "Galleria mellonella as a consolidated in vivo model hosts: New developments in antibacterial strategies and novel drug testing." Virulence **10**(1): 527-541.

Dafopoulou, K., *et al.* (2015). "Colistin-Resistant *Acinetobacter baumannii* Clinical Strains with Deficient Biofilm Formation." Antimicrob Agents Chemother **60**(3): 1892-1895.

Dingsdag, S. A., *et al.* (2017). "Metronidazole: an update on metabolism, structure–cytotoxicity and resistance mechanisms." Journal of Antimicrobial Chemotherapy **73**(2): 265-279.

Dößelmann, B., *et al.* (2017). "Rapid and Consistent Evolution of Colistin Resistance in Extensively Drug-Resistant *Pseudomonas aeruginosa* during Morbidostat Culture." Antimicrobial Agents and Chemotherapy **61**(9): e00043-00017.

ECDC-Annual-Epidemiological-Report (2017). "Healthcare-associated infections acquired in intensive care units." European Centre for Disease Prevention and Control - Surveillance Report - [https://www.ecdc.europa.eu/sites/default/files/documents/AER\\_for\\_2017-HAI.pdf](https://www.ecdc.europa.eu/sites/default/files/documents/AER_for_2017-HAI.pdf).

ECDC-Surveillance-Report (2012). "Point prevalence survey of healthcare- associated infections and antimicrobial use in European acute care hospitals." European Centre for Disease Prevention and Control - Surveillance Report - <https://www.ecdc.europa.eu/en/publications-data?s=healthcare%20associated%20infections&f%5B0%5D=output+types%3A1244&sort+by=search+api+relevance&sort+order=DESC&page=1>.

Edwards, D. I. (1986). REDUCTION OF NITROIMIDAZOLES IN VITRO AND DNA DAMAGE. Bioreduction in the Activation of Drugs. P. Alexander, J. Gielen and A. C. Sartorelli, Pergamon: 53-58.

Elena, S. F., *et al.* (2003). "Evolution experiments with microorganisms: the dynamics and genetic bases of adaptation." Nature Reviews Genetics **4**(6): 457-469.

Etyimologia: Pseudomonas, Emerg Infect Dis. 2012 Aug;18(8):1241. doi: 10.3201/eid1808.ET1808. (2012). "Etyimologia: Pseudomonas." Emerg Infect Dis **18**(8): 1241.

EUCAST (2019). "The European Committee on Antimicrobial Susceptibility Testing. Breakpoint tables for interpretation of MICs and zone diameters. Version 9.0, 2019. <http://www.eucast.org>."

Falagas, M. E., *et al.* (2005). "Colistin: The Revival of Polymyxins for the Management of Multidrug-Resistant Gram-Negative Bacterial Infections." Clinical Infectious Diseases **40**(9): 1333-1341.

Farshadzadeh, Z., *et al.* (2018). "Growth Rate and Biofilm Formation Ability of Clinical and Laboratory-Evolved Colistin-Resistant Strains of *Acinetobacter baumannii*." Front Microbiol **9**: 153.

Fernández, L., *et al.* (2010). "Adaptive resistance to the "last hope" antibiotics polymyxin B and colistin in *Pseudomonas aeruginosa* is mediated by the novel two-component regulatory system ParR-ParS." Antimicrob Agents Chemother **54**(8): 3372-3382.

Fernández, L., *et al.* (2012). "The Two-Component System CprRS Senses Cationic Peptides and Triggers Adaptive Resistance in *Pseudomonas aeruginosa* Independently of ParRS." Antimicrobial Agents and Chemotherapy **56**(12): 6212.

Fernández-Reyes, M., *et al.* (2009). "The cost of resistance to colistin in *Acinetobacter baumannii*: a proteomic perspective." PROTEOMICS **9**(6): 1632-1645.

- Francis, V. I., *et al.* (2017). "Two-component systems required for virulence in *Pseudomonas aeruginosa*." FEMS Microbiol Lett **364**(11).
- Freeman, C. D., *et al.* (1997). "Metronidazole. A therapeutic review and update." Drugs **54**(5): 679-708.
- Fuqua, W. C., *et al.* (1994). "Quorum sensing in bacteria: the LuxR-LuxI family of cell density-responsive transcriptional regulators." Journal of Bacteriology **176**(2): 269.
- Giske, A., *et al.* (2017). "Systemic antibiotic prophylaxis prior to gastrointestinal surgery – is oral administration of doxycycline and metronidazole adequate?" Infectious Diseases **49**(11-12): 785-791.
- Gómez-Zorrilla, S., *et al.* (2016). "Impact of multidrug resistance on the pathogenicity of *Pseudomonas aeruginosa*: in vitro and in vivo studies." International Journal of Antimicrobial Agents **47**(5): 368-374.
- Gould, I. M., *et al.* (1985). "*Pseudomonas aeruginosa*: clinical manifestations and management." Lancet **2**(8466): 1224-1227.
- Guillon, A., *et al.* (2018). "Treatment of *Pseudomonas aeruginosa* Biofilm Present in Endotracheal Tubes by Poly-L-Lysine." Antimicrobial Agents and Chemotherapy **62**(11): e00564-00518.
- Gurung, J., *et al.* (2013). "Association of biofilm production with multidrug resistance among clinical isolates of *Acinetobacter baumannii* and *Pseudomonas aeruginosa* from intensive care unit." Indian J Crit Care Med **17**(4): 214-218.
- Gutu, A. D., *et al.* (2013). "Polymyxin resistance of *Pseudomonas aeruginosa* phoQ mutants is dependent on additional two-component regulatory systems." Antimicrob Agents Chemother **57**(5): 2204-2215.
- Hardalo, C., *et al.* (1997). "*Pseudomonas aeruginosa*: Assessment of Risk from Drinking Water." Critical Reviews in Microbiology **23**(1): 47-75.
- Harmsen, M., *et al.* (2010). "An update on *Pseudomonas aeruginosa* biofilm formation, tolerance, and dispersal." FEMS Immunology & Medical Microbiology **59**(3): 253-268.
- Hauser, A. R. (2009). "The type III secretion system of *Pseudomonas aeruginosa*: infection by injection." Nat Rev Microbiol **7**(9): 654-665.
- Hocquet, D., *et al.* (2013). "Metronidazole increases the emergence of ciprofloxacin- and amikacin-resistant *Pseudomonas aeruginosa* by inducing the SOS response." Journal of Antimicrobial Chemotherapy **69**(3): 852-854.
- Huang, W. M., *et al.* (1983). "Improved section adhesion for immunocytochemistry using high molecular weight polymers of L-lysine as a slide coating." Histochemistry **77**(2): 275-279.
- Iglewski, B. H. (1996). *Pseudomonas*. Medical Microbiology. 4th and S. Baron. Galveston (TX), University of Texas Medical Branch at Galveston  
The University of Texas Medical Branch at Galveston.
- Javed, M., *et al.* (2018). "Colistin susceptibility test evaluation of multiple-resistance-level *Pseudomonas aeruginosa* isolates generated in a morbidostat device." J Antimicrob Chemother **73**(12): 3368-3374.

- Jensen, P. Ø., *et al.* (2007). "Rapid necrotic killing of polymorphonuclear leukocytes is caused by quorum-sensing-controlled production of rhamnolipid by *Pseudomonas aeruginosa*." **153**(5): 1329-1338.
- Jimenez, P. N., *et al.* (2012). "The multiple signaling systems regulating virulence in *Pseudomonas aeruginosa*." *Microbiol Mol Biol Rev* **76**(1): 46-65.
- Jorge, P., *et al.* (2017). "Searching for new strategies against biofilm infections: Colistin-AMP combinations against *Pseudomonas aeruginosa* and *Staphylococcus aureus* single- and double-species biofilms." *PLoS One* **12**(3): e0174654.
- Jørgensen, K. M., *et al.* (2013). "Sublethal Ciprofloxacin Treatment Leads to Rapid Development of High-Level Ciprofloxacin Resistance during Long-Term Experimental Evolution of *Pseudomonas aeruginosa*." *Antimicrobial Agents and Chemotherapy* **57**(9): 4215.
- Juhas, M., *et al.* (2005). "Quorum sensing: the power of cooperation in the world of *Pseudomonas*." *Environmental Microbiology* **7**(4): 459-471.
- Kamali, E., *et al.* (2020). "Evaluation of antimicrobial resistance, biofilm forming potential, and the presence of biofilm-related genes among clinical isolates of *Pseudomonas aeruginosa*." *BMC Research Notes* **13**(1): 27.
- Kang, C.-I., *et al.* (2003). "Pseudomonas aeruginosa Bacteremia: Risk Factors for Mortality and Influence of Delayed Receipt of Effective Antimicrobial Therapy on Clinical Outcome." *Clinical Infectious Diseases* **37**(6): 745-751.
- Karami, P., *et al.* (2020). "The correlation between biofilm formation capability and antibiotic resistance pattern in *Pseudomonas aeruginosa*." *Gene Reports* **18**: 100561.
- Katz, D. E., *et al.* (2016). "Ten years with colistin: a retrospective case series." **70**(9): 706-711.
- Katz, E., *et al.* (1977). "The peptide antibiotics of *Bacillus*: chemistry, biogenesis, and possible functions." *Bacteriol Rev* **41**(2): 449-474.
- Kim, S. K., *et al.* (2016). "Biofilm dispersion in *Pseudomonas aeruginosa*." *J Microbiol* **54**(2): 71-85.
- Klausen, M., *et al.* (2003). "Involvement of bacterial migration in the development of complex multicellular structures in *Pseudomonas aeruginosa* biofilms." *Molecular Microbiology* **50**(1): 61-68.
- Lambert, P. A. (2002). "Mechanisms of antibiotic resistance in *Pseudomonas aeruginosa*." *J R Soc Med* **95 Suppl 41**(Suppl 41): 22-26.
- Lee, D. G., *et al.* (2006). "Genomic analysis reveals that *Pseudomonas aeruginosa* virulence is combinatorial." *Genome Biol* **7**(10): R90.
- Lee, J.-Y., *et al.* (2014). "Mutations and expression of PmrAB and PhoPQ related with colistin resistance in *Pseudomonas aeruginosa* clinical isolates." *Diagnostic Microbiology and Infectious Disease* **78**(3): 271-276.
- Lee, J.-Y., *et al.* (2016). "Evolved resistance to colistin and its loss due to genetic reversion in *Pseudomonas aeruginosa*." *Scientific Reports* **6**: 25543.
- Lee, V. T., *et al.* (2007). "A cyclic-di-GMP receptor required for bacterial exopolysaccharide production." *Mol Microbiol* **65**(6): 1474-1484.



- Levin, A. S., *et al.* (1999). "Intravenous Colistin as Therapy for Nosocomial Infections Caused by Multidrug-Resistant *Pseudomonas aeruginosa* and *Acinetobacter baumannii*." Clinical Infectious Diseases **28**(5): 1008-1011.
- Levin, B. R., *et al.* (1997). "The Population Genetics of Antibiotic Resistance." Clinical Infectious Diseases **24**(Supplement\_1): S9-S16.
- Li, J., *et al.* (2006). "Colistin: the re-emerging antibiotic for multidrug-resistant Gram-negative bacterial infections." The Lancet Infectious Diseases **6**(9): 589-601.
- Lister, P. D., *et al.* (2009). "Antibacterial-resistant *Pseudomonas aeruginosa*: clinical impact and complex regulation of chromosomally encoded resistance mechanisms." Clin Microbiol Rev **22**(4): 582-610.
- Little, J. W., *et al.* (1982). "The SOS regulatory system of *Escherichia coli*." Cell **29**(1): 11-22.
- Liu, Y.-Y., *et al.* (2016). "Emergence of plasmid-mediated colistin resistance mechanism MCR-1 in animals and human beings in China: a microbiological and molecular biological study." The Lancet Infectious Diseases **16**(2): 161-168.
- Liu, Y. Y., *et al.* (2017). "Structural Modification of Lipopolysaccharide Conferred by *mcr-1* in Gram-Negative ESKAPE Pathogens." Antimicrob Agents Chemother **61**(6).
- Livermore, D. M. (2004). "The need for new antibiotics." Clinical Microbiology and Infection **10**: 1-9.
- Löfmark, S., *et al.* (2010). "Metronidazole Is Still the Drug of Choice for Treatment of Anaerobic Infections." Clinical Infectious Diseases **50**(Supplement\_1): S16-S23.
- López-Rojas, R., *et al.* (2011). "Impaired Virulence and In Vivo Fitness of Colistin-Resistant *Acinetobacter baumannii*." The Journal of Infectious Diseases **203**(4): 545-548.
- Lory, S., *et al.* (2009). "Multiple activities of c-di-GMP in *Pseudomonas aeruginosa*." Nucleic Acids Symposium Series **53**(1): 51-52.
- Macfarlane, E. L. A., *et al.* (2000). "Role of *Pseudomonas aeruginosa* PhoP-PhoQ in resistance to antimicrobial cationic peptides and aminoglycosides." **146**(10): 2543-2554.
- Maeda, K., *et al.* (1953). "A new antibiotic, azomycin." J Antibiot (Tokyo) **6**(4): 182.
- Magiorakos, A. P., *et al.* (2012). "Multidrug-resistant, extensively drug-resistant and pandrug-resistant bacteria: an international expert proposal for interim standard definitions for acquired resistance." Clin Microbiol Infect **18**(3): 268-281.
- Maurice, N. M., *et al.* (2018). "*Pseudomonas aeruginosa* Biofilms: Host Response and Clinical Implications in Lung Infections." Am J Respir Cell Mol Biol **58**(4): 428-439.
- McEachran, D. W., *et al.* (1986). "A new method for the irreversible attachment of cells or proteins to polystyrene tissue culture plates for use in the study of bacterial adhesion." Journal of Microbiological Methods **5**(2): 99-111.
- McPhee, J. B., *et al.* (2003). "Cationic antimicrobial peptides activate a two-component regulatory system, PmrA-PmrB, that regulates resistance to polymyxin B and cationic antimicrobial peptides in *Pseudomonas aeruginosa*." Molecular Microbiology **50**(1): 205-217.

- McVicker, G., *et al.* (2014) Clonal expansion during *Staphylococcus aureus* infection dynamics reveals the effect of antibiotic intervention. PLoS Pathog **10**, e1003959 DOI: 10.1371/journal.ppat.1003959
- Melnyk, A. H., *et al.* (2015). "The fitness costs of antibiotic resistance mutations." Evol Appl **8**(3): 273-283.
- Merritt, J. H., *et al.* (2007). "SadC reciprocally influences biofilm formation and swarming motility via modulation of exopolysaccharide production and flagellar function." J Bacteriol **189**(22): 8154-8164.
- Miller, M. A. (2007). "Clinical Management of *Clostridium difficile*-Associated Disease." Clinical Infectious Diseases **45**(Supplement\_2): S122-S128.
- Moradali, M. F., *et al.* (2017). "Pseudomonas aeruginosa Lifestyle: A Paradigm for Adaptation, Survival, and Persistence." Front Cell Infect Microbiol **7**: 39.
- Morga, M., *et al.* (2015). "Monolayers of poly-L-lysine on mica – Electrokinetic characteristics." Journal of Colloid and Interface Science **456**: 116-124.
- Moskowitz, S. M., *et al.* (2012). "PmrB Mutations Promote Polymyxin Resistance of *Pseudomonas aeruginosa* Isolated from Colistin-Treated Cystic Fibrosis Patients." Antimicrobial Agents and Chemotherapy **56**(2): 1019.
- Mulcahy, L. R., *et al.* (2014). "Pseudomonas aeruginosa biofilms in disease." Microb Ecol **68**(1): 1-12.
- Muller, C., *et al.* (2011). "A two-component regulatory system interconnects resistance to polymyxins, aminoglycosides, fluoroquinolones, and  $\beta$ -lactams in *Pseudomonas aeruginosa*." Antimicrob Agents Chemother **55**(3): 1211-1221.
- Müller, M. (1986). "Reductive activation of nitroimidazoles in anaerobic microorganisms." Biochemical Pharmacology **35**(1): 37-41.
- Muriel, C., *et al.* (2019). "The diguanylate cyclase AdrA regulates flagellar biosynthesis in *Pseudomonas fluorescens* F113 through SadB." Scientific Reports **9**(1): 8096.
- Nair, C. G., *et al.* (2013). "Sub-lethal concentrations of antibiotics increase mutation frequency in the cystic fibrosis pathogen *Pseudomonas aeruginosa*." Letters in Applied Microbiology **56**(2): 149-154.
- Nguyen, D., *et al.* (2011). "Active Starvation Responses Mediate Antibiotic Tolerance in Biofilms and Nutrient-Limited Bacteria." Science **334**(6058): 982.
- Noteboom, Y., *et al.* (2015). "Antibiotic-Induced Within-Host Resistance Development of Gram-Negative Bacteria in Patients Receiving Selective Decontamination or Standard Care." Crit Care Med **43**(12): 2582-2588.
- O'Toole, G. A. (2011). "Microtiter Dish Biofilm Formation Assay." JoVE(47): e2437.
- O'Toole, G. A., *et al.* (1998). "Flagellar and twitching motility are necessary for *Pseudomonas aeruginosa* biofilm development." Molecular Microbiology **30**(2): 295-304.
- Olaitan, A. O., *et al.* (2014). "Mechanisms of polymyxin resistance: acquired and intrinsic resistance in bacteria." **5**(643).

- Pamp, S. J., *et al.* (2008). "Tolerance to the antimicrobial peptide colistin in *Pseudomonas aeruginosa* biofilms is linked to metabolically active cells, and depends on the *pmr* and *mexAB-oprM* genes." **68**(1): 223-240.
- Passador, L., *et al.* (1993). "Expression of *Pseudomonas aeruginosa* virulence genes requires cell-to-cell communication." *Science* **260**(5111): 1127.
- Pereira, T. C., *et al.* (2018). "Recent Advances in the Use of *Galleria mellonella* Model to Study Immune Responses against Human Pathogens." *J Fungi (Basel)* **4**(4).
- Qi, L., *et al.* (2016). "Relationship between Antibiotic Resistance, Biofilm Formation, and Biofilm-Specific Resistance in *Acinetobacter baumannii*." *Front Microbiol* **7**: 483.
- Radman, M. (1975). "SOS repair hypothesis: phenomenology of an inducible DNA repair which is accompanied by mutagenesis." *Basic Life Sci* **5a**: 355-367.
- Raetz, C. R., *et al.* (2007). "Lipid A modification systems in gram-negative bacteria." *Annu Rev Biochem* **76**: 295-329.
- Rocchetta, H. L., *et al.* (1999). "Genetics of O-antigen biosynthesis in *Pseudomonas aeruginosa*." *Microbiol Mol Biol Rev* **63**(3): 523-553.
- Rodríguez-Baño, J., *et al.* (2008). "Biofilm formation in *Acinetobacter baumannii*: associated features and clinical implications." *Clinical Microbiology and Infection* **14**(3): 276-278.
- Rolain, J.-M., *et al.* (2011). "Acinetobacter baumannii Resistant to Colistin With Impaired Virulence: A Case Report From France." *The Journal of Infectious Diseases* **204**(7): 1146-1147.
- Rosenthal, A. Z., *et al.* (2011). "Following evolution of bacterial antibiotic resistance in real time." *Nat Genet* **44**: 11.
- Rybtke, M., *et al.* (2015). "Pseudomonas aeruginosa Biofilm Infections: Community Structure, Antimicrobial Tolerance and Immune Response." *Journal of Molecular Biology* **427**(23): 3628-3645.
- Santajit, S., *et al.* (2016). "Mechanisms of Antimicrobial Resistance in ESKAPE Pathogens %J BioMed Research International." **2016**: 8.
- Sato, Y., *et al.* (2018). "Sub-minimum inhibitory concentrations of colistin and polymyxin B promote *Acinetobacter baumannii* biofilm formation." *PLoS One* **13**(3): e0194556.
- Shapiro-Ilan, D. I., *et al.* (2005). "Definitions of pathogenicity and virulence in invertebrate pathology." *Journal of Invertebrate Pathology* **88**(1): 1-7.
- Shima, S., *et al.* (1984). "Antimicrobial action of epsilon-poly-L-lysine." *J Antibiot (Tokyo)* **37**(11): 1449-1455.
- Shinn, D. L. S. (1962). "METRONIDAZOLE IN ACUTE ULCERATIVE GINGIVITIS." *The Lancet* **279**(7240): 1191.
- Steinhaus, E. A., *et al.* (1970). *An Abridged Glossary of Terms Used in Invertebrate Pathology*, U.S. Pacific Northwest Forest and Range Experiment Station.
- Storm, D. R., *et al.* (1977). "Polymyxin and Related Peptide Antibiotics." *Annual Review of Biochemistry* **46**(1): 723-763.

- Stover, C. K., *et al.* (2000). "Complete genome sequence of *Pseudomonas aeruginosa* PAO1, an opportunistic pathogen." Nature **406**(6799): 959-964.
- Sykes, J. E. (2014). Chapter 36 - Gram-negative Bacterial Infections. Canine and Feline Infectious Diseases. J. E. Sykes. Saint Louis, W.B. Saunders: 355-363.
- Tacconelli, E., *et al.* (2018). "Discovery, research, and development of new antibiotics: the WHO priority list of antibiotic-resistant bacteria and tuberculosis." Lancet Infect Dis **18**(3): 318-327.
- Takahashi, K., *et al.* (1992). "Detection of lipopolysaccharide (LPS) and identification of its serotype by an enzyme-linked immunosorbent assay (ELISA) using poly-l-lysine." Journal of Immunological Methods **153**(1): 67-71.
- Tally, F. P., *et al.* (1972). "Metronidazole versus anaerobes. In vitro data and initial clinical observations." Calif Med **117**(6): 22-26.
- Tan, J. H., *et al.* (2017). "In Vitro and In Vivo Efficacy of an LpxC Inhibitor, CHIR-090, Alone or Combined with Colistin against *Pseudomonas aeruginosa* Biofilm." Antimicrob Agents Chemother **61**(7).
- Tang, H. B., *et al.* (1996). "Contribution of specific *Pseudomonas aeruginosa* virulence factors to pathogenesis of pneumonia in a neonatal mouse model of infection." Infect Immun **64**(1): 37-43.
- Tocher, J. H., *et al.* (1988). "Electrochemical Characteristics of Nitro-Heterocyclic Compounds of Biological Interest: I. The Influence of Solvent." Free Radical Research Communications **4**(5): 269-276.
- Tocher, J. H., *et al.* (1992). "The interaction of reduced metronidazole with DNA bases and nucleosides." International Journal of Radiation Oncology\*Biophysics **22**(4): 661-663.
- Toprak, E., *et al.* (2011). "Evolutionary paths to antibiotic resistance under dynamically sustained drug selection." Nat Genet **44**: 101.
- Toprak, E., *et al.* (2011). "Evolutionary paths to antibiotic resistance under dynamically sustained drug selection." Nat Genet **44**(1): 101-105.
- Tsai, C. J., *et al.* (2016). "Galleria mellonella infection models for the study of bacterial diseases and for antimicrobial drug testing." Virulence **7**(3): 214-229.
- Tumbarello, M., *et al.* (2011). "Multidrug-resistant *Pseudomonas aeruginosa* bloodstream infections: risk factors and mortality." Epidemiol Infect **139**(11): 1740-1749.
- Wand, M. E., *et al.* (2015). "Retention of virulence following adaptation to colistin in *Acinetobacter baumannii* reflects the mechanism of resistance." Journal of Antimicrobial Chemotherapy **70**(8): 2209-2216.
- Willmann, M., *et al.* (2018). "Multi-omics approach identifies novel pathogen-derived prognostic biomarkers in patients with *Pseudomonas aeruginosa* bloodstream infection." bioRxiv: 309898.
- Wilson, C., *et al.* (2017). "Quantitative and Qualitative Assessment Methods for Biofilm Growth: A Mini-review." Res Rev J Eng Technol **6**(4).
- Wood, T. K., *et al.* (2013). "Bacterial persister cell formation and dormancy." Appl Environ Microbiol **79**(23): 7116-7121.

## 9 Erklärung zum Eigenanteil der Dissertationsschrift

Die Arbeit wurde am Institut für Medizinische Mikrobiologie und Hygiene des Universitätsklinikums Tübingen unter Betreuung von Prof. Dr. med. MSc Matthias Willmann durchgeführt.

Die Konzeption der Studie erfolgte durch Prof. Dr. med. MSc Matthias Willmann (Gruppenleiter), zusammen mit Mumina Javed (PhD Studentin). Die Protokolle und der Ablauf der Experimente wurden von Prof. Dr. med. MSc Matthias Willmann, Mumina Javed und mir entworfen.

Die Experimente wurden von mir mit Unterstützung durch Mumina Javed etabliert und durchgeführt. Die Methode zur Resistenztestung („Susceptibility tests“) wurde von Viola Ueltzhöffer durchgeführt.

Die statistische Auswertung erfolgte nach Anleitung von Prof. Dr. med. MSc Matthias Willmann und Dr. Ulrich Schoppmeier durch mich. Die Auswertung der Korrelation („Correlation analysis“) wurde von Dr. Ulrich Schoppmeier durchgeführt.

Das Verfassen des Manuskripts für die Veröffentlichung der Daten („Transcriptomic Basis of Serum Resistance and Virulence Related Traits in XDR *P. aeruginosa* Evolved Under Antibiotic Pressure in a Morbidostat Device“), die aus dem Projekt hervorgingen, erfolgte durch Mumina Javed und Prof. Dr. med. MSc Matthias Willmann.

Ich versichere, das Manuskript selbständig verfasst zu haben und keine weiteren als die von mir angegebenen Quellen verwendet zu haben.

Tübingen, den

Benedikt Jentzsch

## 10 Publications

First data of this work have been presented as a poster at the “71st Annual Conference of the German Society for Hygiene and Microbiology (DGHM)” in February 2019 in Göttingen.

Parts of the data shown in this work were published in:

Javed M, Jentsch B, Heinrich M, Ueltzhoeffer V, Peter S, Schoppmeier U, Angelov A, Schwarz S and Willmann M “Transcriptomic Basis of Serum Resistance and Virulence Related Traits in XDR *P. aeruginosa* Evolved Under Antibiotic Pressure in a Morbidostat Device”. *Front. Microbiol.* Published: 25. January 2021. 11:619542. doi: 10.3389/fmicb.2020.619542

## 11 Acknowledgements

I would like to sincerely thank Prof. Dr. med. MSc Matthias Willmann for giving me the opportunity to do my medical doctoral thesis in his working group and to be part of the project. Thank you for your patience and guidance on the challenging journey and for always encouraging me through all the setbacks that occurred during the time.

Furthermore, I would like to thank all the members of AG Willmann, as I was very warmly welcomed, and I am grateful for the very nice time and the familial atmosphere. I also appreciate Dr. Ulrich Schoppmeier's help and advice with the statistical analysis of the data.

My special appreciation goes to Dr. Mumina Javed for her really nice supervision, support and helpful feedback for both my lab work and writing process. I am glad that I could share the path to my MD and your PhD with you.

Also, I want to thank the whole Team of AG Peschel for all their help in the lab especially in the beginning of the project and their advice and guidance regarding the experiments in this work. I felt really welcomed and part of the team right from the start, and I am thankful for all the friends I found in you.

I am grateful to the IZKF Promotionskolleg Tübingen for their financial and advisory support.

Last but not least, I would like to thank my family and friends who have always assisted and encouraged me on the long and stressful journey leading up to the completion of this dissertation. In particular, I want to thank my dear partner Lea, who has managed not only to motivate me, but also to support me during the writing process.

Thank you!